REPORT NO. DOT-TSC-OST-73-29, V

CONCEPT FOR A SATELLITE-BASED ADVANCED AIR TRAFFIC MANAGEMENT SYSTEM

Volume V. System Performance

J. C. Elsey
J. B. King
I. M. Weiss
K. M. Armstrong
C. Chen
J. Hsu
T. C. Lu
R. P. Utsumi

FEBRUARY 1974
FINAL REPORT

Prepared for
DEPARTMENT OF TRANSPORTATION
OFFICE OF THE SECRETARY
Office of Systems Engineering
Washington DC 20590

NOTICE

The contents of this report reflect the views of Rockwell International/Autonetics Division. The contents do not necessarily reflect the official views or policy of the Department of Transportation. This report does not constitute a standard, specification, or regulation.

NOTICE

This document is distributed under the sponsorship of the Department of Transportation in the interest of information exchange. The United States Government assumes no responsibility for contents or use, thereof.

Technical Report Documentation Page

1. Report No.	2. Government Accession No.	3. Recipient's Catalog No.
DOT-TSC-OST-73-29, V		

4. Title and Subtitle	5. Report Date
CONCEPT FOR A SATELLITE-BASED ADVANCED AIR TRAFFIC MANAGEMENT SYSTEM Volume V. System Performance	February 1974
	6. Performing Organization Code
7. Author(s) *J.C.Elsey, J.B.King, I.M.Weiss, K.M. Armstrong, C.Chen, J.Hsu, T.C.Lu, R.P.Utsumi	8. Performing Organization Report No. DOT-TSC-OST-73-29, V
9. Performing Organization Name and Address Autonetics 3370 Miraloma Avenue Anaheim, CA 92803	10. Work Unit No. (TRAIS) OS404/R-4509
	11. Contract or Grant No. DOT-TSC-508
12. Sponsoring Agency Name and Address Department of Transportation Office of the Secretary Office of System Engineering Washington DC 20590	13. Type of Report and Period Covered Final Report October 1972 through October 1973
	14. Sponsoring Agency Code

15. Supplementary Notes

*Under contract to: Department of Transportation, Transportation Systems Center, Kendall Square, Cambridge, MA 02142

16. Abstract

This volume presents the results of the performance evaluation of the Satellite-Based Advanced Air Traffic Management System (SAATMS). The evaluation established the capacity, safety, and delay performance of the system for the Los Angeles Basin terminal area operations. The results of the performance evaluation were compared to the established performance specification. SAATMS provides capacity exceeding the highest traffic demand projected for 1995 while meeting the delay specification and maintaining the safety level provided by the present system. An evaluation of enroute safety is presented, along with a comparison of the enroute safety provided by the present system and a Ground-Based Advanced Air Traffic Management System (GAATMS). The system and subsystem parameters which influence the functioning of SAATMS are discussed, as are the functional relationships between the system performance measures and the system and subsystem parameters. The analytical expressions and the digital simulation used to evaluate SAATMS are presented along with a discussion of the methodology, the scenarios, and the constraints used in the evaluation. This volume also presents the results of a sensitivity analysis which shows the impact of the system and subsystem parameters on the capacity, safety, and delay performance measures.

17. Key Words	18. Distribution Statement
Air traffic control system, system performance evaluation, safety, delay, capacity, and simulation	DOCUMENT IS AVAILABLE TO THE PUBLIC THROUGH THE NATIONAL TECHNICAL INFORMATION SERVICE, SPRINGFIELD, VIRGINIA 22151.

19. Security Classif. (of this report)	20. Security Classif. (of this page)	21. No. of Pages	22. Price
UNCLASSIFIED	UNCLASSIFIED	150	

Form DOT F 1700.7 (8-72)

* U. S. GOVERNMENT PRINTING OFFICE : 1973 725-504/328

CONTENTS

CONTENTS (continued)

ILLUSTRATIONS

ILLUSTRATIONS (continued)

TABLES

GLOSSARY

AATMS	Advanced Air Traffic Management System
ACC	Airport Control Center
ADF	Automatic Direction Finder
ADIZ	Air Defense Identification Zone
AGL	Above Ground Level
AMF	Analog Matched Filter
AOPA	Aircraft Owners and Pilots Association
ARINC	Aeronautical Radio, Inc.
ARTCC	Air Route Traffic Control Center
ARTS	Automated Radar Terminal System
ATC	Air Traffic Control
ATCAC	Air Traffic Control Advisory Committee
ATCRBS	Air Traffic Control Radar Beacon System
ATCS	Air Traffic Control System
ATM	Air Traffic Management
CA	California
CARD	Civil Aviation Research and Development
CAS	Collision Avoidance System
CCC	Continental Control Center
CNI	Communication Navigation Identification
CNMAC	Critical Near Midair Collisions
COMM	Communications
CONUS	Continental United States
CP	Central Processor
CST	Central Standard Time
CW	Continuous Wave

GLOSSARY (continued)

DABS	Discrete Address Beacon System
DOD	Department of Defense
DOT	Department of Transportation
DME	Distance Measuring Equipment
DNSDP	Defense Navigation Satellite Development Program
DNSS	Defense Navigation Satellite System
ERP	Effective Radiated Power
ESRO	European Satellite Reserach Organization
EST	Eastern Standard Time
ETA	Estimated Time of Arrival
FAA	Federal Aviation Administration
F&E	Facilities and Equipment
FL	Florida
FM	Frequency Modulation
FSS	Flight Service Station
GA	General Aviation
GAATMS	Ground-Based Advanced Air Traffic Management System
GDOP	Geometric Dilution of Precision
GFE	Government Furnished Equipment
IAC	Instantaneous Airborne Count
ICAO	International Civil Aviation Organization
ID	Identification
IFR	Instrument Flight Rules
ILS	Instrument Landing System
IMC	Instrument Meteorological Conditions

GLOSSARY (continued)

I/O	Input/Output
IOP	Input Output Processor
IPC	Intermittent Positive Control
IPS	Instructions Per Second
IR	Infrared
JFK	Kennedy International Airport
LA	Los Angeles
LAT	Latitude
LAX	Los Angeles International Airport
LORAN	Long Range Navigation
LOS	Line-of-sight
LRR	Long Range Radar
MIPS	Million Instructions Per Second
MLS	Microwave Landing System
MODEM	Modulator-Demodulator
MSL	Mean Sea Level
MTBF	Mean Time Between Failures
NAFEC	National Aviation Facilities Experimental Center
NAD	North American Datum
NAS	National Airspace System
NASA	National Aeronautics and Space Administration
NAV	Navigation
NDB	Non-Directional Radio Beacon
NEF	Noise Exposure Factor
NFCC	National Flow Control Center

GLOSSARY (continued)

NMAC	Near Midair Collisions
NOTAM	Notice to Airmen
NOZ	Normal Operating Zone
NWS	National Weather Service
O&M	Operations and Maintenance
PCA	Positively Controlled Airspace
PIREPS	Pilot Reports
PN	Pseudo-Noise
PPM	Pulse Position Modulation
PWI	Pilot Warning Indicator
RAM	Random Access Memory
RCAG	Remote Control Air-to-Ground Facility (Present System)
RCAGT	Remote Communication Air-Ground Terminal
RCC	Regional Control Center
R&D	Research and Development
RDT&E	Research, Development, Test, and Evaluation
RF	Radio Frequency
RNAV	Area Navigation
ROM	Read-Only Memory
SAATMS	Satellite-Based Advanced Air Traffic Management System
SAMUS	State Space Analysis of Multisensor System
SID	Standard Instrument Departure
S/N	Signal-to-Noise
SNC	Surveillance, Navigation, Communication
STAR	Standard Arrival Routes
STC	Satellite Tracking Center
STOL	Short Takeoff and Landing

GLOSSARY (continued)

TACAN	Tactical Air Navigation
T&E	Test and Evaluation
TCA	Terminal Controlled Airspace
TOA	Time of Arrival
TRACAB	Terminal Radar Approach/Tower Cab
TRACON	Terminal Radar Approach Control
TRSA	Terminal Radar Service Areas
TRW	Thompson Ramo Wooldridge
TSC	Transportation Systems Center
TX	Texas
VFR	Visual Flight Rules
VHF	Very High Frequency
VMC	Visual Meteorological Conditions
VOR	Very High Frequency Omni-Directional Range
VORTAC	Very High Frequency Omni-Range TACAN
VVOR	Virtual VOR
2D	Two Dimensional
3D	Three Dimensional
4D	Four Dimensional

1. INTRODUCTION

The prime objective of any system design is the achievement of specific performance goals. To be sure that the desired performance levels are met, the system must be evaluated under varying operating conditions using well defined performance criteria or measures. The primary performance measures of an Air Traffic Management System must reflect the capacity, safety, and delay performance of the system. To insure that the performance measures selected to evaluate the system truly reflect the capabilities of the system, these measures must be related to the system characteristics or parameters which affect performance.

There are two categories of parameters which impact the performance of an Air Traffic Management System. The first category concerns those parameters involved in the services provided by the system, the functions performed by the system, and the manner in which these functions are performed. The definition of the performance measures used to evaluate the capacity, safety, and delay performance of the SAATMS are presented in Section 2, System Functional Relationships. Those subsystem and system parameters which influence the functioning of the SAATMS are also presented. The information used by the system to provide services to its users, the characteristics of that information, and the parameters of the system operation which impact SAATMS performance are discussed. Finally, Section 2 presents the functional relationships between the system performance measures and the system and subsystem parameters.

The second category of parameters deals with those parameters which constrain or limit system performance. Section 3, Scenarios, presents data concerning the demand imposed on the SAATMS during the 1995 and post-1995 time period. The characteristics of the user aircraft comprising the demand are discussed. Section 3 also presents a discussion of the terminal facilities available to service the demand and describes the scenarios used in the evaluation of the SAATMS.

The functional relationships involving the system performance measures and the parameters affecting system performance must be developed to obtain a quantitative evaluation of the system capabilities. Digital computer models were used to represent the functional relationships presented in Section 2, and the system constraints and scenarios discussed in Section 3. Analytical expressions involving the system and subsystem parameters were used as models for preliminary estimates of performance. Due to the complexity of an Air Traffic Management System, it is not possible to develop analytical expressions for the entire system and its operation. A digital simulation model was developed to simulate the operation of the SAATMS. Section 4, Performance Models Description describes the analytical expressions and the digital simulation used to evaluate the performance of the SAATMS.

The results of the performance evaluation of SAATMS are presented in Section 5, System Performance. This section presents the capacity, safety, and delay performance of SAATMS for terminal area operations in the Los Angeles region. The SAATMS safety and delay specifications (Ref. 1) were used to

establish the system parameters. The capacity of each of the 43 airports in the Los Angeles area was then evaluated and compared to the demand projected for the 1995 and post-1995 time frames.

The terminal area safety analysis indicates that in-trail separation of aircraft can be reduced to 2 nmi and still provide the same safety as today's system. This safety analysis did not consider the effect of wake turbulence since the purpose was to determine the maximum capacity of the system. Separation of aircraft on parallel approaches can be reduced to 2000 ft and maintain the same level of safety provided by the present system. The capacity of the major aircarrier airports in the Los Angeles region was shown to exceed the post-1995 demand while meeting the safety and delay specification. The capacity of the secondary and feeder airports was shown to exceed the highest projected 1995 demand level. The number of runways at the secondary and feeder airports must be increased to meet the post-1995 demand projection. Section 5 also presents an evaluation of the system safety for enroute operations. It presents a comparison of the enroute safety performance of the SAATMS, the GAATMS, and the present system.

It is important to determine that the system meets the performance specification; it is also important to establish the efficiency of the system to insure that the desired performance is achieved with minimum cost. Trade-off comparison data must be developed to aid in the proper selection of system and subsystem parameter values. Section 6, Sensitivity Data, presents data showing the sensitivity of the system performance measures to important system and subsystem parameters. This section also presents sensitivity data at the subsystem level.

The data presented in this section describe the methodology used in the evaluation of the SAATMS and the results of that evaluation. The performance data and the sensitivity data can be used in the comparison of alternate systems.

The appendices present the complete set of data used as the basis for the airport capacity and enroute safety curves presented in the system performance section.

2. SYSTEM FUNCTIONAL RELATIONSHIPS

The evaluation of the performance of a system requires detailed knowledge of the manner in which the system functions, the constraints imposed on the system, and the parameters which most greatly influence system performance. A functional analysis of SAATMS identified the subsystem and system parameters which are most important in the performance of the functions required to provide the Air Traffic Management services for the user aircraft. SAATMS receives data from the surveillance and navigation subsystems, processes these data to determine information on individual aircraft, makes decisions concerning the status of each aircraft and the functions to be performed to service each aircraft, and takes action to provide these services. The parameters associated with the subsystem data, the processing of these data, and the decisions and actions of the system will influence its performance. The most important measures of performance of an Air Traffic Management System are the capacity of the system, the safety which is afforded to the system user, and the delay to which the user is subjected. The functional analysis was used to show the relationship between subsystem and system parameters involved in performing the system functions and the system performance measures. This section defines the system performance measures used in the study and discusses the important system and subsystem parameters.

2.1 Definition of the Performance Measures Used to Evaluate the SAATMS

The three primary measures of an Air Traffic Management System performance are capacity, safety, and delay. No single definition of these measures can be developed to provide all the information desired due to the complexity of an Air Traffic Management System. The measures defined provide the basic information concerning system performance and will provide data for comparison of alternate systems.

2.1.1 Capacity and Delay

No definition of Air Traffic Management System capacity is complete without specification of the delay imposed on the users by the system. Capacity is a measure of the quantity of aircraft the system can service, while delay is a measure of the quality of the service provided by the system. Two elements of a system which service the same number of aircraft in a given time, one of which imposes no delay while the other forces the aircraft to wait before receiving service, are not equal. Two measures of the ability of a system to service aircraft have been selected to evaluate the SAATMS. The first is the number of aircraft that can be serviced in a unit time under the conditions that the delay experienced by each aircraft be less than a specified value. This measure is called the capacity efficiency. The second is the number of aircraft which can be serviced per unit time when there are always aircraft waiting for service. Under these conditions, the

element of the system providing services is saturated. The number of aircraft that the element can service in a unit time under the assumption of saturation is called the saturation capacity and is the upper bound for that element. The saturation capacity is a special case of capacity efficiency. Both of these measures will be used to compare the capabilities of the system elements. These measures will be primarily applied to runways and airports.

2.1.2 Demand Related to Capacity and Delay

Any aircraft desiring to use an air traffic facility imposes a demand on that facility. A demand may be a request for a runway for arrival or departure, a request for entry into a specific airspace, or a request for aid in determining an aircraft's position. The total demand on a facility is the sum of all these single demands. The demand on any facility is a function of time, the traffic density, and the types or classes of aircraft desiring service. If the facility cannot satisfy the demand at the time it occurs, delays will be imposed on the users of the facility and the performance of that facility will be degraded. If the demand on a facility is so large and so persistent as to continuously exceed the ability of the facility to satisfy that demand, the facility is operating under conditions of saturation. The rate at which aircraft are passed through the facility (i.e., the throughput rate) under these conditions is called the saturation capacity.

An example of the saturation capacity of a facility and its relationship to demand and the facility service time is presented in Fig. 2.1-1. Figure 2.1-1a illustrates a specific form of demand assumed for a facility. Since the demand on the facility consists of discrete events, they are represented by a sequence of impulse functions. The time between the individual demands may assume any distribution, such as Poisson or Erlang, depending on the airspace configuration and the functioning of the system. The sequence of negative impulses in Fig. 2.1-1a represents the time at which the individual demands are serviced. For simplicity, the time required to service a demand has been assumed constant. The accumulated demand and throughput resulting from the distribution of demand and service time is shown in Fig. 2.1-1b. At any instant of time, the length of the queue waiting to be serviced is the vertical difference between the accumulated demand and throughput curves. The horizontal difference between the two curves is the delay associated with an individual aircraft. The delay imposed on the individual aircraft has been plotted on the left side of Fig. 2.1-1b. These data can be used to obtain the total and average delay under these conditions. At a specific time, t_1, the slope of the line connecting the origin to the accumulated demand curve yields the average demand during the interval $(0, t_1)$. The slope of the straight line connecting the origin to the accumulated throughput curve at t_1 will indicate the average throughput during the same interval. The times during which the facility is not servicing aircraft are shown as idle times. The graphs of Fig. 2.1-1c depict a condition when the demand is large, resulting in facility saturation. Under this condition, the slope of the accumulated demand curve is the average demand and the slope of the accumulated throughput curve is the saturation capacity.

a. Demand

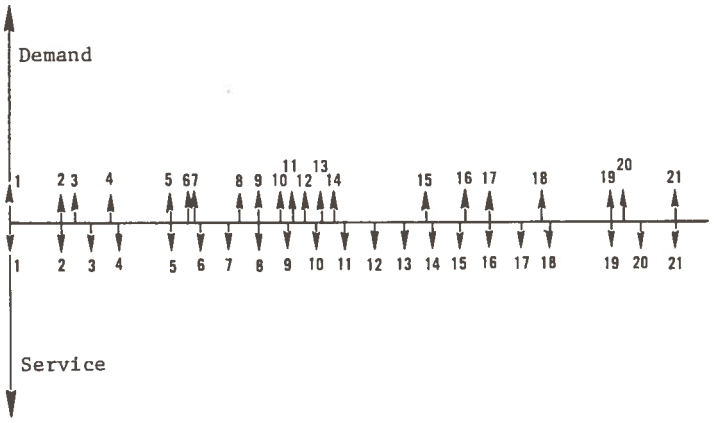

b. Accumulated Demand

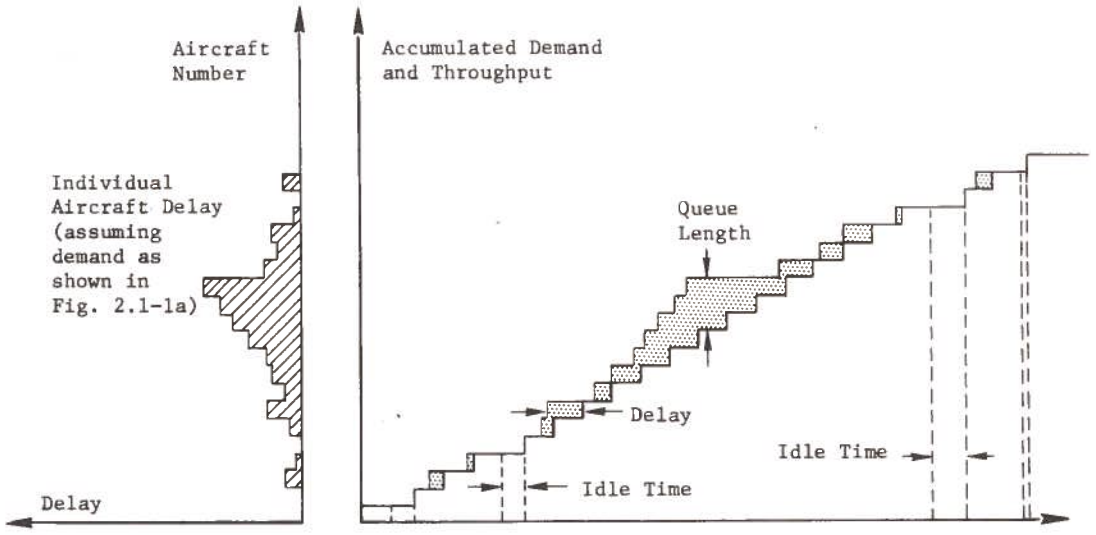

Figure 2.1-1. Capacity and Demand Relationships

c. Facility Saturation

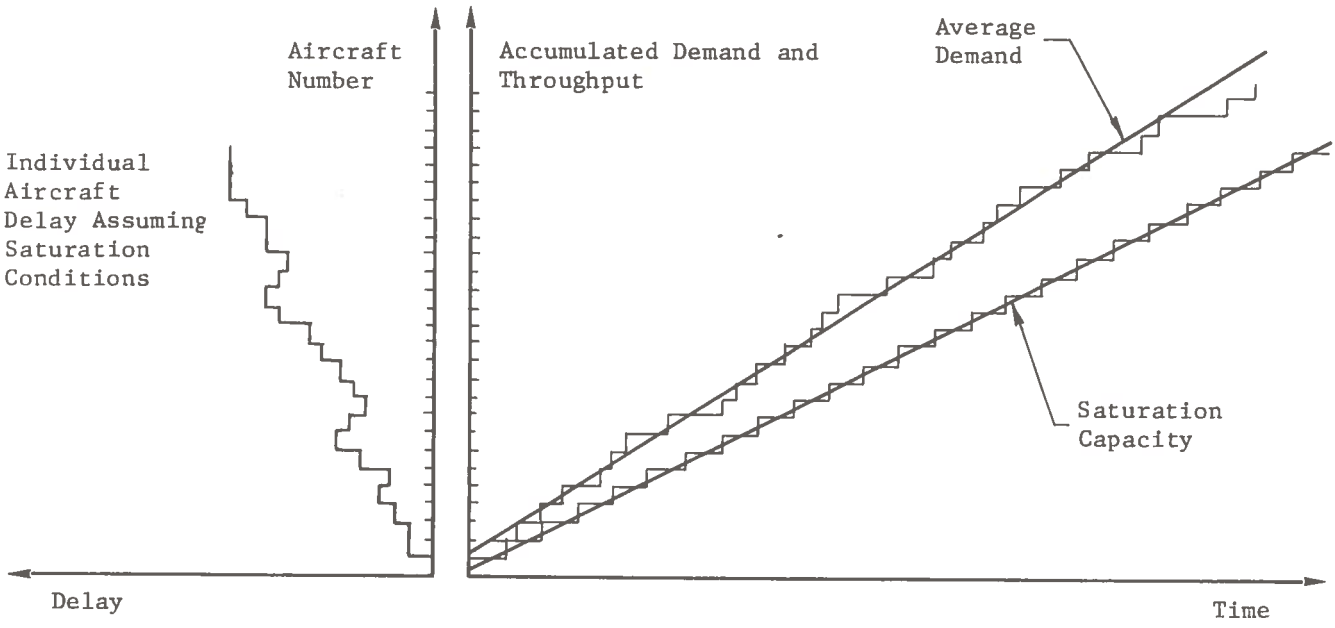

Figure 2.1-1. (continued)

A valid comparison of the saturation capacity and capacity efficiency of two facilities, such as airports, is only possible under the same demand conditions. The description of the demand must include the specification of:

(1) Level (magnitude of the demand rate)

(2) Mix (sequence and performance class of aircraft)

(3) Temporal Distribution (statistics of the time interval between aircraft demanding service)

The manner in which saturation capacity and capacity efficiency are affected by the demand is shown in Fig. 2.1-2 and 2.1-3. The graphs depict the average delay imposed on the aircraft demanding service as a function of the demand level. The curves of Fig. 2.1-2 illustrate capacity measures for two different aircraft mixes. One mix includes both general aviation aircraft and aircarrier aircraft (Mix A), while the other mix consists solely of aircarrier aircraft (Mix B). The time distribution is assumed identical for both demands. The saturation capacity for Mix B is greater primarily because of the uniformity of speed for the aircarrier aircraft; Mix A includes slower GA aircraft and the faster aircarriers. The curve also shows that the capacity efficienty for a constant average delay, D_1, is affected by the demand mix. Figure 2.1-3 depicts the average delay versus demand level for three different demands. The demand level and the mix of aircraft were held constant for the three demand conditions. Curve 1 depicts the average delay curve for a demand with a Poisson distribution of aircraft interarrival times, while the demand resulting in Curve 2 was assumed to have an Erlang distribution. Curve 3 illustrates the average delay resulting from periodic aircraft arrival with a Gaussian distribution about the arrival time. These curves illustrate the effect of aircraft arrival time distributions on the capacity efficiency of a facility. For a given average delay, D_2, the capacity efficiency of a facility is enhanced with a more uniform time between aircraft demand for services. Since any average delay value can be obtained by a large variety of individual aircraft delays, a more precise control of delay can be obtained by specifying the desired delay distribution. Figure 2.1-4 illustrates typical delay distribution functions for four different demand levels. The mix and arrival time distribution were assumed constant for the curves shown. The curves depict the capacity efficiency of a facility for the specification that 90 percent of the aircraft will be delayed less than 4 min. In this case, the capacity efficiency is approximately 145 operations per hour.

2.1.3 Safety

The degree of safety that an Air Traffic Management System provides its user aircraft is related to the physical separation between aircraft or between an aircraft and obstructions such as buildings or terrain. If a system could absolutely guarantee that it would maintain a separation distance between aircraft, no matter how small, the aircraft would be completely safe. The ability of a system to keep aircraft separated is affected by the following:

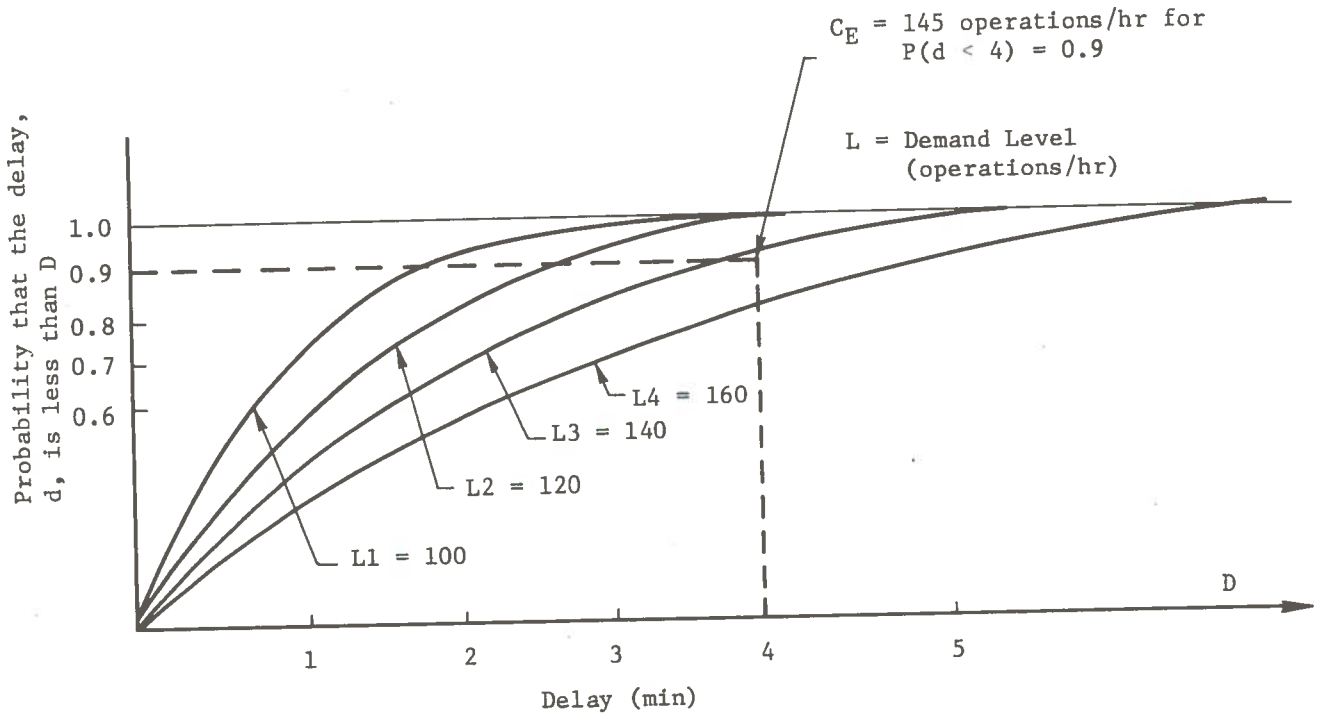

Figure 2.1-4. Probability Distribution Function Used to Define Capacity Efficiency for a Given System

(1) Errors in the surveillance and navigation data

(2) The response time of the system

(3) The aircraft and its pilot

(4) The proficiency of the system operating personnel

If bounds could be precisely determined on all the parameters affecting aircraft separation, a minimum separation distance could be computed and maintained, and no collisions would ever occur between aircraft. Precise specification of all the critical parameters, however, is not possible. One solution to providing safety would be to separate aircraft at extremely large distances to achieve a desired level of safety. The result of this, however, would be an unacceptable decrease in the capacity of the system. The alternative is to develop estimates of the system errors affecting the separation distance and to maintain aircraft far enough apart to provide an acceptable level of safety without degrading capacity to an unacceptable level. This second technique has been utilized in the development of the SAATMS.

Two measures of SAATMS safety performance have been developed. The first defines safety in terms of the blunder protection afforded to each individual aircraft and is independent of the number of aircraft using the system. The second measure determines the expected number of conflicts (collisions between aircraft) per unit time and considers all aircraft using the system. It is a measure of the total system safety rather than individual aircraft safety.

2.1.3.1 Blunder Protection

An aircraft is said to have blundered when it suddenly attains an acceleration toward another aircraft. The system can maintain a minimum separation between aircraft as long as that blunder acceleration is less than a specified value and as long as the system has detected the deviation of the blundering aircraft from its designated flight profile. The safety of individual aircraft is defined in terms of the magnitude of the blunder acceleration for which the system will provide protection and the confidence level with which the system detects the deviation of the blundering aircraft from its intended profile.

As an example, consider the two aircraft, α_1 and α_2, flying along a straight path as shown in Fig. 2.1-5. The aircraft will wander about their respective nominal flight paths due to navigation and pilot errors. If these deviations were large enough, as depicted, the aircraft could collide. The deviation of α_1 from its path would normally be detected by the SAATMS surveillance equipment, and a command would be transmitted directing the aircraft back toward its assigned path. Small deviations from the path are normally corrected by the pilot without intervention from the system. A threshold must be established to determine when the system is required to intervene. Only if an aircraft exceeds that threshold will a command be transmitted to that aircraft. The threshold defines the Normal Operating Zone (NOZ) for the aircraft and is illustrated in the figure. Under normal conditions, the aircraft would remain within its NOZ. Under a blunder

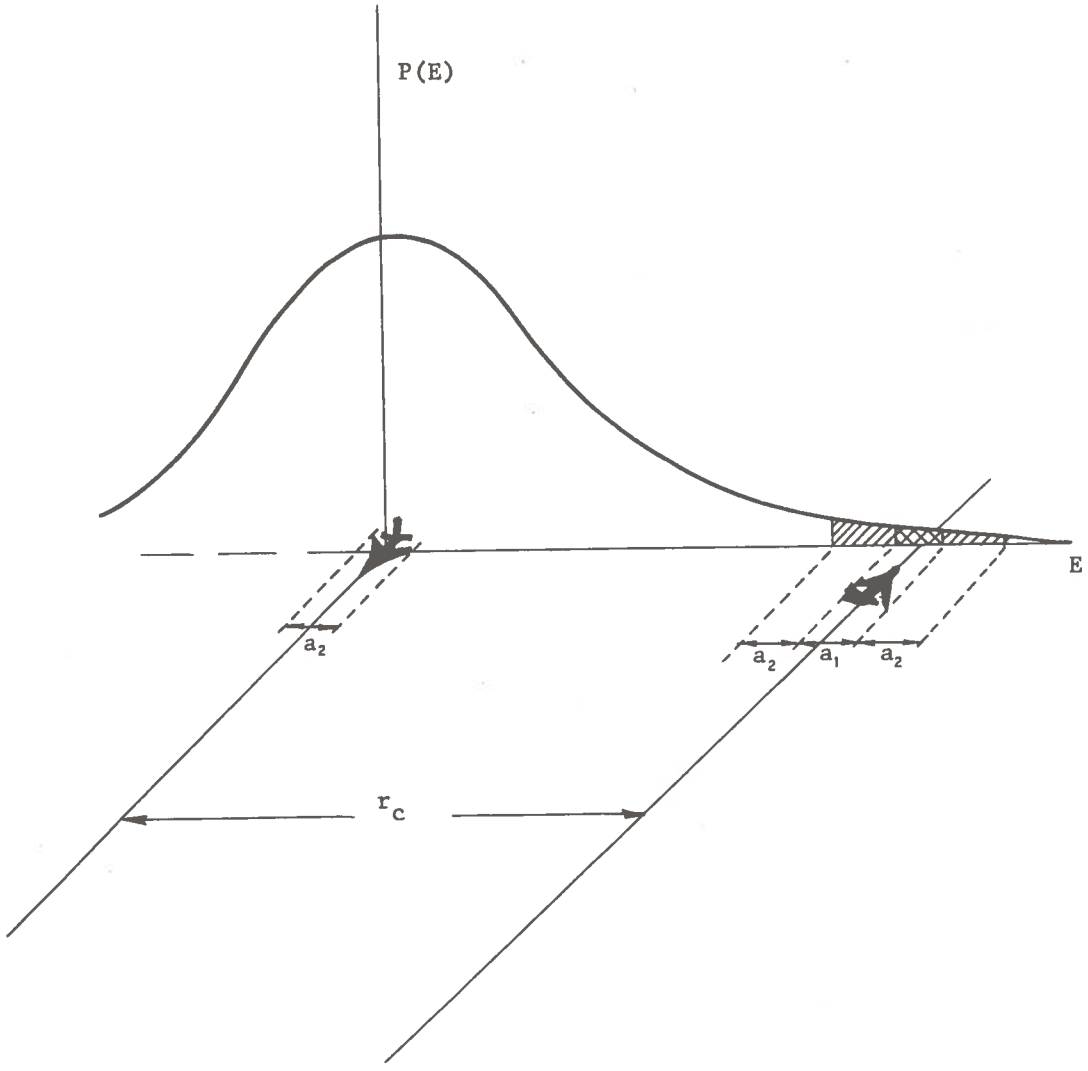

Figure 2.1-6. Crossing Conflict Situation

random variable, which can be described by a probability density function as shown. The conflict measure, for the situation depicted, is equal to the shaded area under the probability density function, P(E). The area represents the likelihood the conflict volumes of the two aircraft will overlap considering all of the parameters which determine the probability density function, P(E). If $N_{C_{ij}}$ is the value associated with the likelihood of conflict volume overlap, it represents the "number of conflicts" which take place as the result of aircraft i crossing aircraft j. If similar values were derived for all crossing aircraft in the system over a given period of time, the total number of conflicts would be given by

$$N_C = \sum_{ij} N_{C_{ij}} \tag{2}$$

Aircraft conflicts arise as a result of aircraft passing and aircraft following each other. They also occur because of the more random flights of GA aircraft without a specified flight profile; however, the measure for these aircraft is determined using a modified version of the equations used to determine the number of conflicts for all other situations. A more detailed discussion of the determination of the number of conflicts is presented in Section 4, which deals with the system evaluation models.

2.2 System and Subsystem Parameters

An evaluation of the performance of an Air Traffic Management System involves a large number of parameters with both complex inter-relationships and relationships to the system performance measures. A functional analysis was conducted to determine those parameters which most greatly impacted the performance of the SAATMS. The values for those critical parameters were established from analyses of the system and subsystem mechanizations of the SAATMS.

2.2.1 Subsystem Parameters

The two subsystems which are most critical to SAATMS safety, capacity, and delay performance are the surveillance and navigation subsystems. The navigation subsystem provides position and velocity information to the user aircraft, while the surveillance subsystem provides position and velocity data to the system for use in the control of aircraft.

The navigation mode parameters which are critical to system performance are

(1) σ_n, the standard deviation of the navigation position errors

(2) $\sigma_n^{\cdot}$, the standard deviation of the navigation velocity errors

(3) τ_n, navigation update interval

In general, the more accurate the navigation position and velocity, the greater the ability of the user aircraft to adhere to a specific flight profile. With more accurate data, the aircraft can be spaced more closely together to achieve a greater capacity at the same safety level. Increasing the rate at which navigation data are received by the aircraft will generally increase the navigation and guidance capability of the aircraft and will enhance the system capacity.

The surveillance mode parameters are similar to the navigation parameters as follows:

(1) σ_s, the standard deviation of the surveillance position error

(2) $\sigma_{\dot{s}}$, standard deviation of the surveillance velocity error

(3) τ_s, surveillance update inverval

The smaller the variance of the surveillance position and velocity errors and the shorter the time between successive surveillance samples, the more accurately the system can determine that an aircraft has deviated from its planned flight profile. The more accurate the surveillance data, the greater the ability of the system to determine potential conflicts or collisions between aircraft.

Both the navigation and surveillance mode parameters affect the system performance in a critical manner. The effects of variation of these parameters on the system performance are discussed in Section 6, which deals with the sensitivity of SAATMS performance.

Two other subsystems which affect the operation of SAATMS are the communications and control processing subsystems. These subsystem parameters are highly sensitive to specific mechanizations. The characteristics of these subsystems have been incorporated into the system parameters since the ultimate mechanization of the communication and data processing will be influenced greatly by the cost effectiveness trade-off studies.

The analysis of SAATMS performance assumed that the data processing and communications subsystems design would provide adequate capacity to handle the load, based on preliminary design analysis using estimates of the communications and data processing loads. It is also assumed that the reliability of all subsystems must be high in order to permit automation of the system processes and functions.

2.2.2 System Parameters

SAATMS utilizes surveillance data as the basis for the control of air traffic. The manner in which the data are utilized will affect the performance of the system. One of the primary system parameters that influences system operation

is the response time or time delay, τ_D. The time delay is the length of time from the reception of surveillance position and velocity data to the initiation of an aircraft maneuver in response to an issued command. The activities performed by the system during the time delay include the following:

(1) Reception of the position and velocity data

(2) Determination of a situation requiring the issuance of a command

(3) Formulation of the command

(4) Transmission of the command

(5) Reception of the command by the affected aircraft

(6) Response of the pilot to the command

(7) Response of the aircraft to the pilot

The length of time required for each of these activities is important; however, the most critical parameter is the overall time.

A second critical parameter involved in the performance of the system is the minimum separation maintained between aircraft. This distance, Q, will affect both system safety and capacity. If the separation distance is large, the capacity will be decreased since fewer aircraft will be allowed to occupy a given airspace. The safety may also be affected depending upon the surveillance and navigation errors, the system time delay, and the blunder protection level.

The rate of interventions or commands, $\dot{N}_I$, the system is required to issue to control aircraft will also affect system performance and the design of the communications equipment. If the system is capable of intervening at a high rate, aircraft can be separated by smaller distances to achieve a higher capacity while maintaining the same level of safety.

There are a large number of other parameters which will impact the performance of the SAATMS. The parameters which have been discussed are those that affect the performance of the system to a greater degree than others.

2.3 Parameter Relationships

This section presents the functional relationships between the system and subsystem parameters. The manner in which system performance measures are affected by these parameters is presented, and the types of models required to represent the inter-relationships between system performance and the system and subsystem parameters are identified.

2.3.1 Capacity and Delay

In its simplist form, capacity of a facility, route, or region of airspace is a function of aircraft separation and velocity. For aircraft with the same velocity, following in trail, the capacity of a route is given by

$$C = \frac{V}{Q}$$

where

V = Aircraft velocity

Q = Aircraft separation

More complicated expressions can be developed to represent aircraft with differing velocities and different separation distances. These expressions are discussed in Section 4.

The capacity efficiency, C_E, is a function of aircraft delay and aircraft separation, thus

$$C_E = f(Q, D)$$

where D = delay. A simulation analysis has been used to relate the capacity efficiency to delay and separation distance. Figure 2.3-1 illustrates this functional relationship where $\overline{D}$ is the average aircraft delay under steady-state conditions. The curves of Fig. 2.3-1 are for a specific scenario (final approach to a single runway) and a specific demand (aircraft mix, performance class, and inter-arrival times distribution). The saturation capacity of the runway corresponds to that value of C_E for which $\overline{D}$ is infinite.

If delay statistics other than average delay are desired, probability distribution functions such as those in Fig. 2.3-2 can be obtained. These curves yield the probability that the aircraft delay is less than a specified value. Each point on the curves of Fig. 2.3-1 is represented by an entire curve in Fig. 2.3-2.

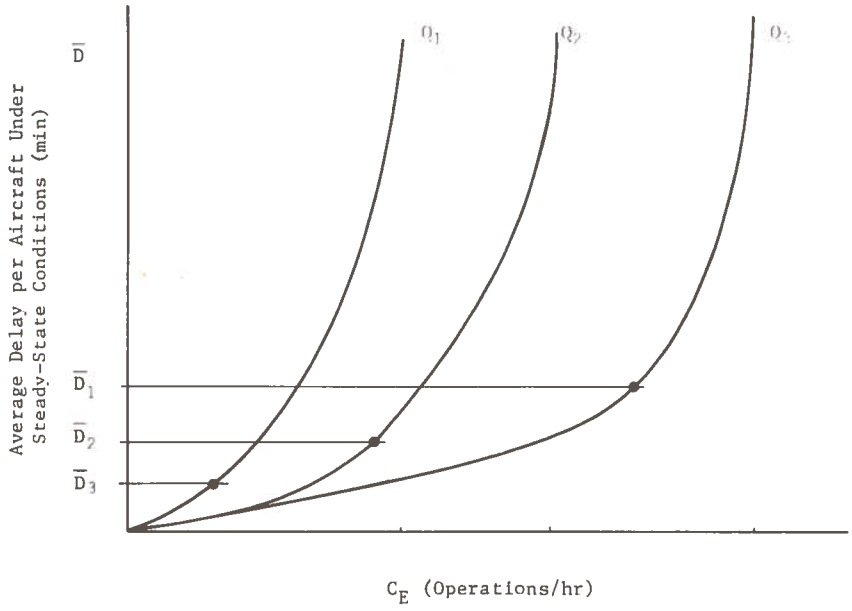

Figure 2.3-1. Capacity Efficiency as a Function of Average Delay and Separation

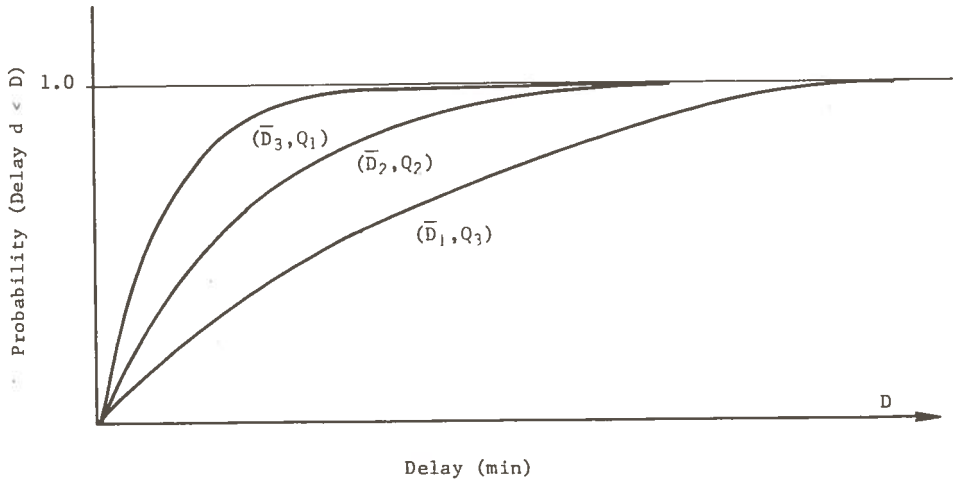

Figure 2.3-2. Delay Probability Distribution Functions

The complexity of the relationships necessitates the use of digital simulation models to obtain the values of capacity and capacity efficiency associated with specific elements of an Air Traffic Management System.

2.3.2 Safety

The safety of individual aircraft or the safety of the total system is primarily related to aircraft separation. Several factors are involved in the determination of the distances by which aircraft must be separated to provide an acceptable level of safety without compromising capacity to an unacceptable degree. Figure 2.3-3 illustrates two aircraft in trail on a common route. The separation standard, Q_S, is defined as the minimum distance between aircraft necessary to satisfy a specific safety criterion. Q_S is the sum of several smaller distances. W_N denotes the width of the aircraft's Normal Operating Zone (NOZ). Aircraft operate within the NOZ without intervention from the system. W_B denotes the width of the Buffer Zone (BZ) which provides a protection against aircraft which blunder outside their NOZ. W_M is the allowable miss distance between aircraft assuming both are at the outer limit of their respective buffer zones. The separation standard, Q_S, is given by

$$Q_S = \frac{W_{NF}}{2} + W_{BF} + W_{BL} + \frac{W_{NL}}{2} + W_{T_{LF}} + W_M$$

$$= W_N + W_B + W_{T_{LF}} + W_M \qquad (1)$$

for $W_{NF} = W_{NL} = W_N$ and $W_B = W_{BF} + W_{BL}$

where

W_{NF} = Width of the NOZ for the following aircraft

W_{NL} = Width of the NOZ for the leading aircraft

W_{BF} = Width of the buffer zone for the following aircraft

W_{BL} = Width of the buffer zone for the leading aircraft

$W_{T_{LF}}$ = Wake turbulence danger distance (function of the leading and following aircraft)

W_M = Aircraft miss distance for both aircraft experiencing maximum protected blunders

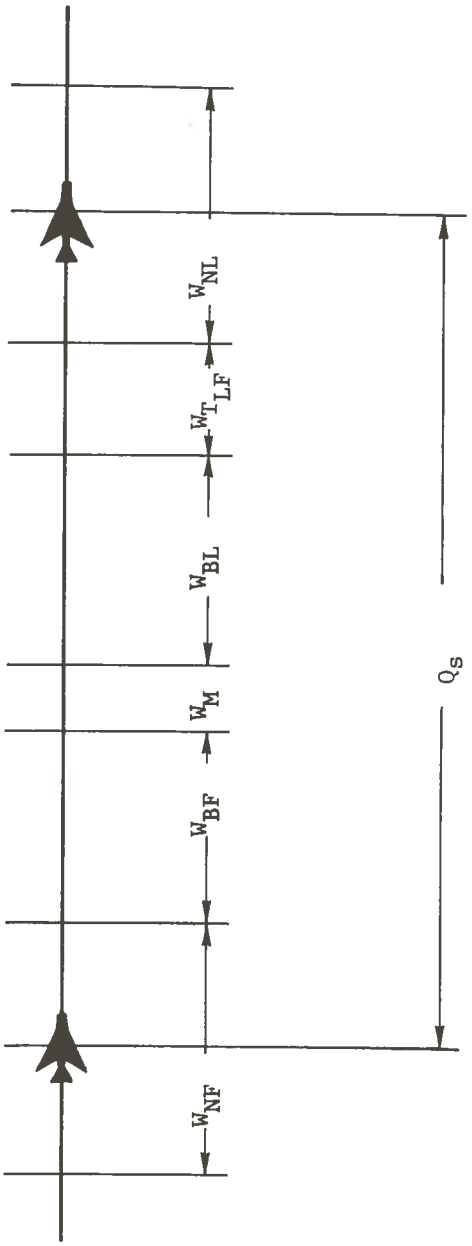

Figure 2.3-3. Separation Standard Distances

For aircraft flying parallel, merging, or crossing routes, Q_S has the same form. The terms comprising Q_S may have different values depending on the geometry, (i.e., $W_{T_{LF}} = 0$ for aircraft on parallel tracks).

The width of the Buffer Zone, W_B, is a measure of system safety and is proportional to the amount of blunder protection provided. Aircraft blunder is measured in terms of aircraft acceleration, A_B, as it crosses the NOZ boundary. Figure 2.3-4 illustrates the relationship between the Buffer Zone and the blunder acceleration, A_B. W_B is also a function of P_B, the probability of not recognizing that an aircraft has blundered across the NOZ threshold in time to prevent the aircraft from crossing the Buffer Zone given that

(1) The aircraft has an acceleration A_B when it crosses the NOZ boundary.

(2) The last surveillance sample showed that the aircraft was just inside the NOZ.

P_B is a function of the surveillance errors (σ_S and $\sigma_S^{\bullet}$) and the surveillance update interval, τ_S. The system time delays, τ_D, and the aircraft return acceleration, A_R, will also affect W_B. Each curve of Fig. 2.3-4 corresponds to specific values of P_B, σ_S, $\sigma_S^{\bullet}$, τ_S, τ_D, and A_R. This is illustrated in the figure by the vector quantity $\bar{\beta}$ which has these parameters as vector components. More details on this relationship, including the equations relating the various parameters are given in Section 3.1.

The width of the Normal Operating Zone, W_N, is a function of several parameters. These include (1) the navigation errors (σ_n, $\sigma_n^{\bullet}$), (2) navigation update interval (τ_n), (3) surveillance errors (σ_S, $\sigma_S^{\bullet}$), (4) surveillance update rate (τ_S), (5) aircraft performance characteristics (including that of the pilot, P), and (6) the system intervention rate ($\dot{\bar{N}}_I$). These relationships are illustrated in Fig. 2.3-5 by the vector quantity $\bar{\rho}$ which has these parameters as vector components. The intervention rate is the number of times the ATC system must intervene in an aircraft's operation in a given time period. An intervention occurs whenever the ATC system determines an aircraft is outside its NOZ. It consists of an acceleration command selected to return the aircraft to the NOZ.

The relationships represented in Fig. 2.3-1 through 2.3-5 provide the means for determining system performance, given specification of the system and subsystem parameters. For example, suppose the problem is to determine the capacity efficiency for an airport for a specified demand type where the average steady-state aircraft delay is to be $\bar{D}$, the safety S_B, and the intervention rate $\dot{N}_I$. The values of the surveillance and navigation parameters are σ_s, $\sigma_s^{\bullet}$, σ_n, $\sigma_n^{\bullet}$, the update rates τ_n and τ_S, and the system response time τ_D. The steps taken to determine C_E are

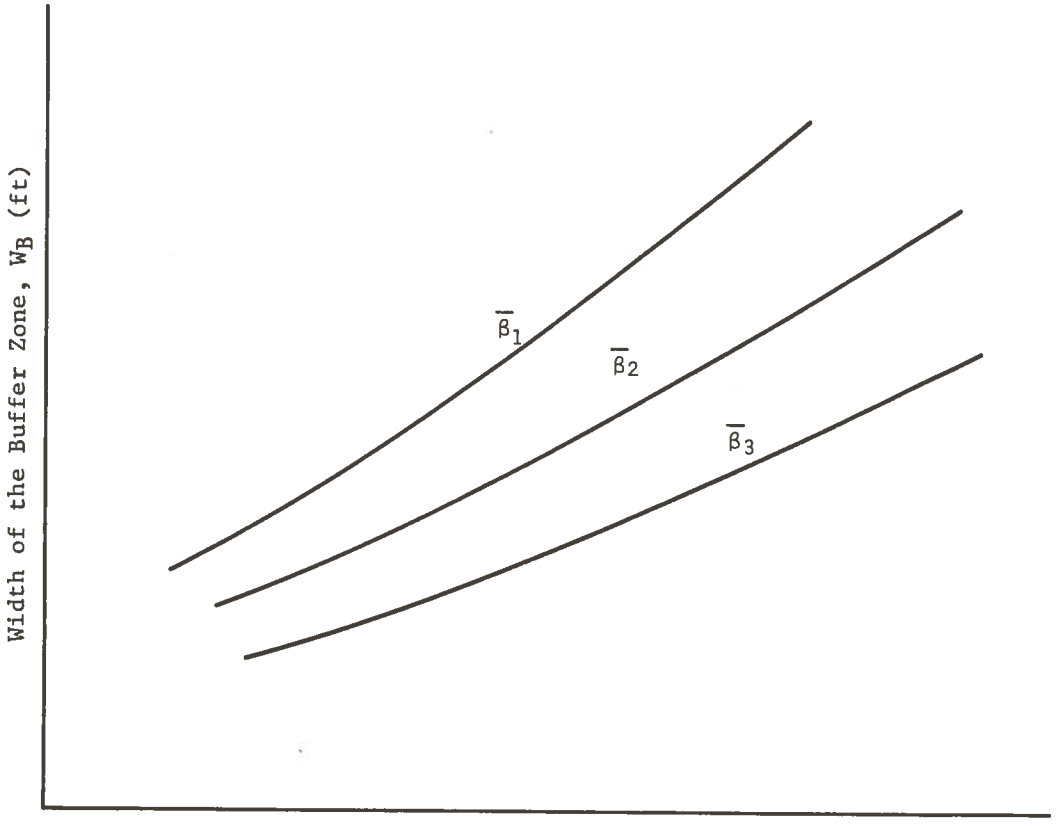

$$\bar{\beta} = \begin{bmatrix} P_B \\ \sigma_s \\ \sigma_{\dot{s}} \\ \tau_s \\ \tau_D \\ A_R \end{bmatrix}$$

where:

$W_B = f(A_B, \bar{\beta})$

$\bar{\beta} = [P_B, \sigma_s, \sigma_{\dot{s}}, \tau_s, \tau_D, A_R]$

P_B = Probability of not recognizing that an aircraft blundered across the NOZ threshold in time to prevent the aircraft from crossing the Buffer Zone

σ_s ($\sigma_{\dot{s}}$) = Standard deviation of position (velocity) surveillance error

τ_s = Surveillance update interval

τ_D = System time delay

A_R = Aircraft return acceleration

Figure 2.3-4. W_B, A_B, β Relationship

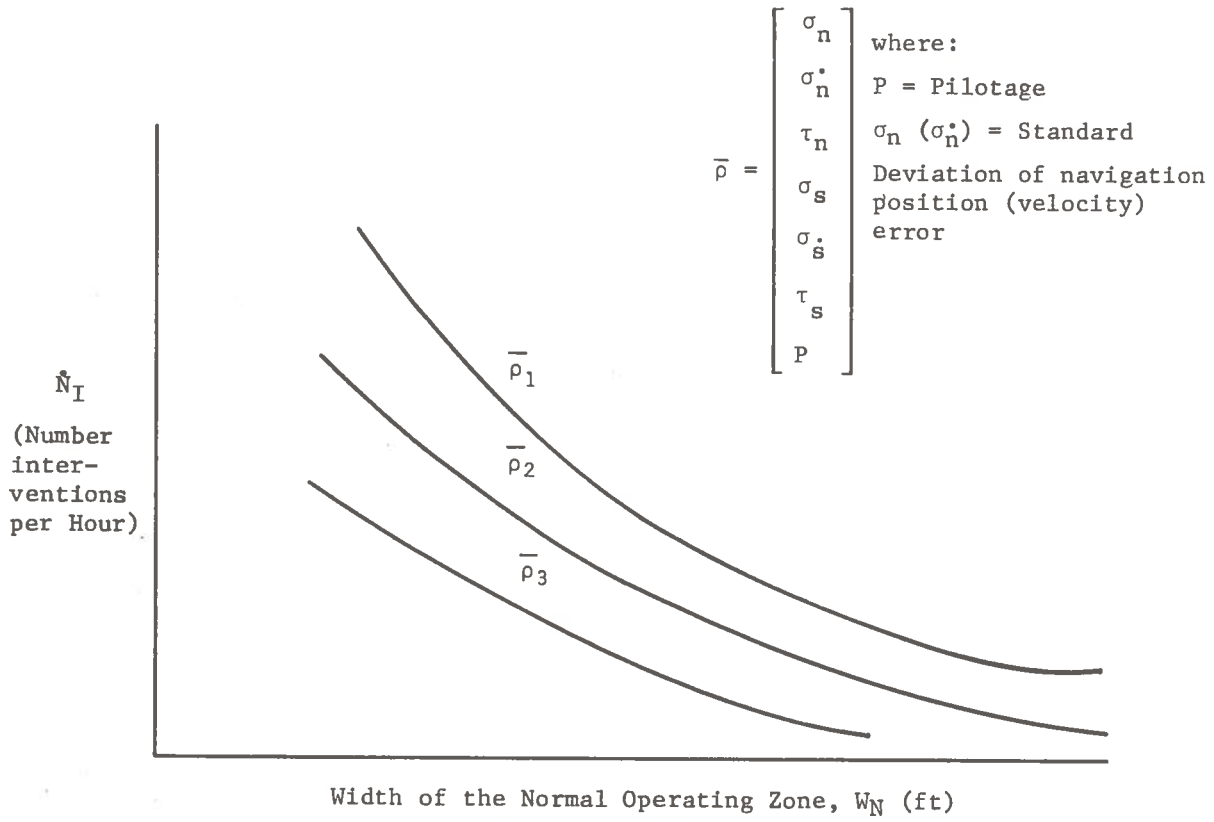

Figure 2.3-5. W_N versus $\dot{N}_I$ Relationship

1. Find W_N for $\dot{N}_I$, σ_n, $\sigma_{\dot{n}}$, τ_n, $\sigma_{\dot{s}}$, σ_s, τ_s, and P from the curves of Fig. 2.3-5.

2. Find W_B for given values of $S_B(P_B, A_B)$, σ_s, $\sigma_{\dot{s}}$, τ_s, τ_D, and a_R from Fig. 2.3-4.

3. Find Q_s for W_N of step 1, W_B of step 2, and specified wake turbulence (assumed given as part of demand data) from Eq. (1)

4. Find C_E for $\bar{D}$ and Q_s from Fig. 2.3-1.

If system safety is to be determined for a given capacity efficiency, a similar procedure would be followed.

It should be noted that specification of the subsystem parameters by themselves does not yield a unique set of system performance parameters. All three system measures (capacity, delay, safety) are inter-related and two must be specified to determine a unique value for the third.

3. SCENARIOS

A number of the parameters which affect system performance are not under the direct control of the system designers. These are the parameters involved with the air traffic demand imposed on the system, the user aircraft characteristics, the airport system, and the physical environment. The Air Traffic Management System can be designed to make optimum use of these factors, where possible, but these parameters do constrain or limit system performance. This section presents a discussion of these parameters.

3.1 Demand

Two different sets of demand data were supplied for the evaluation of AATMS performance. The enroute demand data were supplied by Autonetics and were based on the enroute data generated during the Fourth Generation Air Traffic Control System Concept Formulation Study (Ref. 3). The data provided included the Instantaneous Airborne Count (IAC) during a busy hour for four demand levels. The demand levels were based on the projected national airfleet size for year 1995 and beyond. Table 3.1-1 shows the airfleet size for each of the aircraft classes and demand levels.

Table 3.1-1. National Airfleet Size

Aircraft Classes	Demand Level 1	Demand Level 2	Demand Level 3	Demand Level 4
Aircarrier	5,000	7,000	9,500	14,000
General Aviation	250,000	335,000	500,000	1,000,000
Military	20,000	20,000	20,000	20,000

The enroute IAC's for the demand levels are as follows:

Demand Level 1	11,631
Demand Level 2	15,564
Demand Level 3	22,414
Demand Level 4	41,430

The enroute aircraft were assumed to fly on routes between pairs of cities throughout the Continental United States. The IAC on the city pair routes was used to determine the number of route crossings and aircraft passages. This was used to calculate the number of safety conflicts that would occur.

The second set of demand data concerned busy hour operations and the IAC for the terminal area. The terminal area data were developed by The Mitre Corporation and include the busy hour operations and the instantaneous airborne count for 48 airports in the Los Angeles region (Ref. 11). The IAC data included position, altitude, velocity, origin, and destination of 1840 aircraft projected as airborne during a peak busy hour in 1995 for Demand Level 2. Data for the other demand levels were estimated using a scale factor based on the National Airfleet size given in Table 3.1-1. The IAC's for all demand levels are as follows:

Demand Level 1	1383
Demand Level 2	1840
Demand Level 3	2725
Demand Level 4	5323

These demand data were used to determine the capacity and capacity efficiency of the airports in the Los Angeles region for the 1995 and post-1995 time frame.

3.2 Aircraft Characteristics

The capacity and capacity efficiency of an airport are related to the mix of aircraft comprising the demand. The characteristics of the aircraft will influence how well the system can meter the aircraft to obtain the desired capacity and capacity efficiency performance and will affect the ability of the system to maintain the proper spacing to achieve the desired level of safety. The airfleet is divided into three major classes of aircraft: aircarrier, general aviation, and military. These are separated into several types, each with its own specific performance characteristics. The primary parameters of aircraft performance that affect terminal area operations are the final approach and landing velocities, the takeoff velocities, the distance required for takeoff, and the acceleration and deceleration characteristics. This contrasts with the factors most important in enroute airspace which include cruise velocity, cruise altitude, and aircraft range.

Table 3.2-1 lists the 11 types of aircarrier jet aircraft postulated to be in use in the 1995 and beyond time frame and presents the characteristics assumed for the study. The GA aircraft were divided into three main categories: single engine piston, multi-engine piston and turbo prop, and turbo jet aircraft. Table 3.2-2 lists the pertinent characteristics of the GA aircraft.

TABLE 3.2-1. AIRCARRIER CHARACTERISTICS (FROM REF. 11)

Aircraft Type	SST	4-Engine Jumbo	4-Engine Stretch	3-Engine Jumbo	3-Engine Stretch	2-Engine Jumbo	2-Engine Stretch	2-Engine Standard	Air Taxi Jumbo	Air Taxi Stretch	Air Taxi Standard
Range (nmi)	2,000	2,000	2,000	800-1,500	800-1,500	200-800	200-800	200-800	200	200	200
Typical Speeds (knots)											
Takeoff	250	250	250	220	220	220	220	220	175	175	175
Cruise	813	523	523	496	496	489	489	489	311	311	311
Final Approach	165	165	165	150	150	150	150	150	135	135	135
Landing	150	150	150	135	135	135	135	135	120	120	120
Field Length (ft)											
Takeoff	10,000	10,000	10,000	7,500	7,500	7,500	7,500	7,500	4,500	4,500	4,500
Landing	7,500	7,500	7,500	5,500	5,500	5,500	5,500	5,500	2,000	2,000	2,000
Cruise Altitude (ft)	55,000	39,000	39,000	35,000	35,000	30,000	30,000	30,000	20,000	20,000	20,000
Acceleration/ Deceleration (fps^2)	10	10	10	10	10	10	10	10	10	10	10

Table 3.2-2. General Aviation Aircraft

Aircraft Type	Single Engine	Multi-Engine and Turbo Prop	Turbo Jet
Typical Speeds (knots)			
Takeoff	70	100	120
Cruise	150	225	450
Final Approach	75	90	105
Landing	60	75	90
Field Length (ft)			
Takeoff	1,400	1,700	5,000
Landing	850	1,000	1,200
Cruise Altitude (ft)	12,000	20,000	35,000
Acceleration/Deceleration (fps^2)	6/6	8/6	10/6

These values of the aircraft characteristics were used to establish the runway occupancy times for takeoff and landings. The runway occupancy times for landing were determined for two classes of exits, low speed (12 knots) and moderate speed (30 knots). The aircraft listed in Tables 3.2-1 and 3.2-2 were grouped into classes based on similar landing and takeoff speeds. The GA aircraft are listed as Classes A, B, and C, corresponding to the single engine, multi-engine/turbo prop, and turbo jet aircraft types in Table 3.2-2, respectively. The short-haul aircraft form Class D. The two- and three-engine aircarriers comprise Class E, while the aircarrier SST and four-engine aircraft were combined to form Class F. The values of runway occupancy time for these six classes are shown in Table 3.2-3. Runway occupancy time for landings were determined from

$$R_{OTL} = \frac{V_L - V_E}{A} + T_B$$

where

V_L = Landing velocity (ft/sec)

V_E = Runway exit velocity (ft/sec)

A = Deceleration (ft/sec^2)

T_B = Buffer time (sec)

Table 3.2-3. Aircraft Classes by Speed

Aircraft		Speed (knots)		Runway Occupancy Times (sec)	
Class	Type	Final Approach	Landing	Landing for Exit Speed of 50 fps*	Takeoff
A	Single Engine, GA	75	60	14	21
B	Multi-Engine and Turbo Prop, GA	90	75	19	23
C	Jet, GA	105	90	23	32
D	Ultra Short-Haul, Aircarrier	135	120	21	30
E	Light Weight, Aircarrier	150	135	24	38
F	Heavy Weight, Aircarrier	165	150	26	45

*Landing times for exit speed of 20 fps are 23 and 28 for Classes A and B, respectively.

It is assumed that a continuous exit is available. The buffer time, T_B, was assumed to be 6 sec for exit velocity of 50 ft/sec and 10 sec for exit velocity of 30 ft/sec. The buffer time accounts for possible deviations in pilotage and other factors which may cause an aircraft to remain on the runway longer than the nominal time required for deceleration.

Runway occupancy time for takeoff is determined by the larger of two parameters, namely, T_L and T_A, given by

$$T_L = (2 \frac{D_T}{A_T})^{\frac{1}{2}}$$

and

$$T_A = \frac{V_T}{A_T}$$

where

V_T = Takeoff velocity (ft/sec)

D_T = Takeoff distance (ft)

A_T = Takeoff acceleration (ft/sec^2)

T_L, T_A = Takeoff time (sec)

The larger of the two takeoff times is used to ensure that the proper velocity is achieved prior to liftoff.

3.3 Airports

The Los Angeles region was chosen as the site for the evaluation of the SAATMS terminal area performance. The 48 airports (43 civil airports and 5 military) were structured to represent their 1995 configurations. The airports were divided into eight categories based on the types of air traffic which they would service, their present configuration, and a reasonable expansion of the present facilities. The airport classifications and configurations used in this study are shown in Fig. 3.3-1. A list of the airports in the Los Angeles region and the airport classification is shown in Table 3.3-1.

One of the primary constraints in the development of the airspace structure is the geographic location and the classification of the airports. The airspace structure of the SAATMS was configured to minimize the amount of airspace required for controlled operations into the primary airports (Classes 7 and 8).

Airport System Classification	Primary 8	Primary 7	Secondary 6	Secondary 5	Feeder 4	Feeder 3	Feeder 2	Feeder 1
Airport Layout		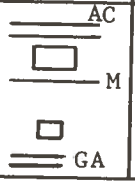	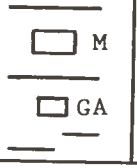					

GA = General Aviation
AC = Air Carrier
M = Mixed

Figure 3.3-1. Airport Classification and Configurations

Table 3.3-1. Airport Classification

Name	Descriptor	Classification
Burbank	BUR	8
Los Angeles International	LAX	8
Ontario International	ONT	8
Santa Ana (Orange County)	SNA	8
Palmdale	PMD	7
Long Beach	LGB	6
Oxnard (Ventura)	OXR	6
Riverside	RAL	6
Torrance	TOA	6
Apple Valley	APV	4
Cable (Upland)	CCB	4
Chino	CNO	4
Compton	CPM	4
Corona	L66	4
El Monte	EMT	4
Fox (Lancaster)	WJF	4
Fullerton	FUL	4
Hawthorne	AHR	4
Laverne Bracket	POC	4
Meadowlark (Huntington Beach)	L16	4
San Fernando	SFR	4
Santa Monica	SMO	4
Santa Paula	SZP	4
Santa Susana	L02	4
Van Nuys	VNY	4
Whiteman	WHP	4
Agua Dulce	X01	3
Capistrano	L38	3
Fla Bob (Riverside)	RIR	3
Redlands	X34	3
Skylark	X42	3
Hemet Ryan	X17	2
Hesperia Air Lodge	X18	2
Rialto	L36	2
Rosamond	X37	2
Tri City	SBT	2
Hawkins	X15	1
Morrow	X25	1
Perris Valley	X31	1
Quartz Hill	X32	1
Rancho California	X33	1
Sterks Ranch	X43	1
Sunhill Ranch	X44	1

The configuration of the airspace structure is fully discussed in Volume IV, Section 1. The SAATMS airspace structure is represented in the digital simulation model by use of a network of parallel speed segregated lanes which merge into a single final approach lane 3 nmi from each runway. The effects of the constraints imposed on the system due to the demand, the aircraft characteristics, and the airport system are presented in Section 5 of this volume.

4. PERFORMANCE MODELS DESCRIPTION

The evaluation of the performance of the SAATMS is accomplished through the use of models to represent system elements and system operation. Models based on analytical expressions were used to establish system separation standards which affect the safety provided the user aircraft in terminal area operations. Analytical models were also used to develop the system safety measures for enroute operations. The capacity and delay performance of the SAATMS in terminal area operations were determined using a digital simulation model. Simulation techniques are required due to the complexity of the system. This section describes the models used to evaluate the SAATMS performance.

4.1 Separation Standard Model

The SAATMS derives position and velocity information on each aircraft in the system from its surveillance mode of operation. This information is processed to determine if conflicts exist when aircraft separation standards are not properly maintained. The separation standard model provides quantitative relationships for determining separation standards applicable to the SAATMS.

4.1.1 Basic Model Structure

The same separation concept applies in all dimensions (along track, cross track, vertical). Thus, the analysis can be done considering only one direction, with the results being applicable in all directions. Three aircraft parameters need to be considered in each direction: position, velocity, and acceleration. Higher order derivatives of position are assumed to be zero. Their effect can be taken into account in the specification of aircraft acceleration.

The model assumes that estimates of aircraft position, r, and velocity, $\dot{r}$, are available from surveillance data every τ_s sec, where τ_s is the time between surveillance samples. The effects of certain levels of aircraft acceleration are examined, and the separation standard is determined based on worst-case acceleration or maximum blunders (defined by an acceleration level) for which protection is to be provided. Surveillance errors and normal aircraft excursions [within the width of the Normal Operating Zone (NOZ)] will also affect the separation standard.

An aircraft position-velocity trajectory for an applied acceleration profile is shown in Fig. 4.1-1. Examination of such trajectories leads to determination of the separation standard, the boundaries of the normal operating zone, and the intervention criteria.

Assume the aircraft acceleration, A(t), has the form shown in the bottom part of Fig. 4.1-1. Then, for $t_o < t < t_1$,

$$r = \frac{1}{2A_B}\dot{r}^2 + r_o - \frac{\dot{r}_o^2}{A_B} \qquad (1)$$

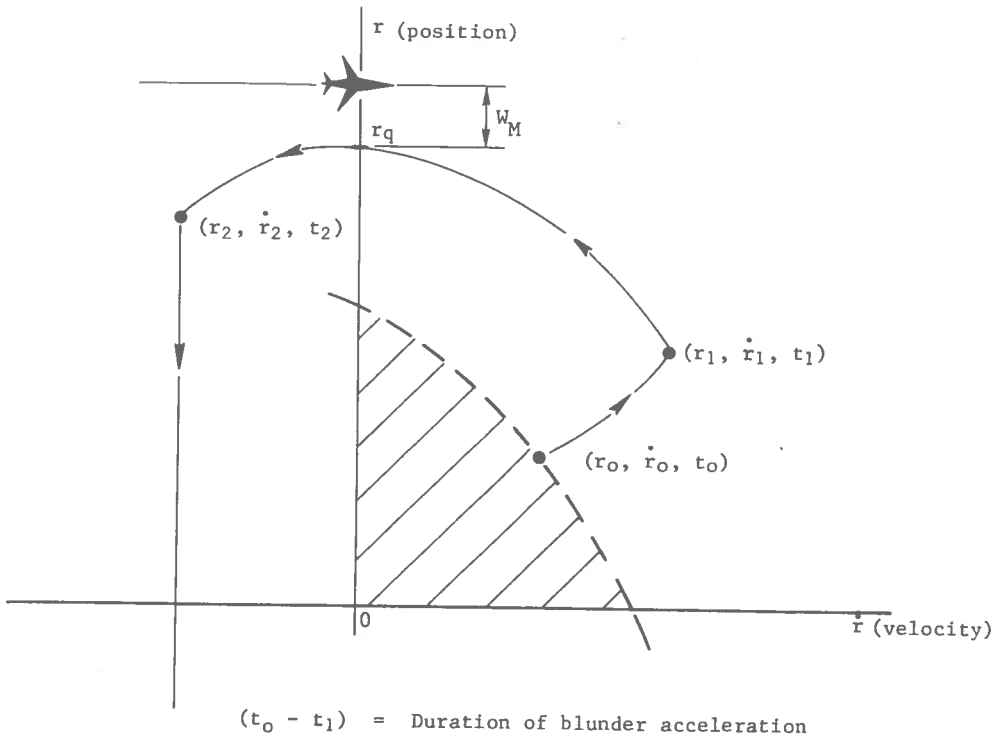

$(t_o - t_1)$ = Duration of blunder acceleration

$(t_1 - t_2)$ = Duration of corrective acceleration

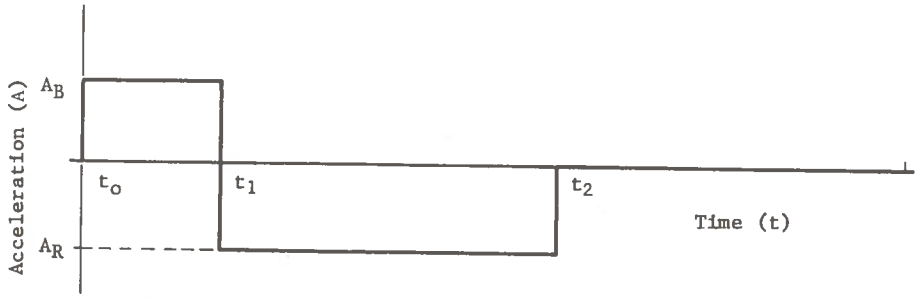

Figure 4.1-1. Aircraft Position-Velocity Trajectories for Applied Acceleration

where, for ease of notation, $r(t) = r$, $\dot{r}(t) = \dot{r}$, $r(t_o) = r_o$, $\dot{r}(t_o) = \dot{r}_o$. Equation (1) shows a parabolic relationship between r and $\dot{r}$. The same equation holds for $t_1 < t < t_2$ with $r_o = r_1$, $\dot{r}_o = \dot{r}_1$, and $A_B = A_R$.

The dashed line in Fig. 4.1-1 represents the boundary of the NOZ in the first quadrant of the r-$\dot{r}$ plane. Considering only the first quadrant, the aircraft is within its NOZ if its state (given by r, $\dot{r}$) is to the left of this line Assume there is an aircraft located at $r = r_q + W_M$, $\dot{r} = 0$ as shown in Fig. 4.1-1. Then an aircraft having the r-$\dot{r}$ trajectory shown would miss this aircraft by a distance W_M.

If (1) A_B represents the maximum acceleration protected against; (2) τ, the sum of the system command delay and the surveillance update interval; and (3) W_M, the minimum miss distance, then the trajectory of Fig. 4.1-1 represents the worst-case blunder that can be protected against. By definition, the initial point of this trajectory lies on the boundary of the NOZ. The locus of all values of r_o, $\dot{r}_o$ for trajectories which pass through r_q with an acceleration of A_B for $t_o \leq t < t_1$ and A_R for $t > t_1$ define the boundary of the NOZ. If $t_o + \tau + T$ is the time the trajectory has the value $\dot{r} = 0$, $r = r_q$ then the boundary equation is

$$r_q = r_o + \dot{r}_o\tau\left(1 - \frac{A_B}{A_R}\right) - \frac{\dot{r}_o^2}{2A_R} + \frac{A_B\tau^2}{2}\left(1 - \frac{A_B}{A_R}\right) \qquad (2)$$

Equation (2) is also a parabola relating r_o and $\dot{r}_o$.

Equation (2) defines the boundary of the NOZ in the first quadrant of the r-$\dot{r}$ plane. The boundary for the third quadrant is found in an identical manner by considering an aircraft at $r = -(r_q+W_M)$. The equation for this boundary is the same as Eq. (1) with $-r_q$ substituted for r_q, and $-A_B$ and $-A_R$ for A_B and A_R, respectively. Figure 4.1-2 shows this curve and the curve of Eq. (2) in the r-$\dot{r}$ plane. The shaded region in the figure is the NOZ. The boundaries in the second and fourth quadrants are defined by the appropriate curves and the specified miss distances. An aircraft is also shown at $r = \dot{r} = 0$ which would be its nominal location in the NOZ.

While the previous discussion has presented the basic structure for the separation standard model, there are still several other items to be included. These are system time delays, surveillance errors, determination of the NOZ, and, finally, a specification of how the component distances combine to give the separation standard for adjacent aircraft.

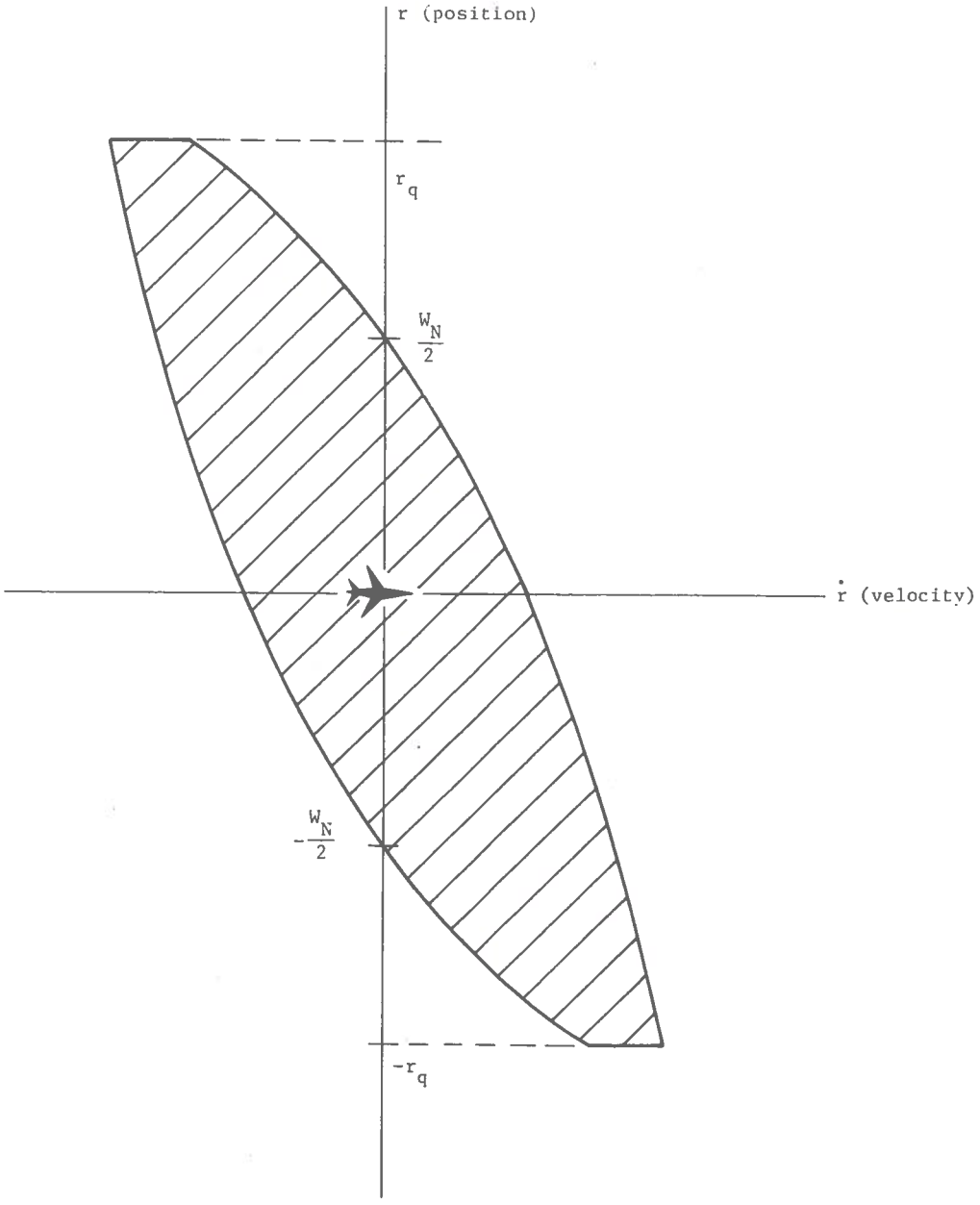

Figure 4.1-2. Normal Operating Zone Boundaries

4.1.2 Effect of System Time Delay

The system time delay, τ_D, is defined as the difference between the time aircraft surveillance data are received by the SAATMS and the time the aircraft responds (changes its acceleration) to commands from the system. The model accounts for such delay by considering τ in Eq. (2) to be the sum of τ_D and τ_s where τ_s is the time between surveillance samples.

4.1.3 Effect of Surveillance Errors

The effect of surveillance position and velocity errors will be to increase the required aircraft separation standard over that implied in Fig. 4.1-2, as illustrated in Fig. 4.1-3. The curves of Fig. 4.1-1 [given by Eq. (1) and (2)] are repeated for the first quadrant of the r-$\dot{r}$ plane and represent the NOZ boundary. The point given by S_a represents the actual aircraft state at time t_o. Due to surveillance errors (a velocity error of $\Delta\dot{r}$ and a position error of Δr), the SAATMS regards the aircraft as being at point S_s. Since S_s is within the NOZ bounds, the SAATMS issues no command to the aircraft. If the aircraft experiences an acceleration as shown in the bottom part of Fig. 4.1-1, it will cross the r axis at r_m rather than at r_q as in Fig. 4.1-1. (Note that if the aircraft had actually been at S_s instead of S_a and experienced the same acceleration profile, it would have reached only r_q instead of r_m.)

The distance, as shown in Eq. (3), represents a distance that must be included in the separation standard to account for surveillance errors.

$$r_e = r_m - r_q \tag{3}$$

In general, r_e is a random number. Its relationship to τ, A_B, A_R, $\dot{r}_s$, Δr, and $\Delta\dot{r}$ can be determined as follows. Let

$\hat{r}_o$ = surveillance value of position at t_o

$\hat{\dot{r}}_o$ = surveillance value of velocity at t_o

r_o = actual value of position at t_o

$\dot{r}_o$ actual value of velocity at t_o

Δr_o = surveillance position error at t_o

$\Delta\dot{r}_o$ = surveillance velocity error at t_o

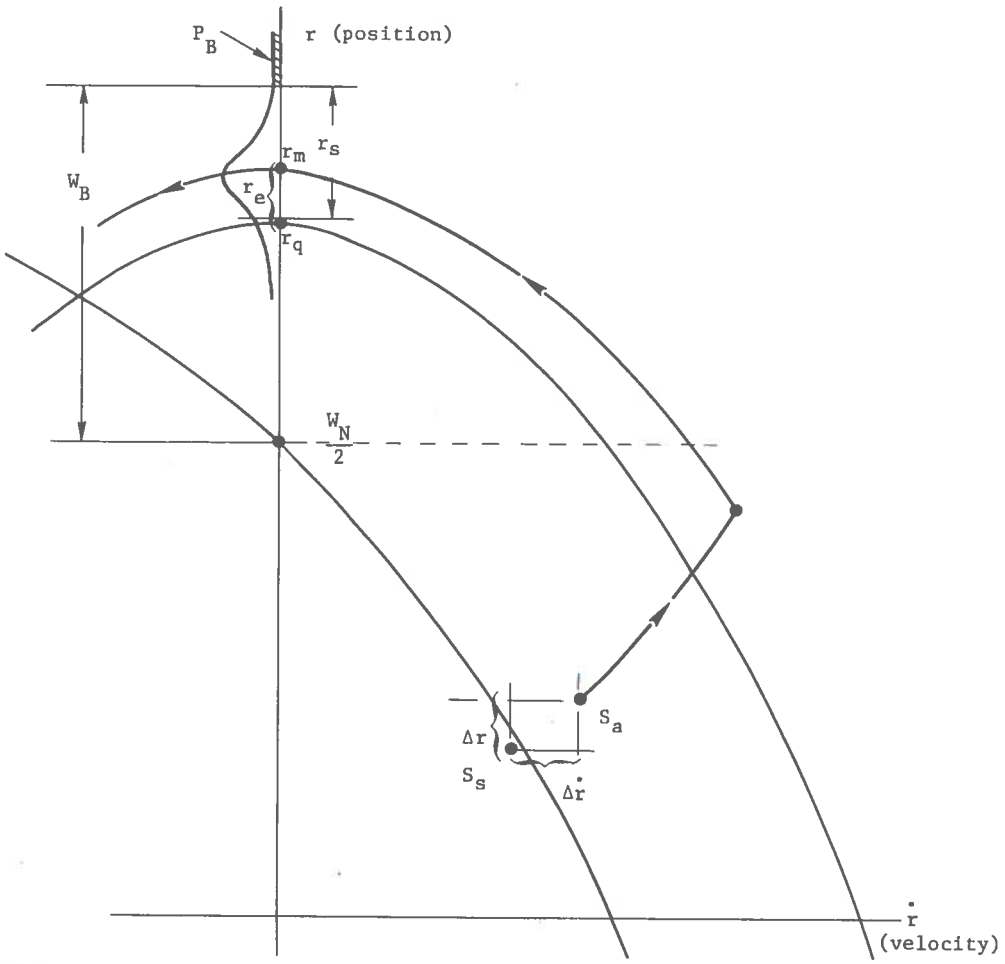

Legend

W_N = Width of Normal Operating Zone

W_B = Width of Buffer Zone

S_a = Actual state of aircraft

S_s = Surveillance state of aircraft

Δr = Position surveillance error

$\Delta \dot{r}$ = Velocity surveillance error

$r_e = r_m - r_q$

r_q = Value of $1/2\ W_N + W_B$ in case there is no surveillance uncertainty

r_m = Value of maximum deviation resulting from a blunder starting at a given S_a

r_s = Additional Buffer Zone needed to insure that a blundering aircraft will not go beyond the buffer zone with probability greater than P_B

Figure 4.1-3. Effect of Surveillance Errors

Then it can be shown that

$$r_e = \Delta r_o + \Delta \dot{r}_o \left[\tau\left(1 - \frac{A_B}{A_R}\right) - \frac{\hat{\dot{r}}_o}{A_R} \right] - \frac{\Delta \dot{r}_o^2}{2A_R} \tag{4}$$

Statistical parameters of r_e can be determined as follows. If Δr_o and $\Delta \dot{r}_o$ have zero mean, the mean value of r_e is given by

$$\bar{r}_e = E(r_e) = -\frac{\dot{\sigma}_s^2}{2A_R} \tag{5}$$

where $\dot{\sigma}_s^2$ = variance of the surveillance velocity error.

Let σ_s^2 = variance of the surveillance position error. Assuming the variables Δr_o and $\Delta \dot{r}_o$ are independent and Gaussian, the variance of r_e, is

$$\sigma_{re}^2 = \overline{r_e^2} - (\bar{r}_e)^2 = \sigma_s^2 + \left[\tau\left(1 - \frac{A_B}{A_R}\right)^2 - \frac{\hat{\dot{r}}_o}{A_R} \right] \dot{\sigma}_s^2 + \frac{\dot{\sigma}_s^4}{2A_R^2} \tag{6}$$

Finally, if Δr_o is Gaussian, r_e is approximately Gaussian. It is assumed to be exactly Gaussian with a mean value given by Eq. (5) and a variance given by Eq. (6).

To allow for the surveillance errors, let r_s = that portion of the separation standard to compensate for the surveillance errors. If r_s is expressed in terms of $\bar{r}_e$ and σ_{r_e} as follows

$$r_s = \bar{r}_e + K_s \sigma_{r_e} \tag{7}$$

then K_s is a constant related to the probability P_B that r_e is greater than r_s. Thus, if $K_s = 3$, from the standard normal distribution tables

$$P_B = \text{Probability } (r_e > r_s) = 0.0013$$

A representation for the probability density function for r_e, the distance r_s, and the probability P_B is shown at the top of Fig. 4.1-3.

4.1.4 Buffer Zone Width

The width of the Buffer Zone, W_B, can now be determined. W_B is also shown in Fig. 4.1-3, and its values are given by

$$W_B = r_q - \frac{W_N}{2} + r_s \tag{8}$$

With appropriate substitution of variables, W_B can be written as

$$W_B = \frac{A_B \tau^2}{2}\left(1 - \frac{A_B}{A_R}\right) - \frac{\sigma_{\dot{s}}^2}{2A_R} + K_s \left\{ \sigma_s^2 + \left[\tau\left(1 - \frac{A_B}{A_R}\right) - \frac{\hat{\dot{r}}_o}{A_R} \right]^2 \sigma_{\dot{s}}^2 + \frac{\sigma_{\dot{s}}^4}{2A_R^2} \right\}^{1/2} \tag{9}$$

4.1.5 Size of the Normal Operating Zone

The size of the NOZ, W_N, will be a function of the aircraft's station keeping ability Δp, (including pilotage if manual steering is used), the SAATMS surveillance errors, Δr, $\Delta \dot{r}$, τ_s, and the desired SAATMS intervention rate, $\dot{N}_I$. There are no precise, analytic relationships between these variables. Assumption could be made concerning the station keeping ability and the surveillance errors so that the effect of the two could be combined to describe the aircraft's position and velocity inside the NOZ by a probability density function, $P(r,\dot{r})$. That portion of $P(r,\dot{r})$ that is outside of the NOZ would represent that portion of time the aircraft is outside of the NOZ. However, to obtain the intervention rate from $P(r,\dot{r})$ would require assumptions about the time correlation of samples of the random variables r and $\dot{r}$. This condition is not zero (aircraft position and velocity are continuous) and there is no information concerning that correlation in $P(r,\dot{r})$. Also, $P(r,\dot{r})$ is not independent of the width of the NOZ, since any aircraft detected to be outside of the NOZ will be directed by the SAATMS to return to the NOZ.

4.1.6 Track Model

Because precise analytic solutions of the relationship between W_N, Δp, Δr, $\Delta \dot{r}$, τ_s, and $\dot{N}_I$ cannot be obtained, a digital computer simulation model was constructed to represent aircraft operation in and around the NOZ. This model is called the Track Model and is shown in Fig. 4.1-4. The various parameters contained in the model are listed below the diagram.

Random numbers are generated to represent the surveillance and navigation errors and the disturbance acceleration. A rectangular integration procedure is used for integration of the various parameters. Aircraft and pilot characteristics are represented by the constants K_a, K_v, P_p, and K_d.

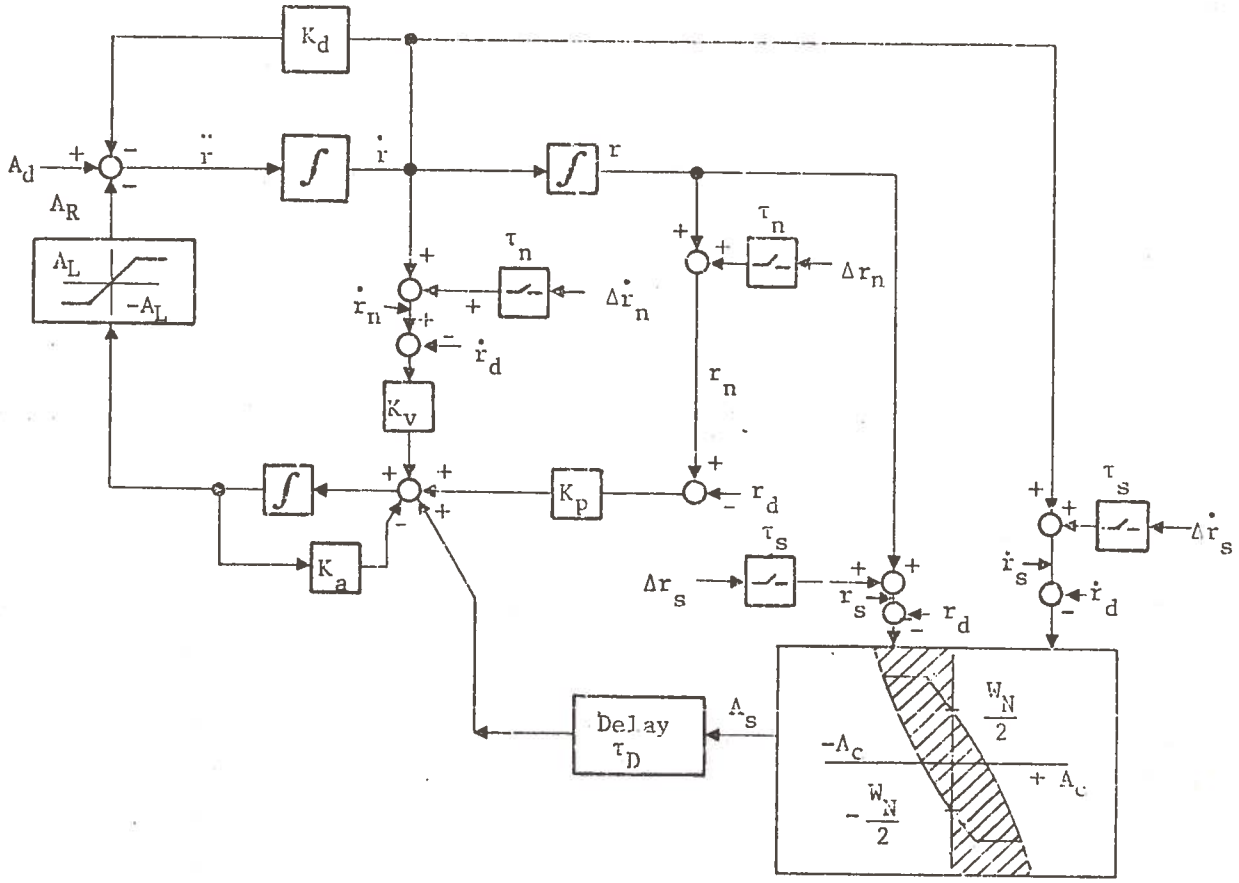

where

A_d	Disturbance acceleration (includes blunder acceleration)
$r, \dot{r}, \ddot{r}$	Actual aircraft position, velocity, acceleration
$r_d, \dot{r}_d$	Desired aircraft position, velocity
$\Delta\dot{r}_n, \Delta r_n$	Navigation velocity and position errors
$\Delta\dot{r}_s, \Delta r_s$	Surveillance velocity and position errors
τ_n, τ_s	Navigation, surveillance update interval
$\dot{r}_n, r_n$	Navigation velocity and position
$\dot{r}_s, r_s$	Surveillance velocity and position
K_a	Aircraft response parameter
K_v, K_p	Velocity and position control loop gains
K_d	Aerodynamic drag term
A_s	Commanded ATC corrective acceleration, $\pm A_c$ (0 if aircraft in shaded region)
W_N	Width of NOZ
A_L	Limit on commanded acceleration

Figure 4.1-4. Diagram of Track Model

The model is one dimensional but is applicable to all dimensions through proper choice of parameter values. The intervention rate is an output from the model and is obtained by counting the number of times a non-zero acceleration command is generated. Time histories of all the model variables are available as model outputs. The phase plane trajectory of an aircraft shown in Fig. 4.1-5 is an example of a time history output. Probability density and distribution functions for r and $\dot{r}$ are also available.

4.1.7 Separation Standard Specification

The separation standard, Q_S, is the sum of several distances as given by Eq. (10) (see Fig. 2.3-3):

$$Q_S = W_N + W_B + W_{T_{LF}} + W_M \tag{10}$$

The purpose of this section is to indicate how the distances comprising Q_S are determined. The width of the buffer zone, W_B, is established utilizing Eq. (9). The width of the normal operating zone, W_N, is obtained from operation of the track model. Curves similar to Fig. 2.3-5 are obtained for the specific system parameters. Specification of an acceptable AATMS intervention rate, $\dot{N}_I$, completes the determination of W_N.

$W_{T_{LF}}$ is the wake turbulence danger distance and is a function of both leading and following aircraft type as well as atmospheric condition. Unfortunately there is little, if any, data to permit exact specification of $W_{T_{LF}}$. For aircraft on parallel routes, $W_{T_{LF}}$ may be small, depending on wind velocity. Because of the lack of firm data on wake turbulence separation requirements, various values of Q_S (which represent various values of $W_{T_{LF}}$) are used to provide sensitivity data.

W_M is a specified miss distance and is arbitrary. Aircraft will only come within W_M feet of each other when one has blundered, with some blunder acceleration A_{BM}. If $A_B > A_{BM}$, the distance between aircraft at their point of closest approach will be smaller than W_M, while if $A_B < A_{BM}$, the aircraft will be farther apart than W_M at their closest point of approach. To prevent metal-to-metal contact for A_{BM} blunders, W_M must be at least as great as the largest aircraft physical dimension (since the aircraft were considered essentially as point masses in the derivation of the equations describing their motion). Based on the largest physical dimensions of aircraft in use today, a value of 300 ft for W_M (between aircraft centers of mass) would preclude physical contact regardless of aircraft orientation. In the present ATC system, a critical near mid-air collision is defined as a near miss of 150 ft or less. No point of reference is specified for this definition, however. In order to provide a higher margin of safety than the present system for SAATMS, a minimum miss distance of 300 ft has been specified. The specific values of Q_S that were used in the evaluation of the SAATMS performance are discussed in Section 5, System Performance.

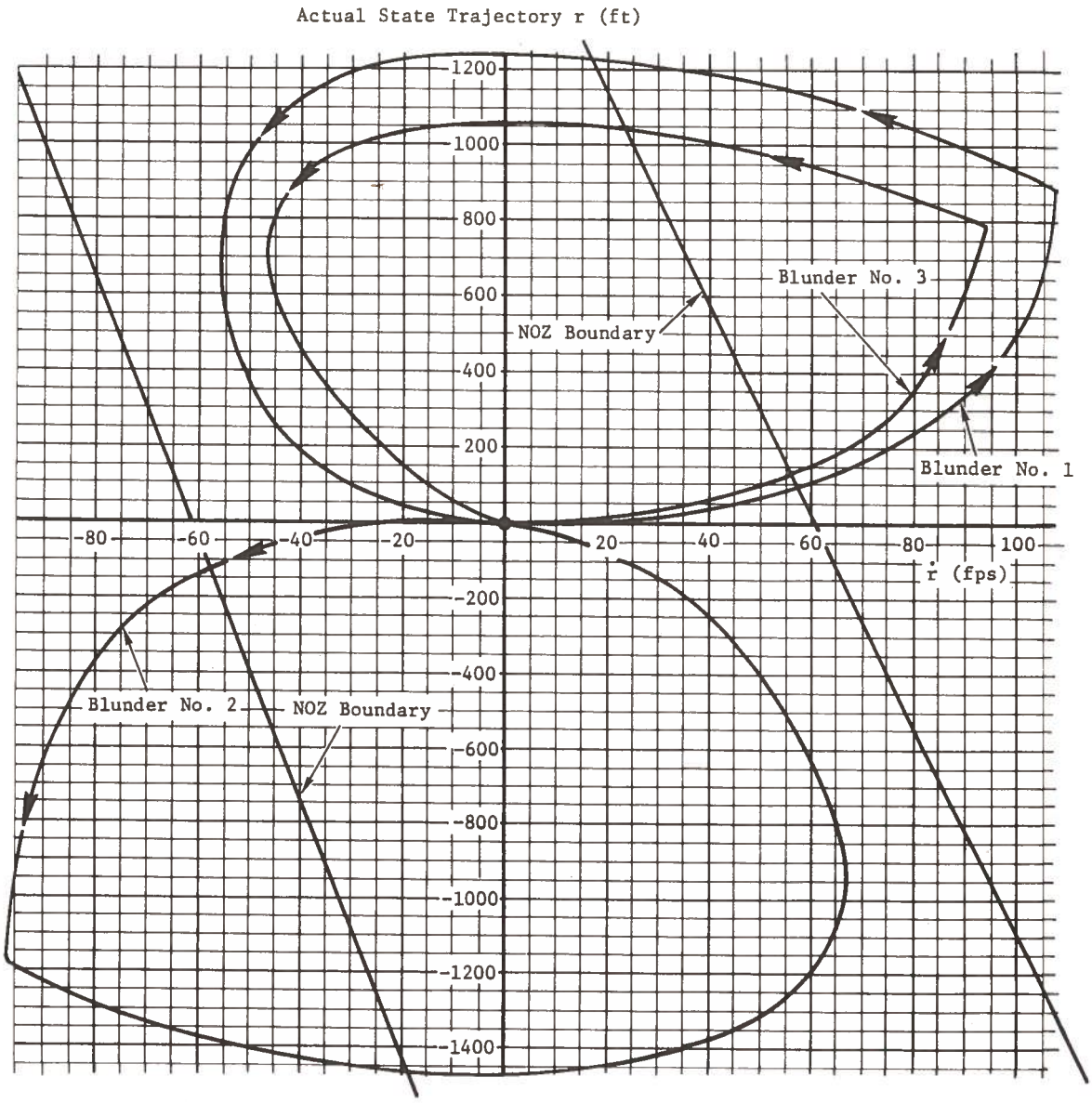

Figure 4.1-5. Example of R-R Trajectory from Track Model, Three Blunders of 16 FT/Sec^2 Occurred

4.2 Capacity and Delay Models

4.2.1 Analytic Expressions

Analytical models of capacity and delay can be derived for some portions of the air traffic system. In most situations, simplifying assumptions are necessary so that expressions may be handled mathematically. Analytical models yielding mathematical relationships between system parameters are used whenever possible. The usefulness of such relationships depends on the number and type of the assumptions used to derive the expressions.

Perhaps the most simple model is the one used to measure the capacity of a single lane of air traffic. This model is usually developed with the assumption that all aircraft travel in trail, are separated by a distance exactly equal to Q, and have the same velocity V. In this case, the capacity C is given by

$$C = \frac{V}{Q} \tag{1}$$

A slightly more complicated model can be developed if Q is assumed to be the sum of two quantities Q_{min} and Q_c, where Q_{min} is a minimum separation that must be maintained (due to the possibility of wake turbulence for example) and Q_c is a buffer distance allocated to account for aircraft control errors (including surveillance, navigation, control errors, and system response times). Then

$$C = \frac{V}{Q_{min} + Q_c} \tag{2}$$

An analytical expression can be derived for the case where there are N different classes of aircraft with velocities V_i (i = 1..., N) and the required minimum separation between each class may be different (possibly due to wake turbulence). Let Q_{ij} be the minimum separation required between aircraft of Class i followed by aircraft of Class j. Assume (1) that the length of the trail is L, (2) that no overtaking of aircraft is allowed, and (3) that the population for each class is P_i. The index i is chosen in such a way that $V_i > V_j$ if i > j. The capacity is then given by:

$$C = \frac{\left(\sum_i P_i\right)^2}{\sum_i \sum_j \left[P_i P_j \frac{Q_{ij}}{V_k} + L\left(\frac{1}{V_i} - \frac{1}{V_j}\right) E_{ij}\right]} \tag{3}$$

where k = maximum (i,j)

$$E_{ij} = \begin{cases} 1 \text{ if } i < j \\ 0 \text{ if } i > j \end{cases}$$

This relationship is more realistic than those mentioned previously but does not provide for control errors.

Some probabilistic models for runway capacity analysis have been suggested by previous investigators (Ref. 17 through 21). The forms of threshold inter-arrival time error, gate arrival time error, speed and time errors in flying a common path are assumed to be known and are introduced in these models. Landing capacities of the runways, under the requirement that violation of separation standard be within a certain bound, are then estimated.

Most of the analytical expressions are for different isolated parts of the air traffic system under restricted or simplified assumptions. Since they generally are easily applied, they are often useful as the first-order estimation of capacities (such as a bottleneck analysis). Many of them can be integrated into computer simulations for the study of larger inter-related systems. They are also readily useful for rough sensitivity analyses.

Many air traffic situations are too complicated to be modeled, with even modest accuracy, by analytic expressions. In some cases, the analytic expressions themselves are cumbersome and difficult to use [e.g., Eq. (3)]. Determination of the capacity of a single runway used for mixed departures and arrivals by several classes of aircraft operating under multiple rules (airspace separation, runway occupancy, departure/departure separation, and departure/arrival separation) is an example of such a situation. Aircraft delay is even more complex. Queuing models can be postulated for determining aircraft delay in a single facility, but the only manageable analytic solutions for such models are for the case of Poisson arrivals and exponential service times or some forms of Erlang distributions.

In view of these limitations on the usefulness of analytic models, a digital computer simulation model was developed to determine system capacity and delay.

4.2.2 Computer Simulation Model

There has been much effort devoted to the computer simulations of air traffic systems. Most of the large scale simulations have been developed with specific objectives in mind. Based on the purpose of those doing the modeling, different aspects of the system are highlighted. For example, a model which is developed to study the work load of an air traffic controller would emphasize the relations which affect the air traffic controllers most while some other factors are either considered as secondary or completely neglected. Use of such a model in evaluating other aspects of the air traffic system would not yield reliable results.

The lack of a suitable simulation model made it necessary to develop a model which would closely represent the SAATMS and which could be used for establishing subsystem and system performance.

This model is called the network model since a network structure consisting of nodes and connecting branches is used to represent the air traffic structure. Figure 4.2-1 shows an example of the network structure for a single runway. Input data are used to define the network structure in terms of node number, location, and type. The number of nodes in a network is constrained only by the computer memory available. Thus, a network can represent any portion of an air traffic system to varying degrees of desired detail. For example, referring to Fig. 4.2-1, more runway exits than the two indicated could be modeled by adding more nodes on the runway. The departure and approach airspace structure as well as the taxiway system could also be expanded by adding more nodes.

The large number of variables and the complex dynamics of the air traffic management system would require a large amount of computer time if a continuous time simulation was used. The network model is an event-oriented simulation. The basic event in the model occurs when an aircraft arrives at a node. Significant points of the airspace are considered as nodes. Selection of nodes depends on the outputs to be sought as well as the size and detail of the simulation. There are destination nodes, which may either be airports or gates in terminals, or origin nodes, where aircraft may first enter the system. A node may be a destination node for some flights and be an origin node for others.

Aircraft move from node to node along the branches of the network. Only the time at which an aircraft passes a node will be used to describe states of the system. Detailed position and velocity of an aircraft will generally be available only at the nodes.

Inputs to the model consist of specification of the following:

Network: the x, y, z values of each node in the structure

Routes: the number and sequence of nodes in each route

Separation Standard: minimum aircraft separation as a function of aircraft type and state

Demand: aircraft types, arrival times, and velocity at each route node

Each aircraft constitutes an entity to the model. For each entity, the time and place (node) of the next event are entered into a matrix. After such an event occurs, the next event to take place for that entity replaces the original entry. New entities enter into the matrix when they appear at the origin nodes. The simulation clock advances from one event to the next in one single step. Thus, it i a fast-time discrete simulation.

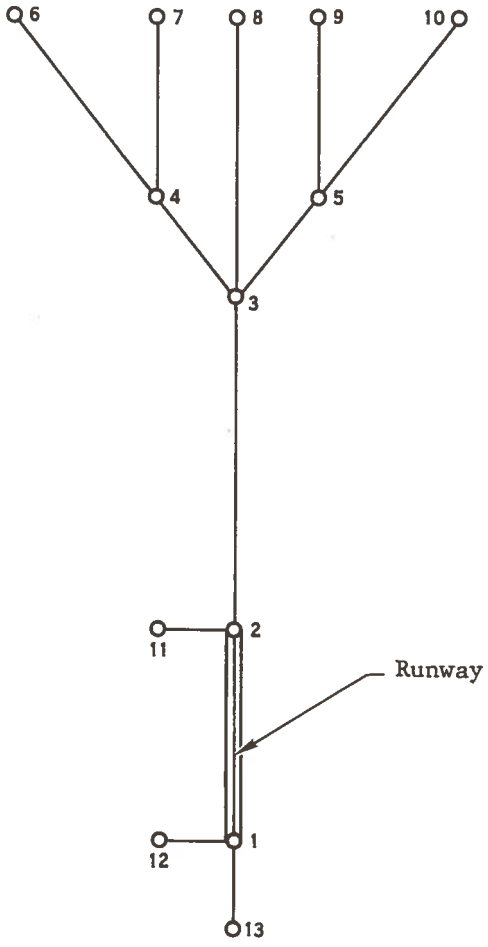

Figure 4.2-1. Example of Network Structure for Single Runway

The simulation clock advances from present time to the earliest time at which an event for any entity is to occur. The node where the event would take place is checked to see the last event that occurred there and to verify the availability of the node. If the node can accept the aircraft at its desired time, the event is then cleared and scheduled to take place. Otherwise, the event is delayed the necessary time and a new schedule is given. In either case, the actual time of the event may contain perturbations which represent time of arrival errors. The actual time of occurrence of the event is recorded and is also used to update the node occupation record. Figure 4.2-2 shows a simple flow diagram of the model computer program.

The following outputs are available from the model:

Capacity: Number of aircraft passing the specific nodes during the run

Delay: Average delay per aircraft, average delay per aircraft type, maximum delay, delay distribution

Congestion: Metering loss at specific nodes can be obtained as part of the output and bottlenecks can be identified.

The node concept used in the network model offers considerable flexibility. The level of detail describing the network of airspace may be extended depending upon the extent of detail one is seeking. For studying the air traffic in a region, each airport may be considered as a node. Detailed behavior of aircraft at airports is ignored at this level. If, however, there is an interest in the delay and the capacity of an airport, the airport may be modeled with a large number of nodes to represent each significant point on the runways and taxiways. In either case, the same node concept model can be used. Only the network arrays which describe the graph structure will differ.

In view of this flexibility, the main model can be used to obtain data for most phases of operations and different parts of the airspace. The model can be used to analyze a single runway, an airport, a terminal area, or enroute airspace. If it is decided that additional information along certain critical branches is desirable, additional nodes can be inserted. If certain parts of a subsystem do not have much influence on the aspect being investigated, the number of nodes for that subsystem can be reduced. The results of the evaluation of the performance of the SAATMS derived from use of the network model are presented in Section 5, System Performance.

4.2.3 Safety Models

4.2.3.1 Number of Conflicts

The number of conflicts expected in a Satellite-Based Advanced Air Traffic Management System over a period of time was chosen as a measure of total system safety because it provides an absolute measure of one facet of safety. In addition,

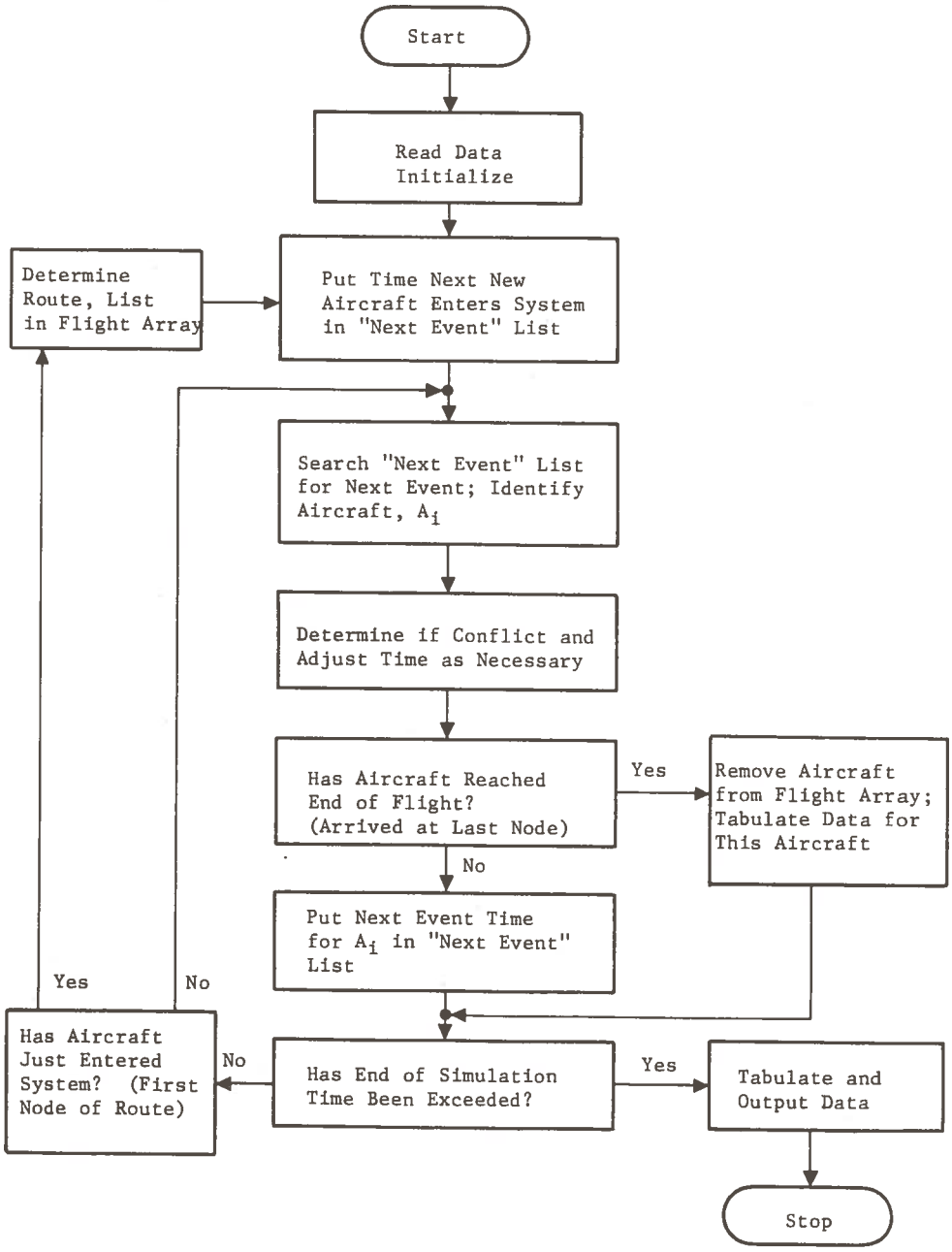

Figure 4.2-2. Simplified Flow Diagram of Network Event-Step Computer Simulation Program

the conflict equations are compatible with the format of the demand data projected for the 1995 time frame and they are computationally easy to use. The equations are also compatible with past data concerning collisions and critical near mid-air collisions (CNMAC). The conflict equations can be normalized to past data (1968 data were available) (Ref. 2), thereby reducing the effects of conservative simplifying assumptions utilized in this derivation. A conflict or a critical near mid-air collision is defined as a near miss of 150 ft or less before physical contact occurs.

The number of conflicts model was used to compute the expected number of conflicts in the enroute airspace in 1995. The values computed were based on the projected demand data supplied by TSC, which provided the number of flight path crossings and aircraft passages in the enroute airspace for 1995. The expected number of conflicts for the SAATMS, the Ground-Based Advanced Air Traffic Management System (GAATMS), and the present system were computed. The results of that analysis are presented in the System Performance Section, Section 5.

The number of crossing and passage conflicts for the year 1995 is given by Ref. 1 as

$$N_{C\ 1995} = \frac{3 \cdot q \cdot K}{2\sqrt{2}\,\pi} \sum_{h} \frac{A_c\ (h)\ r_{cn}\ (h)}{\sqrt{\frac{27}{8}\, r_{cn}^3\ (h) - r_{qn}^3}}\ N_{P\ 1995}\ (h) \qquad (4)$$

where

K = Normalization factor obtained from the 1968 CNMAC data (Ref. 2)

q = Fraction of the relative position error distribution, E, that lies outside the ellipsoid given by the semi-axes x_q, y_q, z_q (chosen components of a vector $\bar{r}_q$)

$$r_{qn} = \left[\left(\frac{x_q}{\sigma_x}\right)^2 + \left(\frac{y_q}{\sigma_y}\right)^2 + \left(\frac{z_q}{\sigma_z}\right)^2\right]^{1/2} = \text{normalized magnitude of } \bar{r}_q$$

$N_{P\ 1995}\ (h)$ = Number of crossings or passings per year in an altitude band, h, derived from the demand level data and the airspace structure

σ_x, σ_y, σ_z = Standard deviations of the relative position error distribution, E, of aircraft pairs along ellipsoid semi-axes.

$A_c\ (h)$ = Conflict cross-sectional area determined for 150 ft conflict and the aircraft mix at altitude band, h, normalized with respect to σ_x, σ_y, σ_z

r_{cn} = minimum normalized nominal passage distance

$$= \left[\left(\frac{x\ (h)}{\sigma_x}\right)^2 + \left(\frac{y\ (h)}{\sigma_y}\right)^2 + \left(\frac{z\ (h)}{\sigma_z}\right)^2\right]^{1/2}$$

where x (h), y (h), z (h) are the relative closest approach coordinates of two vehicles along axes of σ_x, σ_y, σ_z in an altitude band h.

Equation (4) was normalized (or calibrated) to the 1968 base year using the 1968 CNMAC data. The normalization factor was obtained by solving for K from Eq. (4) using the 1968 CNMAC data as the number of conflicts and by using parameters applicable to the 1968 system. The normalization equation is

$$K = \frac{4\ \text{CNMAC}_{1968}}{\left(\frac{3q'}{2\sqrt{2}\,\pi}\right)\sum_h \frac{A'_c\ (h)\ r'_{cn}\ (h)}{\left(\sqrt{\frac{27}{8}}\, r^3_{cn}\ (h)' - r'^3_{qn}\right)} \cdot N_{P1968}\ (h)} \qquad (5)$$

where the primed values imply the use of 1968 parameters and $4\ \text{CNMAC}_{1968} = N_{C1968}$. The factor of four is predicated on an estimate that only 25 percent of the CNMAC are reported.

To compute the number of conflicts expected in 1995, resulting from use of the present system, the GAATMS, and the SAATMS, estimates of their relative position error statistics were derived. The relative position errors (σ_x, σ_y, σ_z) were treated as independent errors in the horizontal and vertical dimensions (σ_H, σ_Z). These values were estimated from the surveillance error statistics. The navigation and surveillance data were not combined statistically to obtain a composite relative position error estimate. This is a reasonable method for estimation in that the surveillance data are used to provide aircraft separation, while the navigation data are used to determine the normal operating zones which result in acceptable intervention rates. The horizontal accuracy values estimated for the present and GAATMS assume that the aircraft are uniformly distributed within the radar range and that the angle of the position vector to the radar line of sight is uniformly distributed.

The average value of the closest approach distance for crossing and passage is estimated from the airspace structure and is normalized to obtain

$$r_{cn}\ (h) = \left[\left(\frac{x_H\ (h)}{\sigma_H}\right)^2 + \left(\frac{z\ (h)}{\sigma_z}\right)^2\right]^{1/2} \qquad (6)$$

where

x_H (h) = nominal horizontal passage separation distance for altitude band h

z (h) = nominal altitude separation distance in altitude band h

An IFR/IFR enroute example of x_H (h) is the specified 10 min separation (Ref. 4) for crossing aircraft and an assumed 7 nmi separation for passing aircraft. The 10 min separation corresponds to different average separation distances for each altitude band due to differing aircraft velocities in each altitude band.

The average collision cross-section, A_c (h), is determined by the aircraft dimensions, the specified 150 ft miss distance, and possibly wake turbulance. The average collision cross-section is dependent on the mix of aircraft in each altitude band. The average collision cross-section is normalized by the position keeping accuracy and is given by

$$A_c \text{ (h)} = \frac{\ell}{\sigma_H} \cdot \frac{S}{\sigma_z} \tag{7}$$

where

ℓ = diameter of the collision cross-section cylinder

S = height of the collision cross-section cylinder

The magnitude of q is related to the chosen ellipsoid semi-axes x_q, y_q, z_q; q is the probability that the relative position error, E, exceeds x_q, y_q or z_q. Equivalent probability distribution axes were chosen for the horizontal and vertical dimension, $r_{x,y}$ and z_q, respectively (components of $\bar{r}_q$). The horizontal and vertical values chosen were kept constant in the evaluation of the three systems. The normalized magnitude of r_q is given by

$$r_{qn} = \left[\left(\frac{r_{x,y}}{\sigma_H}\right)^2 + \left(\frac{z_q}{\sigma_z}\right)^2\right]^{1/2} \tag{8}$$

where

σ_H = Horizontal position keeping accuracy

σ_z Vertical position keeping accuracy

For fixed values of $r_{x,y}$ and z_q, if σ_H and σ_z become smaller (i.e., the position keeping accuracy improves), the value of q will become smaller. The magnitude of q thus reflects the relative system surveillance accuracies. Conservative estimates of q were obtained for the SAATMS and GAATMS through the use of the Tchebycheff inequality. These estimates are independent of the actual shape of the tails of the relative position error distribution. The tacit assumption involved in the use of the Tchebycheff inequality is that the actual shape of the relative position error distribution remains constant from system to system. The concept implicit in the assumption of a constant distribution is that the probability of a blunder occurrence is proportional to system accuracy.

The values for the number of conflicts for the three systems are obtained by Eq. (4) through (8), along with estimates of q based on the statistics of the systems and the projected 1995 demand data. The number of conflicts computed were for the crossing and passage of IFR/IFR enroute aircraft. The crossing and passage conflicts for VFR/VFR and VFR/IFR aircraft under surveillance by the system can also be determined by the same equations if the demand data are properly defined.

4.2.3.2 Enroute VFR/VFR and VFR/IFR Conflict Model as a Function of Surveillance Coverage

Estimates of the average number of VFR/VFR and VFR/IFR random crossings and passages that will occur within 150 ft in 1995 can be obtained from the enroute demand model in Section 4.2.3.3. These crossings and passages must be modified to include the effects of the see-and-avoid factor (Ref. 6) to obtain a more realistic number of crossing and passages. The model must be normalized with respect to the 1968 NMAC data (Ref. 2) appropriate for VFR/VFR and VFR/IFR aircraft. The resulting conflicts must then be scaled over the altitude band according to the relative density of itinerant VFR aircraft (Ref. 7) to obtain an estimate of the number of unsurveyed conflicts as a function of altitude.

The number of VFR/VFR and VFR/IFR crossings and passages was obtained by scaling the IFR/IFR data. The scaling factor is dependent on the density of VFR traffic along the city pair routes. The crossings from the enroute traffic data are given in terms of the number of 10 min crossings; these must be adjusted to determine the number of 500 ft (used to normalize the model to the 1968 VFR/VFR and VFR/IFR NMAC data) or 150 ft conflicts. Once these data have been determined, the yearly crossing rate can be developed. The number of passages within 150 ft are estimated using a uniform position distribution of interacting aircraft over a 5 nmi VOR route. The probability of a passage being within 150 ft at the point of closest approach has been determined to be 0.0098 (see Volume IX of this report). This probability is then multiplied by the number of passages on the route.

The number of VFR/VFR and VFR/IFR conflicts is given by

$$N_{C_i} = n_C \cdot N_{SAC} \cdot D_{C_i}$$
$$N_{P_i} = n_P \cdot N_{SAP} \cdot D_{P_i} \quad (9)$$

and

$$n_C = \frac{NMAC_C}{N_{SAC} \cdot D_{C1968}}$$
$$n_p = \frac{NMAC_P}{N_{SAP} \cdot D_{P1968}} \quad (10)$$

where

D_{C_i}, D_{P_i} = number of random 150 ft conflicts for the 1995 system for crossings and passages, respectively

N_{C_i}, N_{P_i} = number of 150 ft conflicts including the see-and-avoid factor normalized with respect to the 1968 NMAC data

i = demand level

N_{SAC}, N_{SAP} = see and avoid factor for crossings and passages, respectively (Ref. 6) $N_{SAC} = 0.2$ and $N_{SAP} = 0.05$

n_C, n_P = normalization factors from the 1968 NMAC data

$NMAC_C$, $NMAC_P$ = 1968 VFR/VFR and VFR/IFR enroute NMAC data (Ref. 2) for crossing and passages, respectively

D_{C1968}, D_{P1968} = 500 ft random conflicts for the 1968 system for crossings and passages, respectively

The number of midair collisions per 150 ft CNMAC is calculated by either of two methods. A factor of 0.0138 midair collisions/CNMAC has been determined on the basis of random interaction of the aircraft when the pilots fail to see and avoid. Using the 150 ft CNMAC data (Ref. 2) and the number of random flight midair collisions, a factor of 0.0174 has been determined. This latter factor was used in the analysis to determine the VFR/VFR and VFR/IFR mid-air collisions.

4.2.3.3 Enroute Demand Model

The enroute demand model (Ref. 3) was used to obtain the number of crossings and passages in each altitude band for the number of conflicts models. Estimation of crossing conflicts assumes a Poisson distribution of intersection crossing times. The equation for the rate at which conflicts occur as derived below is

$$n_C \simeq 2\, n_a\, n_b\, T \tag{11}$$

where

n_a and n_b are average traffic flow in aircraft per hour, at the same altitude, on crossing routes

T is the minimum separation time used to define a conflict

Given two routes that intersect at the same altitude, assume that the intersection crossing times of aircraft on each of the two routes are randomly distributed in accordance with the Poisson process. Let n_a and n_b be the number of aircraft per hour on Routes A and B, respectively, crossing the intersections. At the instant an aircraft on Route A crosses the intersection, the event where one or more crossing times of Route B aircraft is within an interval T will be defined as a conflict. Its probability is

$$P\ (n=0) = e^{-n_b T} \quad \text{(one side)} \tag{12}$$

$$P\ (n>0) = 1 - e^{-2n_b T} \quad \text{(both sides)} \tag{13}$$

The total conflicts are defined as half of the sum of conflicts computed for each route with the other

$$n_C \simeq 1/2\left[n_a\left(1 - e^{-2n_b T}\right) + n_b\left(1 - e^{-2n_a T}\right)\right] \tag{14}$$

for $2n_aT$ and $2n_bT < 1$, this can be approximated by $n_C \simeq 2n_an_bT$. The number of 10-min or 2-min crossings can be obtained from this equation. Similarly, the number of 500-ft or 150-ft near misses can be obtained by using the average aircraft speed and near miss distances and converting them into a crossing time.

The busy hour crossings and passages are converted to yearly crossings and passages by

$$Y_{C,P}(h) = BH_{C,P}(h)\ \frac{\text{Hours} \times 365}{PF(h)} \tag{15}$$

where

$BH_{C,P}(h)$ = busy hour crossings or passages in altitude band h

$Y_{C,P}(h)$ = yearly crossings or passages in altitude band h

Hours = average number of hours per day to assume constant busy hour operation (13 hours) (Ref. 9)

PF(h) = peaking factor; peak hour to average hour aircraft ratio for aircraft mix in altitude band h.

The rate at which passage conflicts occur per mile of route is a function of the speeds of each aircraft class and the percent of the population in each class.

Assume that aircraft using airways belong to J ground-speed classes having speeds:

$$V_1 < V_2 < V_3 < V_j < V_J$$

Let N_j be the average number of aircraft of class j per mile of airways. An aircraft of Type j will overtake (i.e., pass) aircraft of Classes 1 to j-1 producing C_j conflicts per unit of time:

$$C_j = \sum_{i=1}^{j-1} N_i \, (V_j - V_i) \tag{16}$$

The total number of conflicts for all aircraft in unit distance is given by:

$$C = \sum_{j=1}^{J} N_j \sum_{i=1}^{j-1} N_i \, (V_j - V_i) \tag{17}$$

This can be expressed in matrix form as follows:

$$C = \underline{n}^T \underline{\underline{M}} \, \underline{n} \tag{18}$$

where the ij^{th} element of matrix $\underline{\underline{M}}$, m_{ij}, is given by

$$m_{ij} = \begin{cases} V_i - V_j, \text{ if } V_i > V_j \\ 0, \text{ otherwise.} \end{cases}$$

5. SYSTEM PERFORMANCE

5.1 Introduction

The three system performance measures used in the evaluation of the SAATMS are capacity, safety, and delay. These three performance measures are interrelated; two of these measures must be specified to obtain a unique specification of the third. The delay and safety have been specified as requirements (Ref. 1); the capability of the system to provide capacity must be evaluated.

The safety specification requires that the safety provided by the SAATMS be the same as it is in today's system or better. The safety provided by today's system has been established in terms of the blunder protection afforded each user aircraft. This section discusses the results of the evaluation and shows that the SAATMS provides the same level of blunder protection for each user in the terminal area as is presently provided.

The safety of the SAATMS for enroute area operations has been determined in terms of the number of collisions expected in the 1995 and post-1995 time frame. These data have been normalized to the Critical Near Mid-Air Collision (CNMAC) data for the year 1968. The number of collisions expected in 1995, assuming that today's system was used for control of air traffic, has also been determined. The two safety values have been compared; the safety afforded by the SAATMS is orders of magnitude greater than that provided by the extension of today's system.

The specification for delay is stated as a probability distribution of delay associated with each airport. The specification is that the departure delays and landing delays during an average busy hour shall be 6 min or less for 50 percent of the flights, 15 min or less for 90 percent of the flights, and 30 min or less for 99.9 percent of the flights. This section determines the capacity efficiency of each airport under the conditions that the delay characteristics associated with each airport meet the specification.

The design goal of the SAATMS is to provide a capacity at each airport, and throughout the entire terminal region, that satisfies the demand. The capacity of each airport used by the SAATMS is determined and compared with the four specified demand levels to evaluate the efficiency of the system design in meeting its goal.

This section presents the results of the safety analyses and the evaluation of the capacity efficiency provided by the SAATMS. This section also presents the values of the system parameters, the subsystem parameters, and the system constraints used in the evaluation and analysis of the SAATMS.

5.2 System and Subsystem Parameter Values

5.2.1 Surveillance and Navigation Subsystem Parameters

The values of the surveillance and navigation subsystem parameters used in the evaluation of the SAATMS were obtained from subsystem performance analyses (Volume III). The values used are as follows:

σ_s, σ_n = 100 ft = Standard deviation of the surveillance and navigation position errors, respectively

$\sigma_{\dot{s}}$, $\sigma_{\dot{n}}$ = 10 ft/sec = Standard deviation of the surveillance and navigation velocity errors, respectively

$\tau_s = \begin{cases} 8 \text{ sec} = \text{Surveillance update interval for in-trail aircraft} \\ 2 \text{ sec} = \text{Surveillance update interval for aircraft on parallel approaches and for aircraft entering the system} \end{cases}$

τ_n = 5 sec = Navigation update interval

M_s, M_n = 0 = Mean value of the surveillance and navigation position errors, respectively

$M_{\dot{s}}$, $M_{\dot{n}}$ = 0 = Mean value of the surveillance and navigation velocity errors, respectively

The surveillance and navigation errors, ε_s and ε_n, respectively, are assumed to be the sum of two random variables which possess means of zero and equal variances. One of the random variables is exponentially correlated with a time constant of 1800 sec; the second is assumed to be uncorrelated.

5.2.2 System Parameters

One of the most important system parameters is the separation standard, Q_s. The separation standard is given by

$$Q_s = W_N + W_B + W_T + W_M \qquad (1)$$

where

W_N = Width of the aircraft's normal operating zone (NOZ)

W_B = Width of the buffer zone (BZ)

W_T = Separation distance allowed to protect against wake turbulence

W_M = Miss distance (given that the maximum protected blunder has occurred)

Each of these distances must be established to evaluate the AATMS performance.

5.2.2.1 Normal Operating Zone

The track model, discussed in Section 4, was exercised using the appropriate values of the SAATMS subsystem parameters. Figure 5.2-1 is a curve of W_N as a function of the SAATMS intervention rate, $\dot{N}_I$. The constants K_a, K_p, K_v, K_d shown on the figure represent aircraft dynamics. Their values were chosen such that the actual position and velocity errors for $r_d = \dot{r}_d = 0$ were approximately the same as the navigation position and velocity errors. The selection of a value for W_N is dependent on the specification of an acceptable intervention rate. In enroute airspace where the aircraft density is generally low and capacity is not constrained, large values of W_N can be used to yield a low intervention rate. In the terminal area, and especially in the final approach zone, higher values of intervention rates can be used to reduce W_N and to enhance airport capacity. The value of W_N selected as appropriate for the SAATMS is 1800 ft. This yields an intervention rate of approximately one intervention per aircraft per hour, which is well within the capacity of the SAATMS communications subsystem. Decreasing W_N below 1800 ft would greatly increase the intervention rate without achieving a comparable gain in capacity.

5.2.2.2 Buffer Zone

The selection of the appropriate value for the buffer zone width, W_B, involves establishing the blunder protection for the system, since the aircraft safety is directly dependent on the size of the buffer zone. The width of the Buffer Zone is given by:

$$W_B = \frac{A_B\tau^2}{2}\left(1 - \frac{A_B}{A_R}\right) - \frac{\sigma_{\dot{s}}^2}{2A_R} + K_s\left(\sigma_s^2 + \left[\tau\left(1 - \frac{A_B}{A_R}\right) - \frac{\hat{\dot{r}}_o}{A_R}\right]^2 \sigma_{\dot{s}}^2 + \frac{\sigma_{\dot{s}}^4}{2A_R^2}\right)^{1/2} \qquad (2)$$

where

A_B = Blunder acceleration for which protection is to be provided

A_R = Return acceleration commanded by the system

σ_s^2 = Variance of the surveillance position errors

$\sigma_{\dot{s}}^2$ = Variance of the surveillance velocity errors

K_s = Constant related to the probability of detecting a maximum blunder

τ = Total system time delay

$\hat{\dot{r}}_o$ = Measurement of the aircraft velocity at time t_o

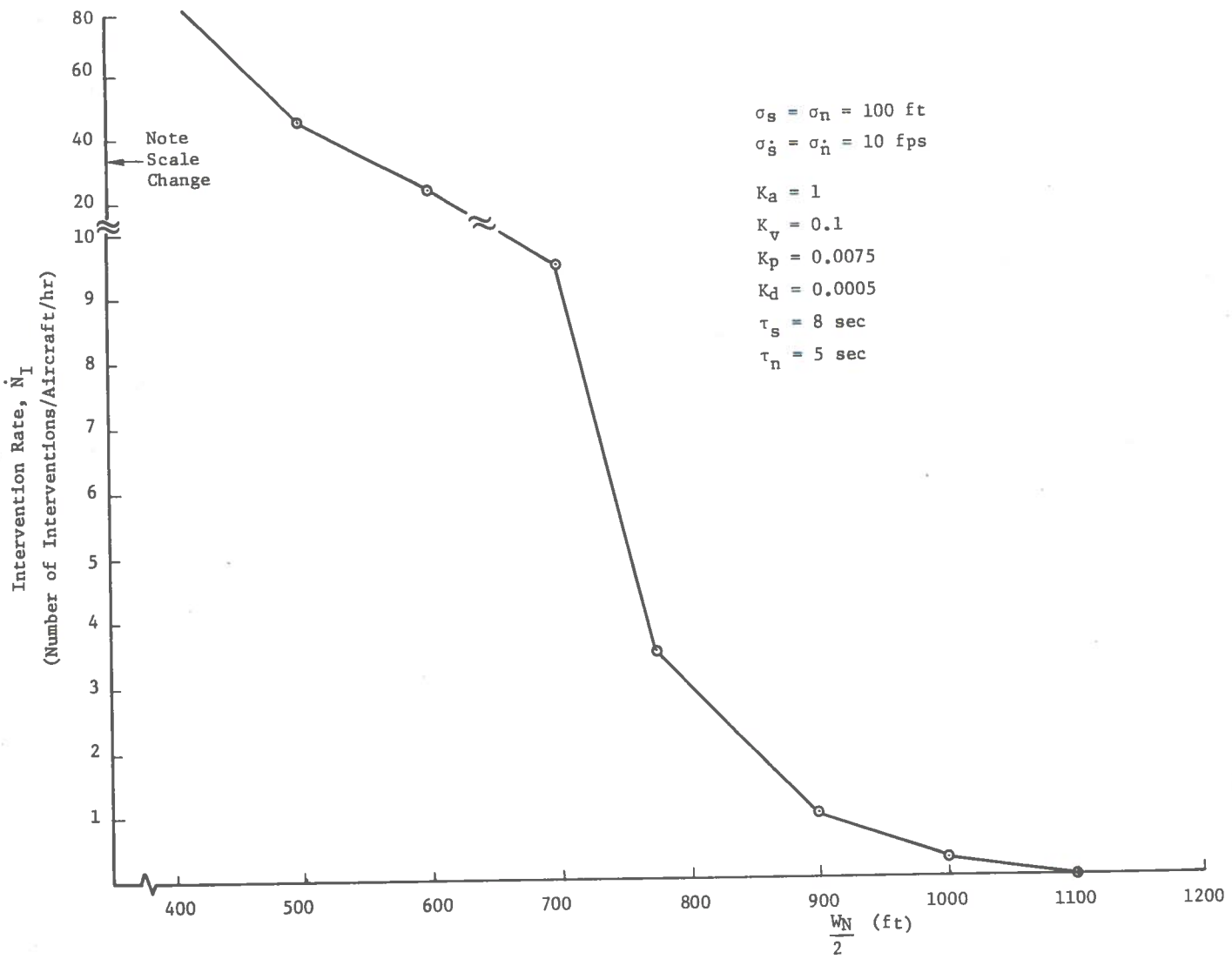

Figure 5.2-1. W_N vs N_I

The values of these parameters for the SAATMS are as follows:

(1) $\sigma_s = 100$ ft

(2) $\sigma_{\dot{s}} = 10$ ft/sec

(3) $\tau = 12$ sec (τ is the sum of the surveillance update interval, τ_S, and the system command delay time, τ_D; $\tau_S = 8$ sec and $\tau_D = 4$ sec)

(4) $K_S = 3$ (corresponding to a 3-σ case)

(5) $\hat{\dot{r}}_o = 20$ ft/sec

(6) $A_R = -16$ ft/sec^2

In order to determine A_B, the protected blunder acceleration, the safety afforded aircraft by today's system must be established. The level of safety of today's system can be obtained by solving Eq. (2) for A_B using the appropriate parameter values. The values assumed for the present system are

$\sigma_s = 1000$ ft

$\sigma_{\dot{s}} = 100$ ft/sec

$\tau = 18$ sec

The values of A_R, K_S, and $\hat{\dot{r}}_o$ were assumed to be the same as those used for the SAATMS. The separation standard, Q_S, used in the present system is 3 nmi. The width of the buffer zone would then be given by

$$W_B = Q_S - W_N - W_T - W_M \qquad (3)$$

If wake turbulence is not considered, then $W_T = 0$. The miss distance, discussed in Section 4, is somewhat arbitrary. The value selected for W_M for the SAATMS is 300 ft, which is larger than the largest physical dimension of any aircraft in use today. Finally, if the value of W_N selected for the SAATMS is used for today's system, then the blunder protection can be determined. This is a conservative estimate since the values of the SAATMS surveillance and navigation errors are much smaller than today's system. The value of W_N for the present system should then be larger than that for the SAATMS. Using the conservative estimate

$$W_B = 18{,}000 - 1{,}800 - 300 = 15{,}900 \text{ ft}$$

Figure 5.2-2 is a plot of the buffer zone width, W_B, as a function of the blunder acceleration, A_B, for both the SAATMS and the present system. For W_B = 16,000 ft, the blunder acceleration for which the present system will protect aircraft is A_B = 14 ft/sec^2. Using this value of A_B for the SAATMS yields a buffer width, W_B = 2700 ft, as can be seen from the lower curve in Fig. 5.2-2.

5.2.2.3 Separation Standard for In-Trail Aircraft

The minimum value of the separation standard, Q_S, for in-trail aircraft using SAATMS is

$$Q_S = W_B + W_N + W_M = 2700 + 1800 + 300 = 4800 \text{ ft}$$

The separation standard of 0.8 nmi for SAATMS will provide the same safety as the present system, assuming no wake turbulence. Conditions under which no wake turbulence exists were used in the evaluation of SAATMS performance in order to determine the maximum capacity for the specified values of safety and delay. If wake turbulence exists, aircraft must be separated by a greater distance, reducing the system capacity. At present, the separation standard for aircraft following heavy jet aircraft is increased from 3 to 5 nmi, employing a wake turbulence distance, W_T, of 2 nmi. The evaluation of the SAATMS performance was parametric in nature, so that the capacity of the system can be obtained using varying values of W_T to determine the effects of increased separation due to wake turbulence.

5.2.2.4 Parallel Path Operations

The 3 nmi separation standard used in the present system applies to in-trail aircraft (along track dimension) in the terminal area. Cross-track separation is allowed to be less than the along-track separation under certain conditions. Aircraft on parallel approach paths to parallel independent runways may be separated by as little as 5000 ft under IFR conditions. This 5000 ft separation distance impacts aircraft safety. Establishing the safety of today's system under these conditions will permit the establishment of the safety requirements for the SAATMS and will permit the specification of parallel independent runway spacing for the SAATMS. Figure 5.2-3 shows the buffer zone width, W_B, as a function of the protected blunder acceleration for parallel approach paths to parallel independent runways. The upper curve represents the operation of today's system; the lower curves are representative of the SAATMS capabilities. The figure illustrates that a Buffer Zone of 5000 ft yields a protected blunder acceleration of 11.5 ft/sec^2 for today's system. Using this blunder acceleration, the two potential Buffer Zones for SAATMS are 2270 ft or 850 ft. The 2270 ft zone resulted from use of an 8-sec surveillance update interval coupled with a 4-sec system command delay time; the 850-ft zone resulted from a 2-sec surveillance update interval coupled with the same 4-sec system command delay time.

The width of the SAATMS normal operating zone for final approach conditions is shown in Fig. 5.2-4 as a function of the intervention rate, $\dot{N}_I$. During final approach, navigation data are obtained from a system such as MLS or an advanced ILS. The errors are assumed to be smaller than that provided by the SAATMS navigation subsystem. The values used as inputs to the track model to obtain the curve of Fig. 5.2-4 are

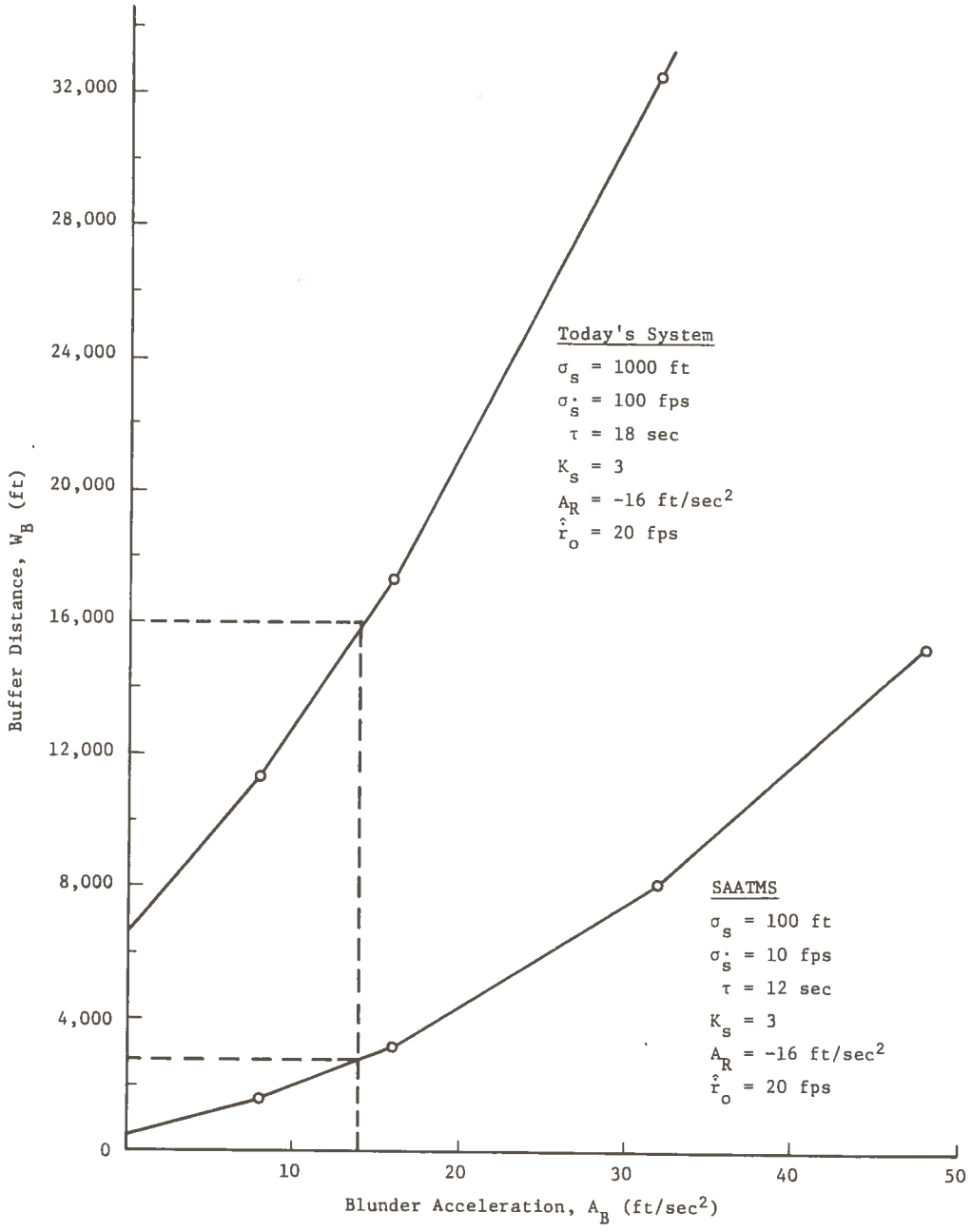

Figure 5.2-2. W_B vs A_B for the SAATMS and Today's System

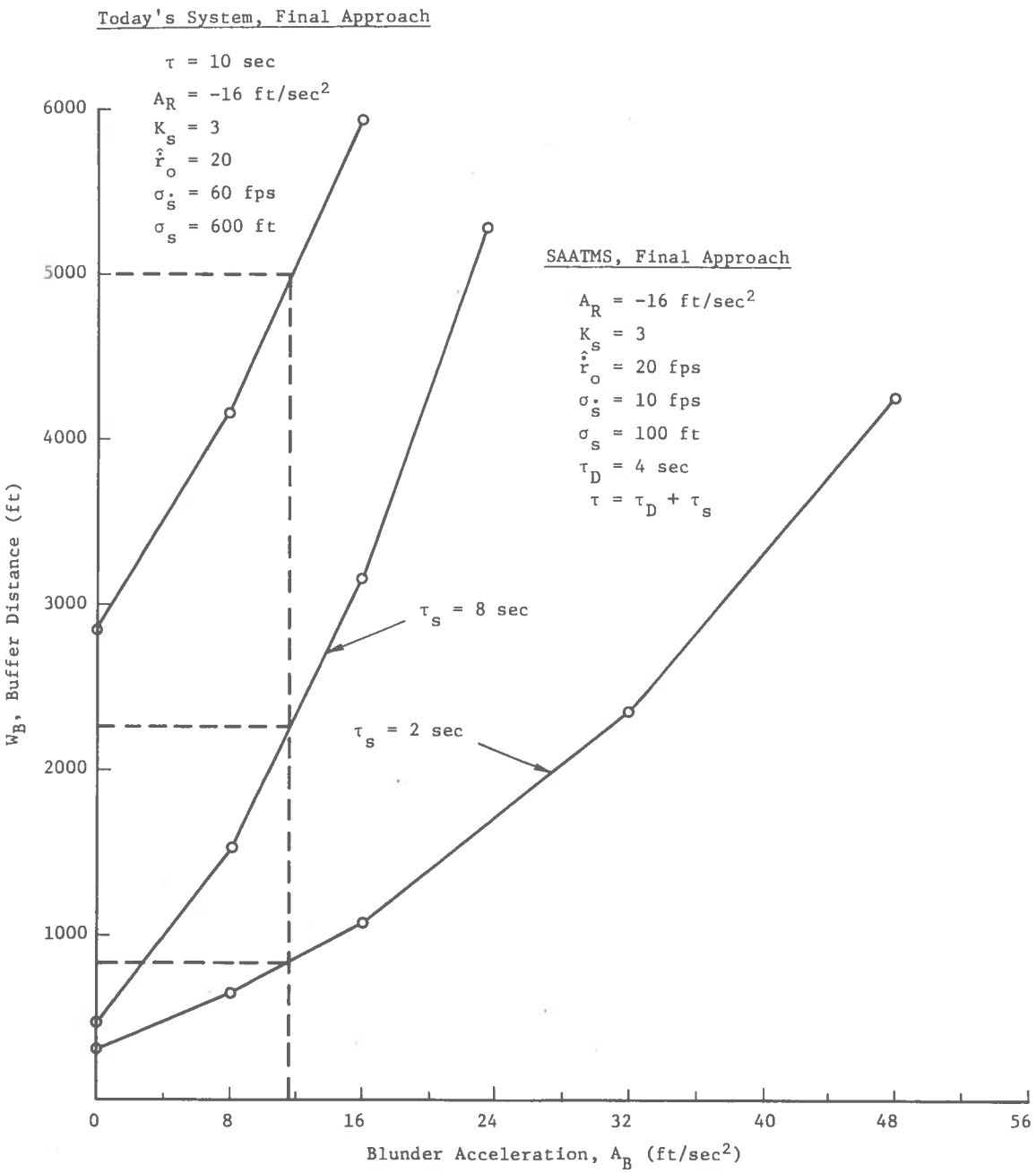

Figure 5.2-3. W_B vs A_B for Final Approach Cross-Track Separation

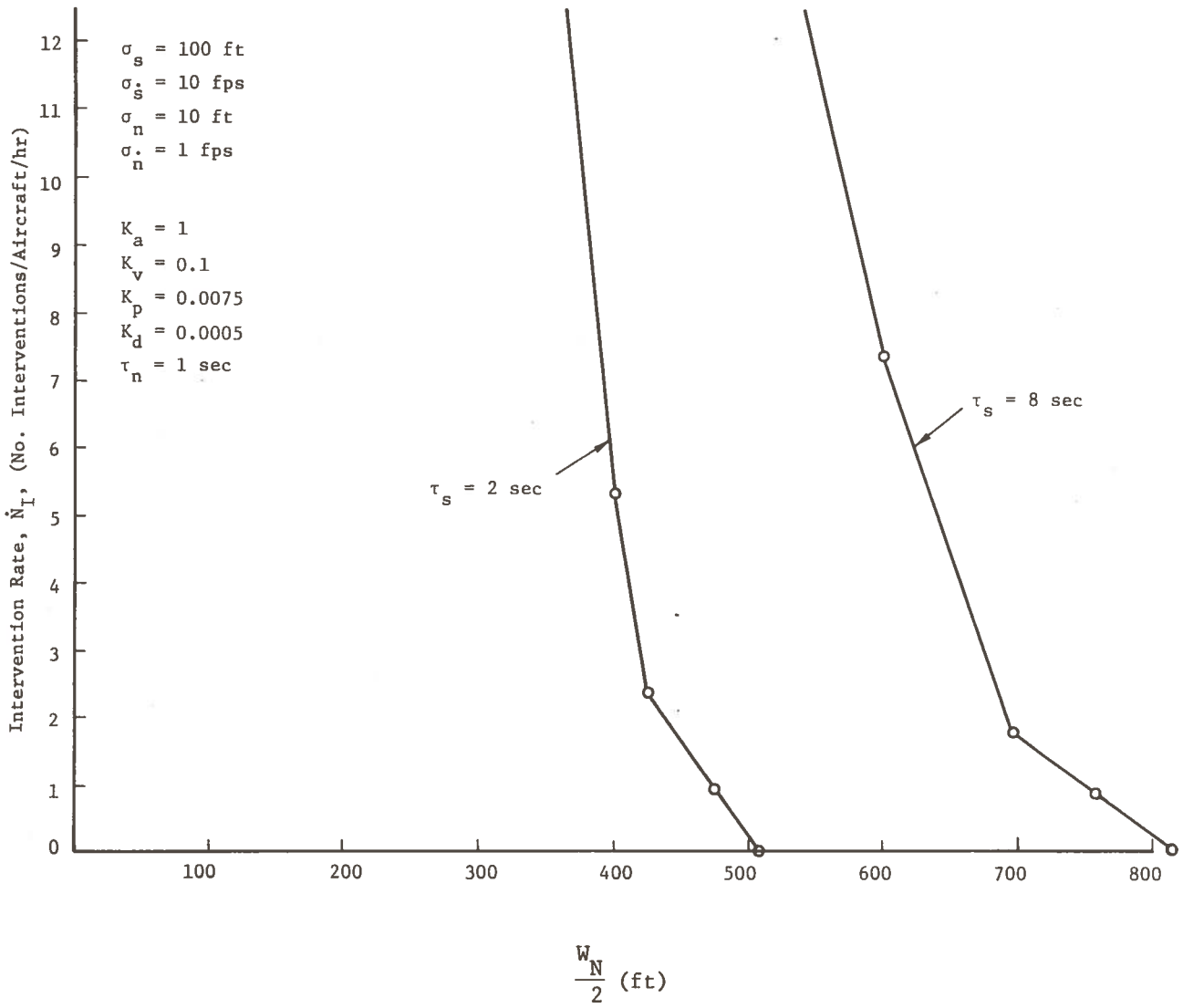

Figure 5.2-4. W_N vs $\dot{N}_I$ for Final Approach Conditions

σ_n = 10 ft = Landing system position error standard deviation

$\sigma_{\dot{n}}$ = 1 ft/sec = Standard deviation of the landing system velocity error

τ_n = 1 sec = Landing system update interval

Figure 5.2-4 shows the potential values of the width of the SAATMS Normal Operating Zone, W_N, vs the intervention rate, $\dot{N}_I$. For an intervention rate of one intervention per aircraft per hour, the values of W_N could be 1500 ft and 950 ft. The 1500-ft zone results from an 8-sec surveillance update interval while the 950-ft zone results from a 2-sec update interval.

Combining the width of the Normal Operating Zone with the width of the Buffer Zone and the selected miss distance yields the following cross-track separations:

For τ_s = 8 sec and τ_D = 4 sec,

$$Q_s = 1500 + 2270 + 300 = 4070 \text{ ft}$$

And for τ_s = 2 sec and τ_D = 4 sec,

$$Q_s = 950 + 850 + 300 = 2100 \text{ ft}$$

Use of a 2-sec surveillance update interval, τ_s, would allow SAATMS to separate aircraft on parallel final approaches by 2100 ft, with an intervention rate of one intervention per aircraft per hour. Use of a 2-sec update interval would require a higher processing capability, since a greater amount of surveillance data must be processed. Use of an 8-sec update interval with the same intervention rate would require less processing capability but would necessitate an aircraft separation of 4070 ft. In both cases a higher intervention rate, $\dot{N}_I$, would permit smaller separation of aircraft but would increase the required capacity of the communications subsystem. The ultimate SAATMS mechanization will depend upon the costs involved with the control processing and communication subsystems for the specified aircraft separation. The recommended mechanization for SAATMS requires a 2-sec surveillance update interval for aircraft on parallel final approach paths.

In summary, the system and subsystem parameters of SAATMS yield an along-track separation standard of less than 1 nmi and a cross-track separation standard on final approach of less than 0.4 nmi while maintaining safety at the same level as the present system.

5.3 Capacity

The network model described in Section 4 was exercised to determine runway capacity for various mixes of aircraft classes for various separation standards. Airport capacity was determined by adding the capacity of each runway at the airport.

It is conceivable that the capacity of an air traffic system is limited by some portion of the system other than the runway. A bottleneck analysis was performed to determine that portion of the system that does limit capacity. (Under saturation conditions there will be a bottleneck at some point.) This analysis readily indicated the runways (including the approach airspace) as the limiting constraint on capacity, assuming adequate taxi and gate facilities. If the capacity of a single runway is determined, the airport capacity can then be determined as the sum of the capacity of each airport runway.

5.3.1 Single Runway Capacity

The capacity of a single runway is a function of the mix of aircraft using the runway. The mix for each runway of the airports in the Los Angeles region was derived from the terminal area demand data supplied by The Mitre Corporation. The snapshot demand data consisted of the position, altitude, velocity, origin, and destination of 1840 instantaneous airborne aircraft. The number and type of the aircraft using each runway at each of the 43 airports of concern were derived from the snapshot data. The data cover 48 airports in the region; however, the 5 military airports were not considered because of the limited demand projected for these airports in 1995.

Using the aircraft classes designated in Section 3, Scenarios, the mix at the 43 airports of interest was determined in terms of the percentage of aircraft in each of these six classes. The resultant 43 mixes were examined for similarities; these similarities were used to combine mixes, resulting in a specification of 13 mixes which accurately represent the aircraft mix at the 43 airports. Details of the airports and aircraft mixes can be found in Appendix A.

Exit velocities can affect runway occupancy time and in turn runway capacity. The exit velocity is assumed to be 50 fps (30 knots) for all mixes with the following exception. A low exit velocity of 20 fps (12 knots) is used for mixes M1 and M2, which consist of class A (single engine GA) and class B (multi-engine and turbo prop GA) aircraft only.

Another factor affecting the capacity of a runway is the set of rules regarding aircraft use of a runway. The following five rules are assumed to apply to runway operation in the SAATMS:

(1) The minimum safety separation between two airborne aircraft on approach will not be violated.

(2) Two aircraft may not be on the same runway at the same time.

(3) An IFR departure cannot be initiated unless the following arrival is more than 40 sec from the threshold.

(4) A departure followed by another departure must be appropriately spaced (60 sec between IFR departures).

(5) Aircraft on final approach are given priority.

Rules 3 and 4 contain timing restrictions on IFR operations. These same constraints are assumed not to exist for VFR conditions. Thus, runway capacity will be a function of meteorological conditions. Runway capacity was determined for both VFR and IFR conditions.

Using the system performance models, capacity values for each of the 13 mixes of aircraft for various separation standard values, Q_s, under IFR conditions were determined and are shown in Table 5.3-1. Three different capacity values are shown for each separation standard value and each aircraft mix. The first capacity value shown in Table 5.3-1 is the runway saturation capacity. The second is a capacity efficiency value, corresponding to a landing or departure delay for each aircraft, that satisfies the most constraining of the following specified delay conditions:

(1) The probability that the delay is 6 min or less is 0.5; $P(D \leq 6) = 0.5$.

(2) The probability that the delay is 15 min or less is 0.9; $P(D \leq 15) = 0.9$.

(3) The probability that the delay is 30 min or less is 0.999; $P(D \leq 30) = 0.999$.

The third capacity measure in Table 5.3-1 is the capacity efficiency value for an average aircraft delay of 3 min.

Aircraft delay depends on the time spacing between successive aircraft. This spacing was determined from the snapshot data mentioned earlier. These data contain the position and velocity of 1840 airborne aircraft at one instant of time. For each aircraft traveling to a given airport, its arrival time at the airport was determined by dividing its distance from the airport by its velocity. Statistics on the differences between these arrival times were determined in the form of a histogram. These statistics were found to be Poisson. That is, the probability distribution function describing the time, t_a, between successive arrivals is given by

$$P(t_a < T) = 1 - e^{-\lambda T}$$

where λ is the arrival rate.

For VFR conditions and for the case of dual runway operations (arrivals only on one runway and departures only on the other) capacity values similar to those of Table 5.3-1 were determined.

The values shown in Table 5.3-1 were obtained by use of the network simulation model using Poisson statistics for aircraft arrivals. The saturation capacity values were also determined analytically as a check on the simulation results. The results shown are for mixed operation of arrivals and departures on each runway with a departure/arrival ratio of one. Capacity values for arrivals or departures only on a runway are of interest for the case of parallel runways at an airport. Depending on the spacing between the runways and meteorological conditions, the runways may be operated either as independent runways or dependent dual runways. Mixed arrivals and departures are allowed on independent runways, while parallel runways operated in a dual mode only permit arrivals on one runway and departures on another.

Capacity values for very small separation standard values (0.1 and 0.5 nmi) were obtained from the network simulation model to determine the effect of runway occupancy rules on capacity. The limits on capacity for small values of Q_s are due to runway constraints (rules 2 through 4 above). Examination of Table 5.3-1 shows

Table 5.3-1. Runway Capacities for Each Mix for A/D_R Case

Runway Mix	Saturation Capacity (ops/hr)					Capacity Efficiency (ops/hr)									
						P(D<6)=0.5; P(D<15)=0.9; P(D<30)=0.999					Average Delay = $\overline{D}$ = 3 (min)				
	Q_s = (nmi)					Q_s = (nmi)					Q_s = (nmi)				
	3	2	1	0.5	0.1	3	2	1	0.5	0.1	3	2	1	0.5	0.1
M1	50	75	114	114	114	47	71	110	110	110	42	62	94	94	94
M2	51	76	113	113	113	46	72	111	111	111	38	60	101	101	101
M3	60	90	119	119	119	59	89	116	116	116	54	81	103	104	104
M4	50	73	118	120	120	48	70	113	113	113	42	64	106	106	106
M5	51	75	118	120	120	49	71	116	116	116	46	67	102	102	102
M6	53	77	116	119	119	49	76	117	117	117	42	64	102	102	102
M7	55	80	118	120	120	52	77	115	115	115	45	65	104	104	104
M8	55	80	117	120	120	53	79	117	118	118	46	65	104	104	104
M9	56	81	117	120	120	55	81	113	113	113	51	74	101	102	103
M10	95	114	114	114	114	91	112	112	112	112	84	106	106	106	106
M11	100	108	108	108	108	96	104	104	104	104	89	102	102	102	102
M12	86	102	110	111	111	84	99	106	109	109	77	92	101	103	103
M13	61	86	114	118	118	59	85	109	111	112	56	77	101	103	103

that for IFR conditions, there is little increase in capacity as Q_s decreases below 1 nmi. For all of the cases in Table 5.3-1, there is a departure between each arrival pair under saturation conditions. Under VFR conditions, where rules 3 and 4 do not apply, there is a significant increase in capacity with decreasing Q_s (for Q_s greater than or equal to 0.5 nmi) for all mixes composed primarily of GA aircraft. For the arrivals only case, there is an increase in capacity for decreases in Q_s down to 0.1 nmi for all mixes except the aircarrier mixes because the aircarriers have a longer runway occupancy time.

5.3.2 Airport Capacity

Using the capacities for each runway (as in Table 5.3-1) and the proper number of runways for each airport, the capacity for each airport as a function of separation standard for each case (VFR and IFR with either dual or independent parallel runway operation) was determined by summing the appropriate capacity values.

A comparison between demand and capacity for busy hour operations is given by the curves of Fig. 5.3-1. (The demand data for each airport was furnished by The Mitre Corporation.) In this figure, comparisons are made for three different airport classes (primary, secondary, and feeder) for VFR, IFR-independent runways, and IFR-dual runway operation. Three demand levels are shown where demand level three is taken to be 1.5 times demand level two and demand level four is three times demand level two. The curves show the number and percent of airports in each class, for which the busy hour demand exceeds the capacity.

5.4 Demand-Capacity Comparisons by Airport Class for the Los Angeles Area

The demand data supplied by The Mitre Corporation specified the busy hour operations at each of the airports in the Los Angeles area. The demand data for each airport was influenced by the capacity The Mitre Corporation assumed for the busiest airports, considering the unconstrained demand for 1995 (demand level 2). Whenever the unconstrained demand exceeded the assumed capacity for the busiest airports, the excess demand was redistributed to other airports. The redistributed or constrained demand results in the demand-capacity comparison data presented in Fig. 5.3-1. The airport capacities that The Mitre Corporation computed were based on the use of a 2 nmi aircraft in-trail separation and a 5000 ft parallel independent runway separation. The SAATMS can provide the same level of safety for 0.8 nmi in-trail separation and 2000 ft parallel independent runway separation. The airport capacities for SAATMS will be different than that computed by The Mitre Corporation, since the reduced separation standards will provide higher capacities. Figure 5.3-2 presents capacity-demand comparison data by classes of airports. The curves were obtained by summing the capacity efficiencies of the airports in each class; the curves also show the demand level associated with each airport class. The curves illustrate that at the 0.8 nmi aircraft in-trail separation standard, the SAATMS will be capable of meeting demand levels 2 and 3. The system will be able to support demand level 4 at the primary airports but not at the secondary and feeder airports. These curves reflect the constrained demand resulting from the redistribution of aircraft by The Mitre Corporation, based on a 2 nmi separation. If the aircraft were redistributed based on the airport capacities that the SAATMS can provide, it may be possible to support demand level 4 at a greater number of airports; however, the total capacity achieved by SAATMS is insufficient to satisfy demand level 4.

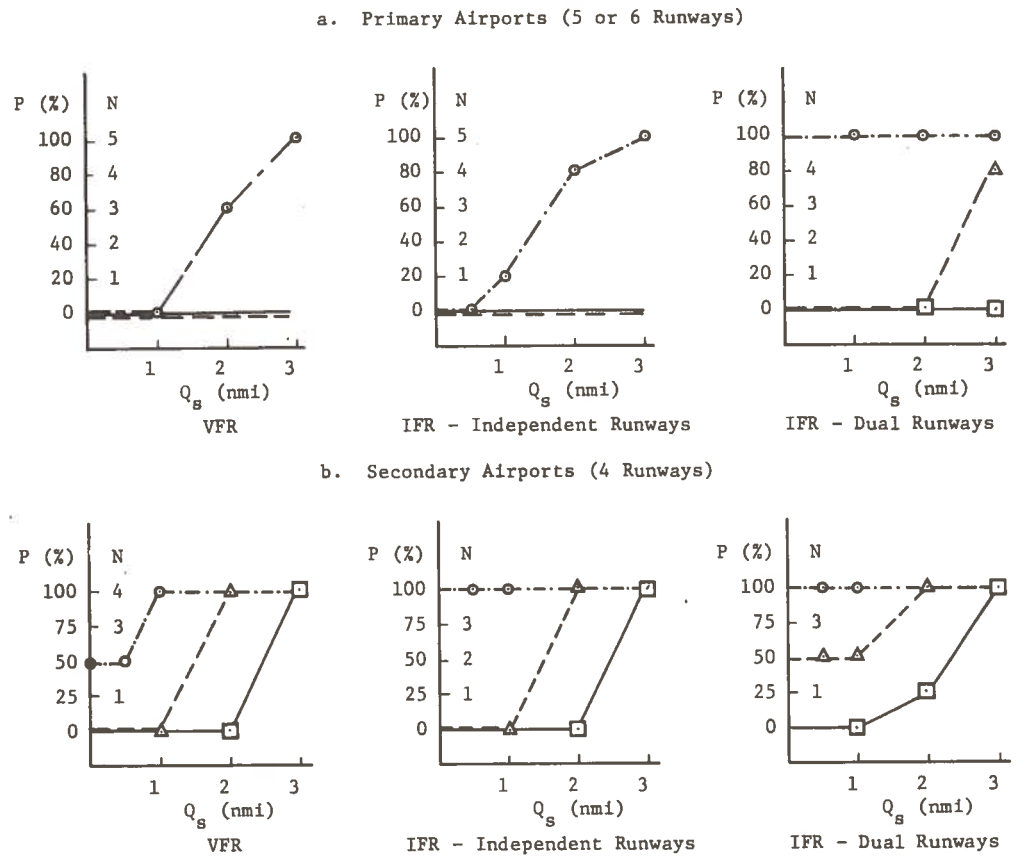

Figure 5.3-1. Demand-Capacity Comparison for Individual Airports by Class

c. Feeder Airports (1 to 3 Runways)

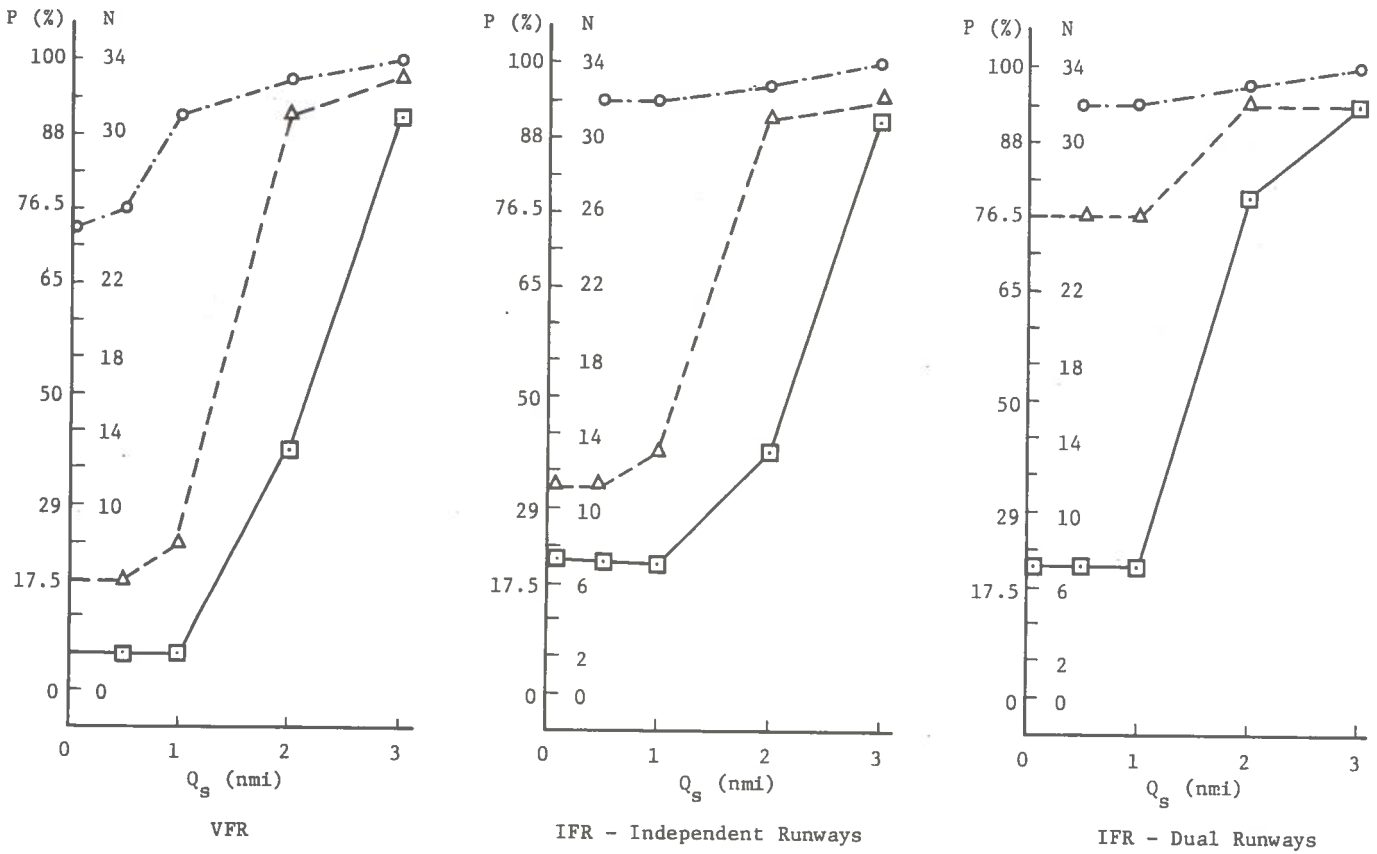

Figure 5.3-1. (Continued)

The effects of increased separation as a result of wake turbulence can be observed from Fig. 5.3-2. If the separation between aircraft using SAATMS must be increased from approximately 1 to 3 nmi due to wake turbulence, the capacity efficiency would be decreased. The major concern would be the capacity efficiencies at the primary and secondary airports, since they are the only airports that service the large jet aircraft. The capacity efficiency of the primary airports would decrease below the projected post-1995 traffic demand level (L4) but would still exceed the highest demand level (L3) projected for 1995. The capacity efficiency of the secondary airports would drop below the nominal traffic demand level (L2) postulated for 1995. This decrease in capacity efficiency would result in increased delay during those times when wake turbulence exists.

The major conclusion is that the primary constraint to achieving the capacity required to support the post-1995 postulated demand (demand level 4) is the number of feeder and secondary runways.

It should be noted that these demand-capacity comparisons are only for the demand during the busy hour. If the demand in the preceding or succeeding hour is less than that specified for the busy hour, the demand schedule could be arranged to smooth the peak demand. Unless the busy hour extends over a longer time than an hour, aircraft could be delayed until the demand decreased. All aircraft would eventually be serviced; however, the average delay would be increased. The demand-capacity comparison data have not considered the diurnal variation in the demand for each airport and its effect upon the aircraft delay or airport capacity efficiency.

5.5 Safety as Measured by Number of Conflicts

Results for the following three aspects of system safety are presented in this section.

(1) The number of enroute conflicts for the year 1995 for CONUS

(2) The effect of limited surveillance coverage

(3) The effect of not providing surveillance at non-tower airports

The 1995 enroute demand data developed by Autonetics was processed to provide an estimate of the number of enroute aircraft crossings and passages for the year 1995 for CONUS. Safety, as measured by number of aircraft conflicts, was then computed for the SAATMS, the GAATMS, and the present system. The conflict models and equations of Section 4.2 were used to compute the number of conflicts. The results are presented by IFR, VFR categories since the data contained this distinction and since different separation standards are used for these categories in some ATC systems. An IFR/IFR conflict involves only IFR aircraft while an IFR/VFR conflict involves both VFR and IFR aircraft.

Table 5.5-1 lists the expected number of IFR/IFR conflicts per year for each of the three ATC systems. These values indicate that SAATMS provides a safety level orders of magnitude greater than either GAATMS or the present system. Use of the present system in the 1995 scenario would result in 2,070 IFR/IFR conflicts; for the same scenario, the upper bound estimate for the GAATMS is 2.78 conflicts; while the upper bound estimate for SAATMS is 0.013 conflicts.

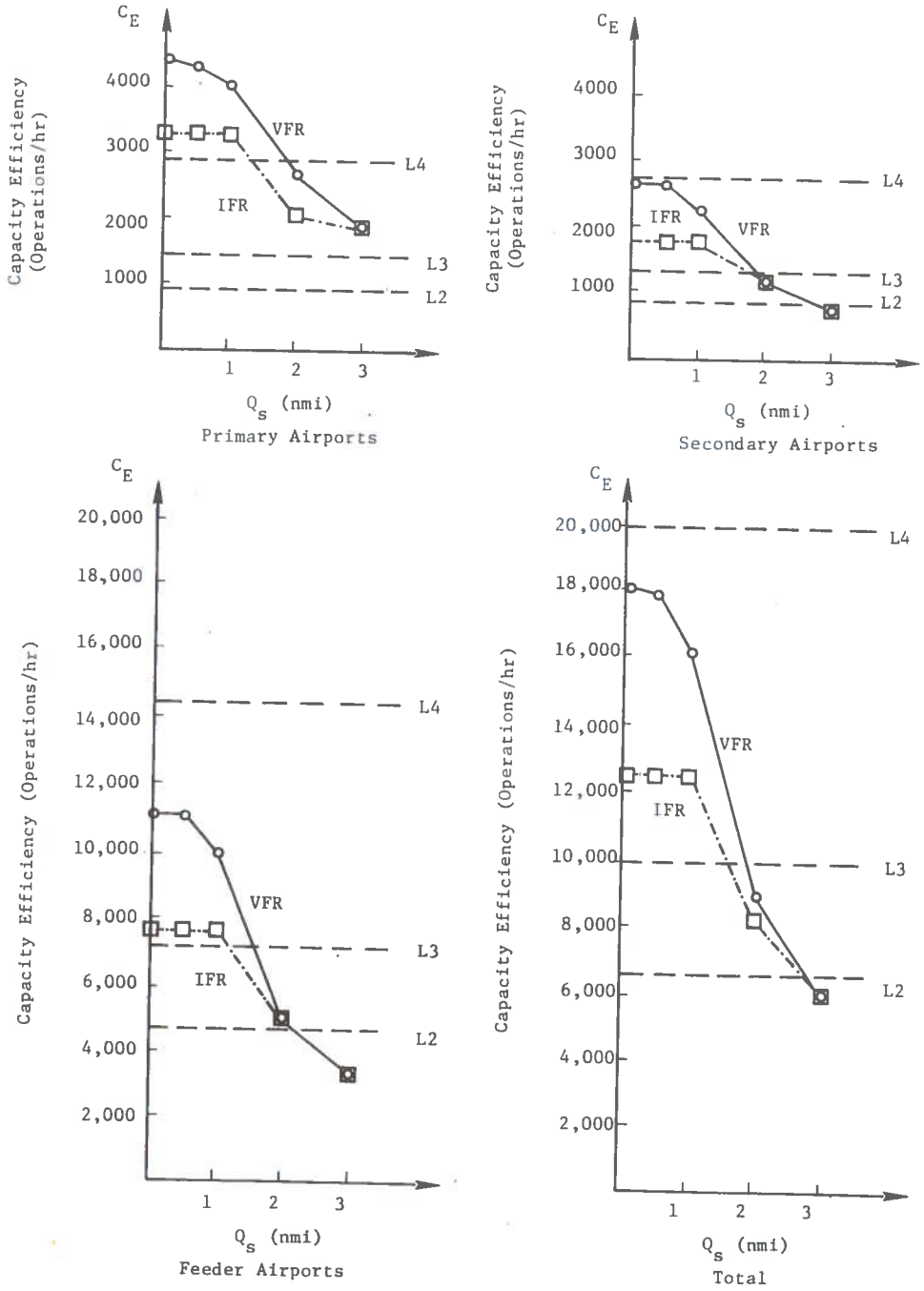

Figure 5.3-2. Demand-Capacity Comparison for Classes of Airports

Table 5.5-1. Number of Enroute IFR/IFR Conflicts per Year by ATM Systems

ATC System	Crossing Conflicts Per Year	Passage Conflicts Per Year	Total Conflicts
SAATMS	0.0125	0.0008	0.0133
GAATMS	2.620	0.165	2.780
Present	1870	200	2070

Note: In 1968, 106 crossing conflicts and 11 passage conflicts occurred.

The demand data used for this portion of the analysis was based on a national airfleet which included 6,700 aircarrier, 500,000 General Aviation, and 20,000 military aircraft. The data included the number of route intersections in the enroute area and the expected number of aircraft crossings and passages (Ref. 3). The data used is a conservative approximation of the demand level 3 data discussed in Section 3.1. The set of demand data used in the enroute IFR/IFR conflict analysis was selected because of its compatibility with the past data concerning collisions and critical near mid-air collisions used for normalization of the conflict equations.

The enroute IFR/VFR and VFR/VFR conflict analysis indicates that the SAATMS is 52.7 times as safe as GAATMS for the same surveillance coverage.

A unique characteristic of the SAATMS is that it provides surveillance coverage down-to-ground level throughout CONUS. This additional coverage allows surveillance of a significant number of potential conflicts that would not be detected by the other systems and results in a substantial improvement in system safety. Table 5.5-2 lists the estimated potential conflicts and midair collisions for two different levels of coverage.

Table 5.5-2. 1995 Enroute IFR/VFR and VFR/VFR Conflicts and Collisions in Uncovered Area as a Function of Coverage, Demand Level 2

No Coverage	Crossing		Passages	
	IFR/VFR, VFR/VFR Conflicts in Uncovered Areas	Midair Collisions in Uncovered Areas	IFR/VFR, VFR/VFR Conflicts in Uncovered Areas	Mid-Air Collisions in Uncovered Areas
Below 6000 ft	2064	36	1548	27
Below 2000 ft	586	10	440	8

As a result of the ground level surveillance coverage, the SAATMS provides coverage at non-tower airports. In the 1964-1971 interval, 100 midair collisions occurred at non-tower airports. Most of these collisions were between aircraft in the traffic pattern. The annual number of such collisions is expected to increase in 1995 due to the increase in air traffic. An optimistic estimate of such collisions in 1995 is 35 compared to a yearly average of 14 for the 7 years from 1964-1971. The surveillance coverage provided by SAATMS will allow separation assurance services to be provided to aircraft using the non-tower airports and will greatly increase system safety.

The following subsections present a more detailed discussion of the results of the safety evaluation.

5.5.1 Enroute IFR/IFR Conflicts

The number of enroute IFR/IFR conflicts was calculated using Eq. (4) of Section 4.2. Use of this conflict equation requires specification of aircraft passages and crossings (number and separation distance at point of closest approach), aircraft position keeping accuracies, and collision cross-sectional areas.

The number of aircraft crossings and passages per year by altitude bands for 1968 and those projected for 1995 were obtained by appropriate processing of the Autonetics enroute demand data. The average value of the separation distance at the point of closest approach for aircraft crossings was assumed to correspond to the existing 10 min separation requirement. For aircraft passages, this distance was assumed to be 7 nmi. Due to different aircraft speeds, the 10 min separation requirement results in different separation distances. The mix of aircraft in each altitude band (Ref. 3, 12) was used to determine the average separation distance. The aircraft position keeping errors were assumed to be the same as the ATM surveillance errors since the surveillance errors indicate the uncertainty in aircraft position as seen by the system. These surveillance data are used to keep aircraft separated, whereas navigation and pilotage errors determine the nominal route separation distances which result in acceptable intervention rates. The relative surveillance position errors for the present and the GAATMS were calculated from published data (Ref. 11) and the errors are shown in Table 5.5-3.

The collision cross-section area is a function of the conflict distance and the physical dimensions of the aircraft involved in the conflict. A 150-ft conflict was assumed (the aircraft are less than 150 ft apart). The mix of aircraft by altitude bands was used to determine the average aircraft dimensions. Combining the conflict distance with the average aircraft dimensions yields the average collision cross-section area.

Table 5.5-3. System Relative Position Surveillance Errors

System	Standard Deviation of Surveillance Position Error (ft)		Comment
	Horizontal, σ_H	Vertical, σ_z	
Present	11,400	350	200 nmi Radar Coverage
GAATMS	900	350	100 nmi Radar Coverage
SAATMS	100	100	Satellite Coverage

The normalization factor K in Eq. (4) of Section 4.2 was determined using 1968 demand and conflict data (Ref. 2). The 1968 conflict data were assumed to be 106 crossing conflicts and 11 passage conflicts. This estimate is four times the reported number, based on the assumption that only 25 percent are reported (Ref. 2). The conflicts were classed as Critical Near Mid-Air Collisions (CNMAC) where aircraft were separated by 150 ft or less at their point of closest approach.

The number of conflicts is a function of the aircraft position keeping accuracy and the separation distance at the point of closest approach. As an indication of the sensitivity to surveillance errors and crossing separation, Table 5.5-4 and Fig. 5.5-1 show the number of enroute IFR/IFR conflicts as a function of surveillance errors for both a 10-min and a 2-min crossing separation. As can be seen from the curves and the tabulated data, there is a significant decrease in the number of conflicts with a decrease in surveillance errors. Note that the calculation of the number of conflicts is based upon use of the present airway structure.

For the case of IFR/VFR and VFR/VFR conflicts in airspace that is under surveillance, the normalization of the conflict equation using 1968 data is not possible since VFR aircraft were not controlled by the ATC system in 1968. The IFR/IFR normalization factor should provide a reasonable estimate for this case, however, and this was used. The IFR/VFR and VFR/VFR crossings and passages were determined from the Autonetics enroute demand data. The minimum separation distance at the point of closest approach in this case was assumed to be 1 nmi. This corresponds roughly to the separation standard for the SAATMS given in Section 5.2. The normalized number of IFR/VFR and VFR/VFR enroute conflicts as a function of surveillance errors is given in Table 5.5-5 where the conflict numbers are normalized with respect to the SAATMS safety.

Table 5.5-4. Number of Enroute IFR/IFR Conflicts per Year as a Function of System Accuracy

System Designation	System Accuracy		Crossing Conflicts per Year		Passage Conflicts per Year	Total Conflicts per Year	
	σ_H (ft)	σ_z (ft)	10-min Separation	2-min Separation		10-min Separation	2-min Separation
A	50	50	0.0031	0.0153	0.0004	0.0034	0.0157
B (SAATMS)	100	100	0.0125	0.0625	0.0008	0.0133	0.0633
C	500	350	0.4400	2.200	0.0283	0.4683	2.230
D (GAATMS)	900	350	2.620	13.10	0.1650	2.780	13.30
E Present	11,400	350	1870	9350	198	2070	9550

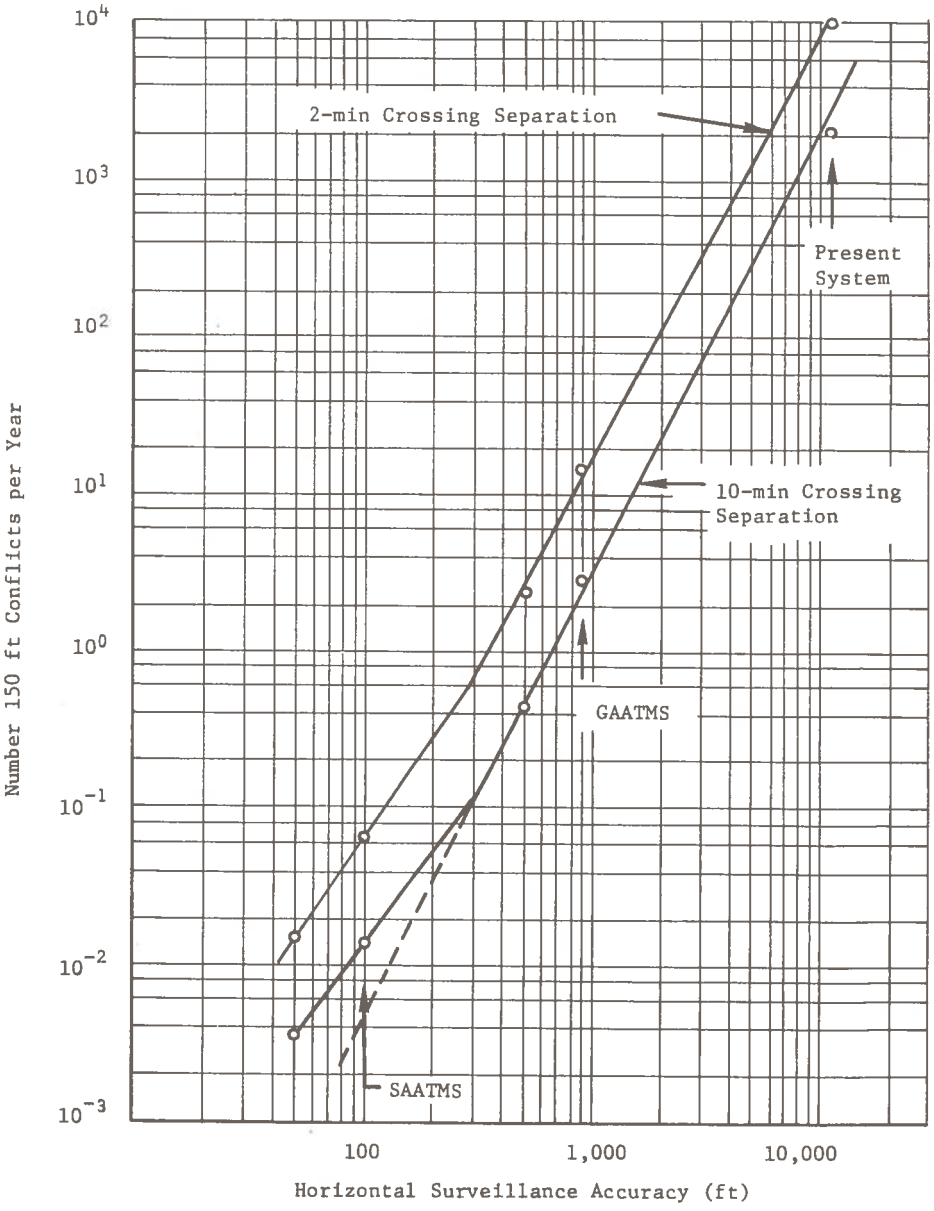

Figure 5.5-1. 1995 Enroute IFR/IFR Conflicts per Year for Demand Level 1A

Table 5.5-5. IFR/VFR and VFR/VFR Normalized System Safety for Crossing and Passage Conflicts

System Designation		Surveillance Errors		Normalized Conflicts
		σ_H (ft)	σ_z (ft)	
A		50	50	0.20
B	SAATMS	100	100	1.00
C		500	350	32.9
D	GAATMS	900	350	52.7

A comparison of the values in Table 5.5-5 shows 52.7 times as many conflicts for the GAATMS as for the SAATMS. These values assume all systems provide surveillance data at all altitudes.

5.5.2 Enroute Safety as a Function of Altitude Coverage

For an ATC system to prevent aircraft conflicts, it must have surveillance data giving relative aircraft states (e.g., position and velocity). If surveillance data are not available below a certain altitude, the ATC system cannot prevent conflicts below that altitude. To determine the effect of limited altitude surveillance coverage, the curves of Fig. 5.5-2 were generated. The lower curve shows along the Y-axis the number of IFR/VFR and VFR/VFR collisions that occurred in the year 1968 below a certain altitude (as given by values along the X-axis). The upper four curves represent the same relationship for the four projected demand levels. For demand level 2, if coverage were limited to altitudes 6,000 ft and above, over 60 midair collisions would occur below this altitude (where there is no surveillance).

These curves were obtained by assuming that the number of collisions in an altitude band are roughly proportional to the aircraft density in that band (Ref. 7). The number of enroute collisions considered here for 1968 was estimated from published data (Ref. 2, 10).

The curves of Fig. 5.5-2 indicate the importance of providing surveillance coverage to ground level to keep safety comparable to that achieved in 1968. For example, for demand level 2, if coverage is not provided down to 1500 ft, the number of collisions in the uncovered airspace will exceed the total number of collisions that occurred in 1968.

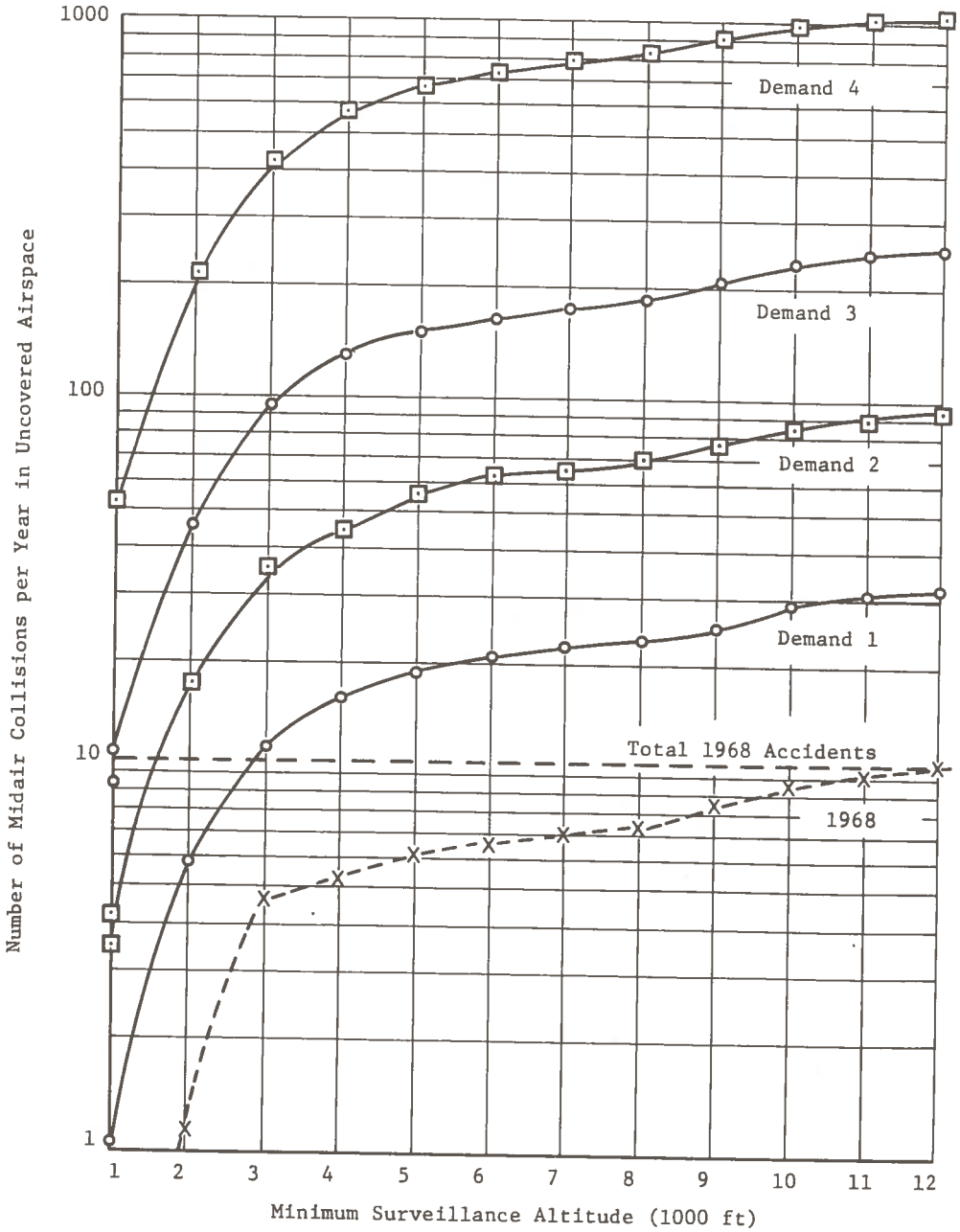

Figure 5.5-2. Midair IFR/VFR, VFR/VFR Enroute Collisions as A Function of Minimum Surveillance Altitude

5.5.3 Effect of Surveillance Coverage at Non-Tower Airports

Surveillance coverage at non-tower airports is another important factor affecting the safety of the SAATMS. In the 7-year interval from 1964 to 1971, 100 midair collisions (Ref. 10) occurred at non-tower airports, mainly in the traffic pattern. Since there were 76.3 million operations at uncontrolled airports in 1971, this results in an average of 0.1872 accidents per 10^6 operations. Assuming the following:

(1) That the number of midair collisions is proportional to the number of operations (Ref. 10)

(2) That the projected operations rise as a linear function of GA fleet size

Then, the number of non-tower midair collisions, NTA, is given by

$$NTA = OP_{1971} \times \frac{GA_{1995}}{GA_{1971}} \times AR \qquad (4)$$

where

OP_{1971} = Operations at non-tower airports 1971 (76.3×10^6)

GA_{1995} = Number of GA aircraft in 1995 (demand levels 1 through 4 have 250,000; 335,000; 500,000; and 1,000,000, respectively)

GA_{1971} = Number of GA aircraft in 1971 (137,000)

AR = Accident rate (0.1872 per 10^6 operations)

Using this equation, the number of midair collisions was computed for the four projected demand levels. The results are listed in Table 5.5-6. The comparisons with the 1971 values are quite striking: for demand level 2, there will be 35 collisions in 1995 compared with 14 in 1971.

The assumptions used to obtain these estimates are optimistic, since Ref. 2, 13, and 14 indicate that midair collisions increase as the square of operations in the terminal area. Also, the increase in operations might exceed the increase in the GA fleet size (Ref. 15).

Additional tower coverage or SAATMS surveillance coverage will keep these midair collisions from rising significantly over the 1971 level.

Table 5.5-6. Midair Collisions for Non-Tower Airports Without SAATMS Surveillance

Demand Level	Midair Collisions
1	26
2	34
3	52
4	104
1971	14

6. SENSITIVITY DATA

The performance of the SAATMS has been evaluated using the specific values of system and subsystem parameters derived from analyses of the system design. This section presents data showing the sensitivity of the system performance measures to variations in the most critical subsystem parameters. Not all system variables have been considered due to the enormity of the task; rather, results are presented for single parameter variations around the baseline values. The first set of sensitivity data concerns the separation standard and the level of blunder protection safety. The second set shows the sensitivity of capacity to variations in separation standard and aircraft mix.

6.1 Separation Standards

The sensitivity of the width of the normal operation zone, W_N, to navigation and surveillance position and velocity errors is shown in Fig. 6.1-1. The operating point for SAATMS is noted on the figure; both the surveillance and navigation position errors standard deviations, σ_p, are 100 ft. The standard deviation of the velocity errors, σ_v, are one-tenth the position values or 10 ft/sec^2. Increasing the position and velocity error standard deviations to 200 ft and 20 ft/sec^2 would increase the width of the normal operating zone to 3200 ft or an increase of 1400 ft. Decreasing the values by the same factor of two would reduce the zone to 1000 ft or a decrease of 800 ft.

Figures 6.1-2 through 6.1-7 illustrate the sensitivity of the width of the buffer zone, W_B, to parameter variations. Figure 6.1-2 shows the sensitivity of W_B to the standard deviation of the surveillance position and velocity errors for several blunder accelerations. The operating point of SAATMS is marked; SAATMS protects against blunder accelerations of 14 ft/sec^2 which is the same protection afforded system users today. Figure 6.1-3 presents the variation of W_B with various values of the total system time delay, τ. The total system time delay is the sum of the surveillance update interval, τ_S, and the command delay, τ_D. The command delay value is assumed to be 4 sec for the curves shown. Figure 6.1-4 shows the effect on the buffer zone width due to variations in the acceleration command issued to aircraft to return them to their normal operating zone. Figure 6.1-5 shows the sensitivity of W_B to the aircraft velocity at the start of the blunder. There is little sensitivity evidenced, which is expected since the system is designed to account for velocity. Figure 6.1-6 presents the sensitivity of the width of the buffer zone to a constant, K_S, which reflects the probability of an aircraft crossing the entire buffer zone and intruding into an airspace that may be assigned to another aircraft. Finally, Fig. 6.1-7 shows the sensitivity of the entire separation standard, Q_S, to variations in the standard deviation of surveillance and navigation position errors, σ_s and σ_n, respectively. Varying σ_s, σ_n will affect both W_N and W_B; the curves reflect the cumulative effect of these variations.

The sensitivity data presented have considered variations of the system and subsystem parameters. The variations of these parameters were concerned primarily with the effect of degradation, rather than improvement, to allow comparison of the SAATMS with the GAATMS and the present system, since these systems do not provide as high accuracies as the SAATMS.

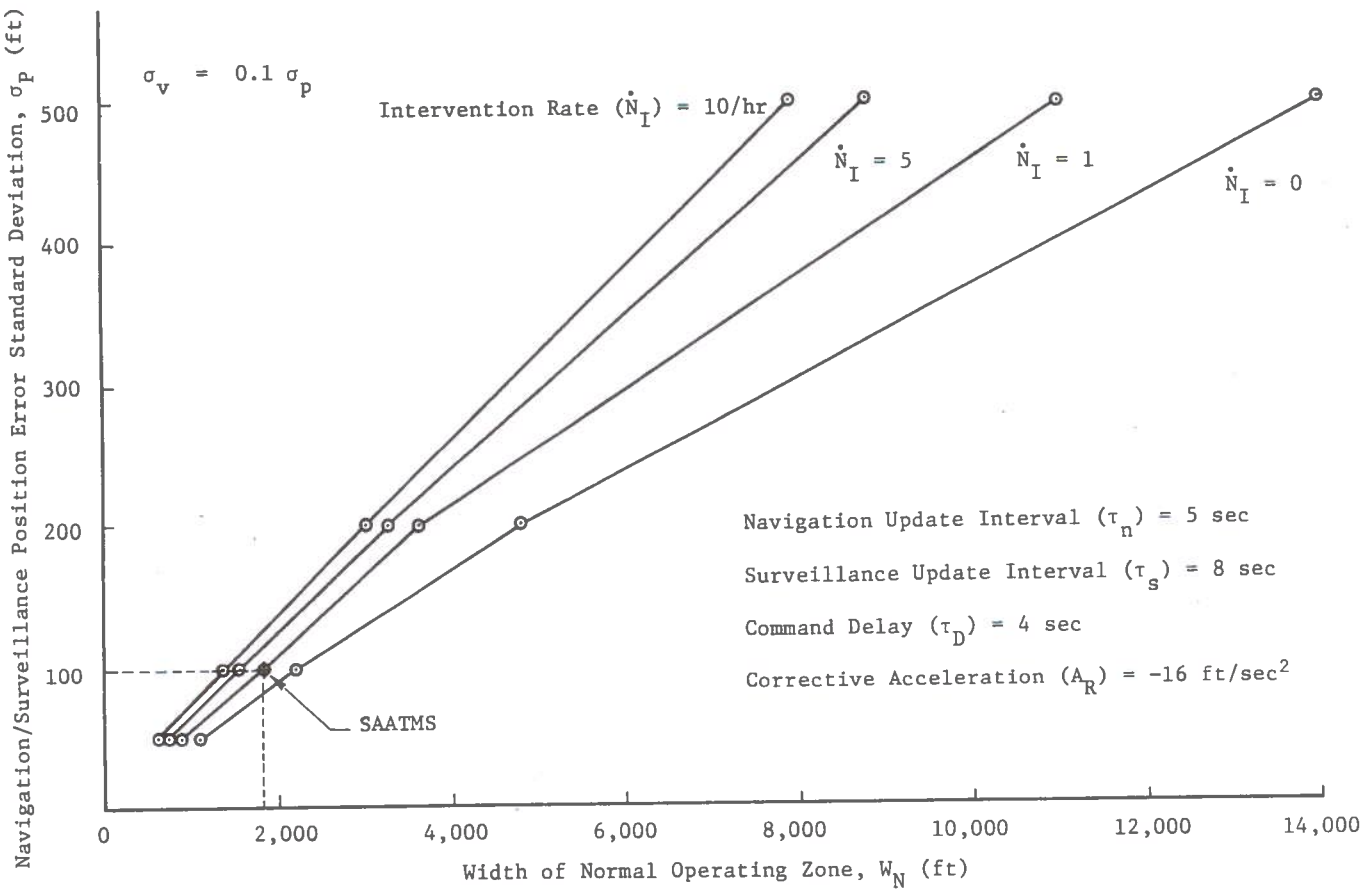

Figure 6.1-1. W_N vs Surveillance/Navigation Errors

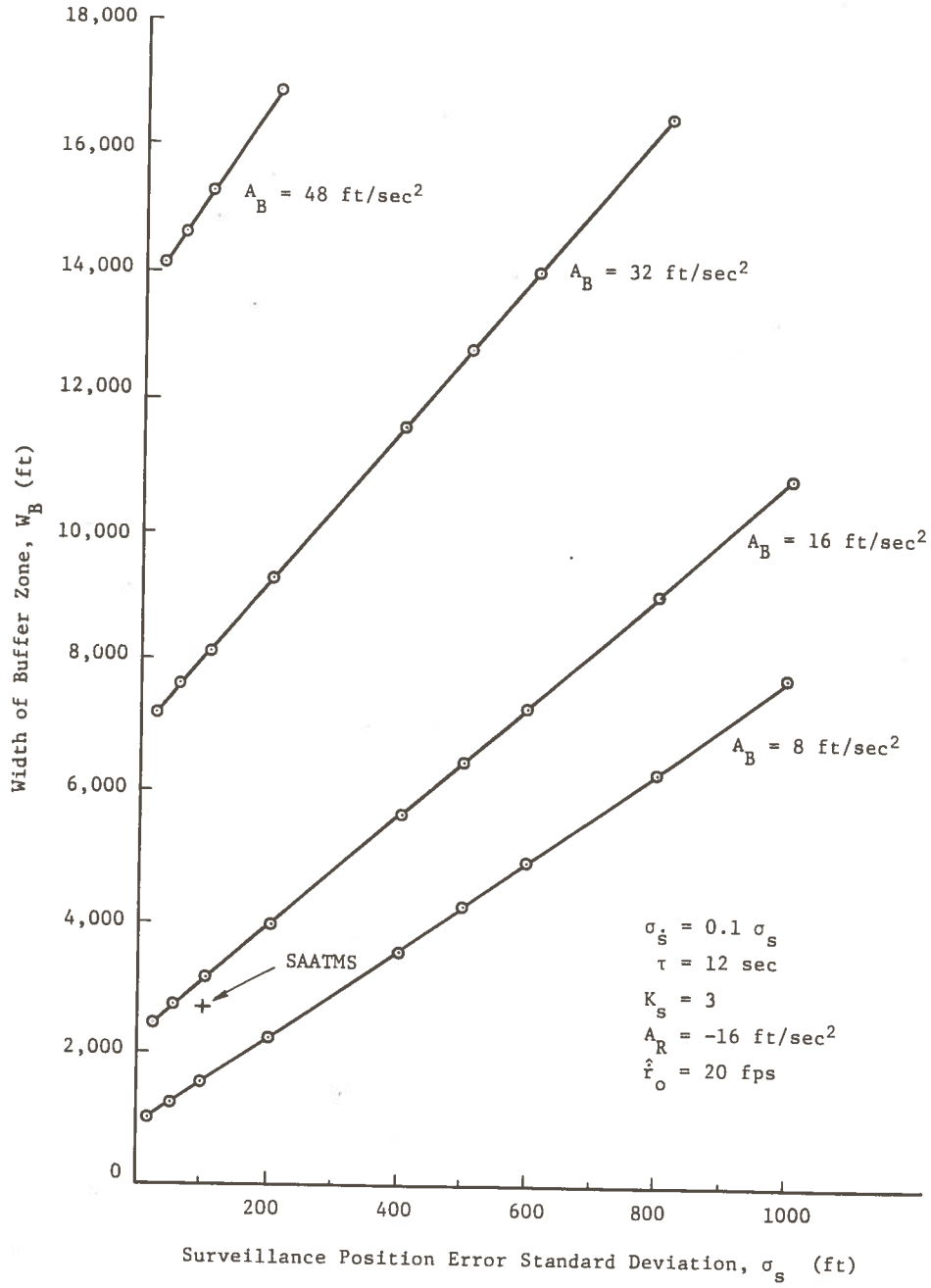

Figure 6.1-2. W_B vs σ_s, A_B

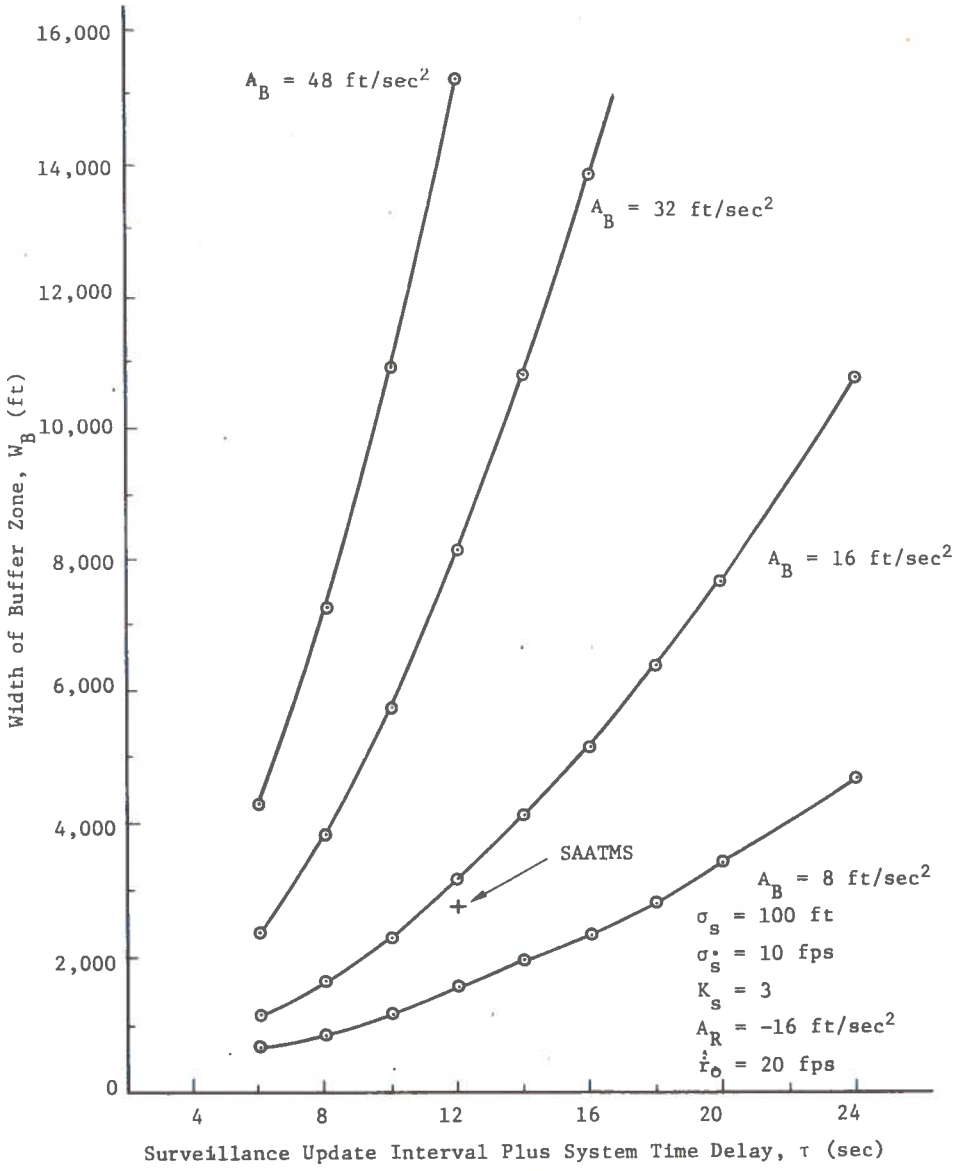

Figure 6.1-3. W_B vs τ Sensitivity Data

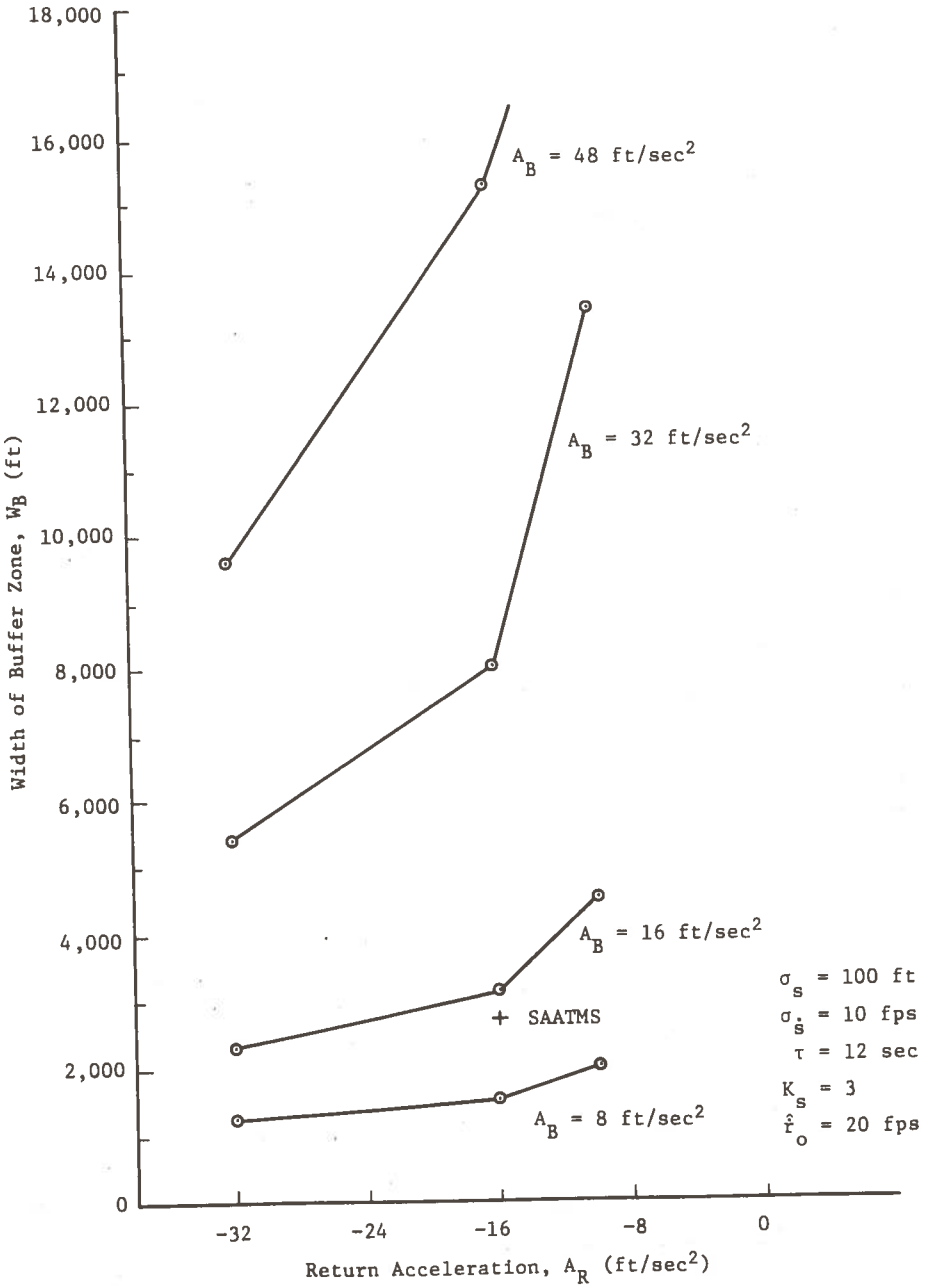

Figure 6.1-4. W_B vs A_R Sensitivity Data

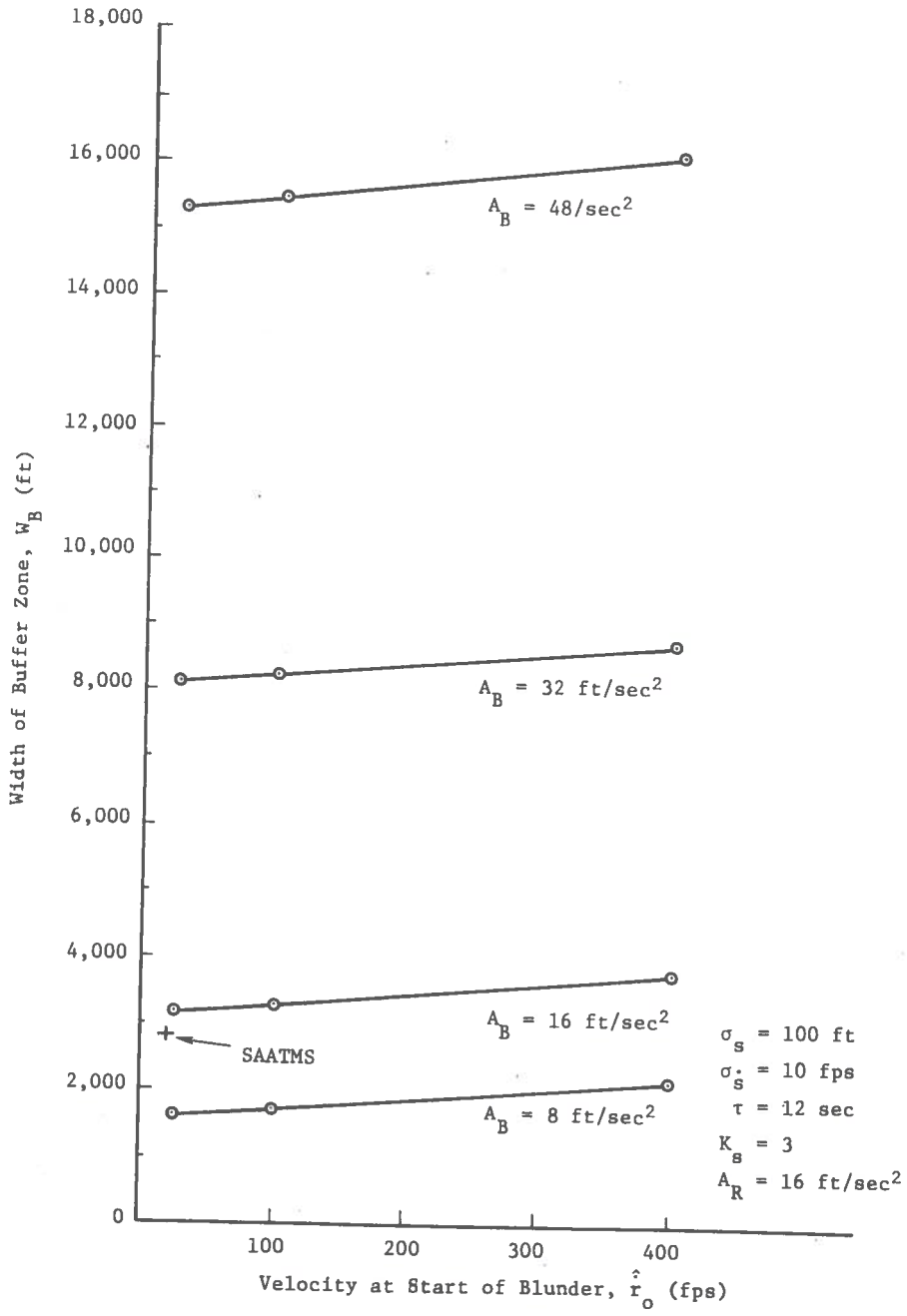

Figure 6.1-5. W_B vs $\hat{\dot{r}}_o$ Sensitivity Data

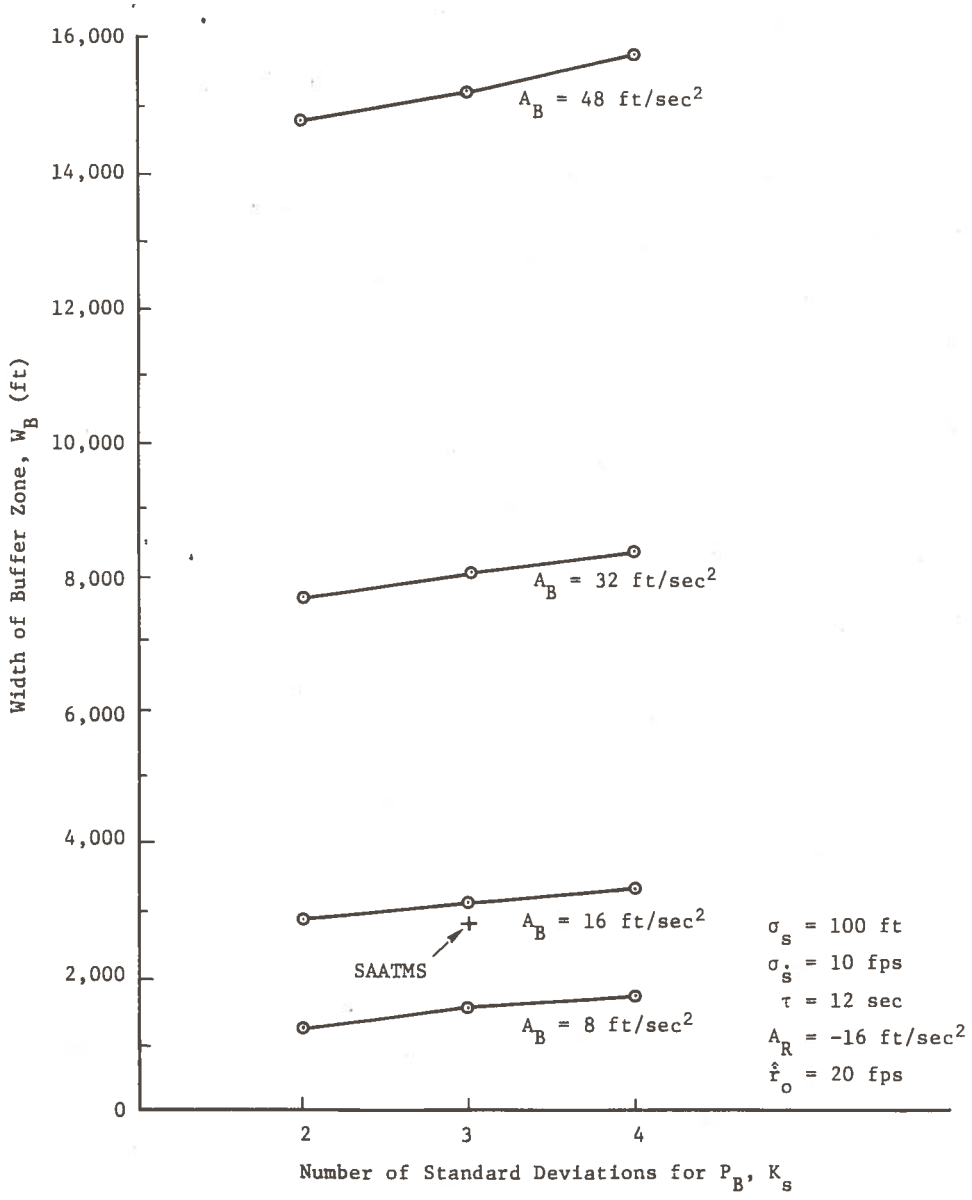

Figure 6.1-6. W_B vs K_S Sensitivity Data

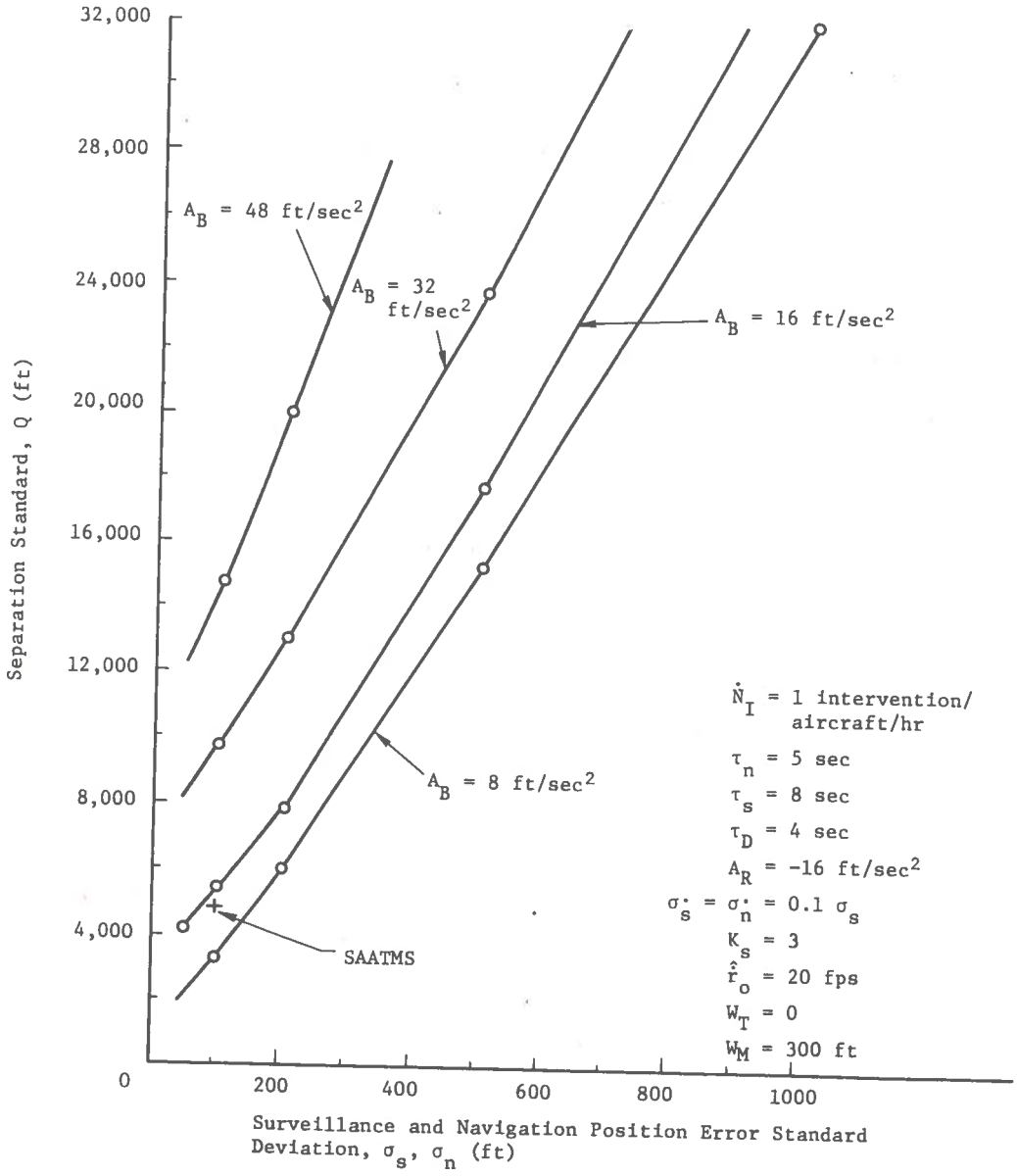

Figure 6.1-7. Q_S vs σ_s, σ_n Sensitivity Data

Figure 6.1-8 presents trade-off comparison data for surveillance errors and surveillance update interval as a function of the width of the buffer zone. These curves can be used to establish the required surveillance update interval for a specific surveillance error and a desired buffer zone width.

6.2 Capacity and Delay Sensitivities

The capacity of an airport or a runway may be sensitive to variations in separation standard and aircraft mix. That is, the capacity of a runway or airport may vary over a large range for relatively small changes in separation standard or aircraft mix. Figures 6.2-1 and 6.2-2 show runway saturation capacity as a function of separation standard for VFR and IFR conditions for the 13 mixes of aircraft discussed in Section 5. The curves show an increase in capacity with decreasing separation standards up to the point where the rules and procedures governing runway operations limit capacity. This break point occurs at different places for different mixes. For the mixes containing primarily aircarrier aircraft, the break point is at Q_S = 2 nmi. The effect of the more severe IFR runway rules (60 sec between IFR departures, 40 sec between an IFR departure and an arrival) is seen by comparison of the set of curves in Fig. 6.2-1 with those in Fig. 6.2-2 for values of the separation standards less than 1 mile. Under IFR conditions, it is apparent that decreasing the separation standard below 1 mile will not result in an increase in capacity (i.e., the capacity is insensitive to variations in separation standards below that point).

The relationship between average steady-state delay and capacity for a runway is illustrated by the curves of Fig. 6.2-3 and 6.2-4. Each circled point on the curves was obtained from a Monte Carlo simulation using the network model to simulate 5 hr of aircraft operations at a runway. The saturation capacity, C_S, is that value of capacity efficiency for which the average steady-state delay is infinite. In Fig. 6.2-3, for a separation standard of 2 nmi, C_S is 90. For an average delay of 3 min, for Q_S = 2 nmi in Fig. 6.2-3, the capacity efficiency is 76. The shape of the curves indicates a very large increase in delay with increasing capacity efficiency for capacity values close to the saturation capacity. The delay rapidly approaches and remains at a small value as the capacity efficiency is decreased below the saturation capacity value. For all of the delay data, the time interval between the appearance of arrivals and departures in the Monte Carlo simulations was a random number having an exponential probability distribution function (Poisson).

The curves of Fig. 6.2-5 and 6.2-6 show runway capacity efficiency curves with delay expressed as a probability distribution function. Each computer simulation run made with the network model for a given demand level generated data for one such curve. The required delay specification is illustrated by the dashed piecewise linear curve in both Fig. 6.2-5 and 6.2-6. This delay specification requires that the landing and departure delay be less than 6 min for 60 percent of all user

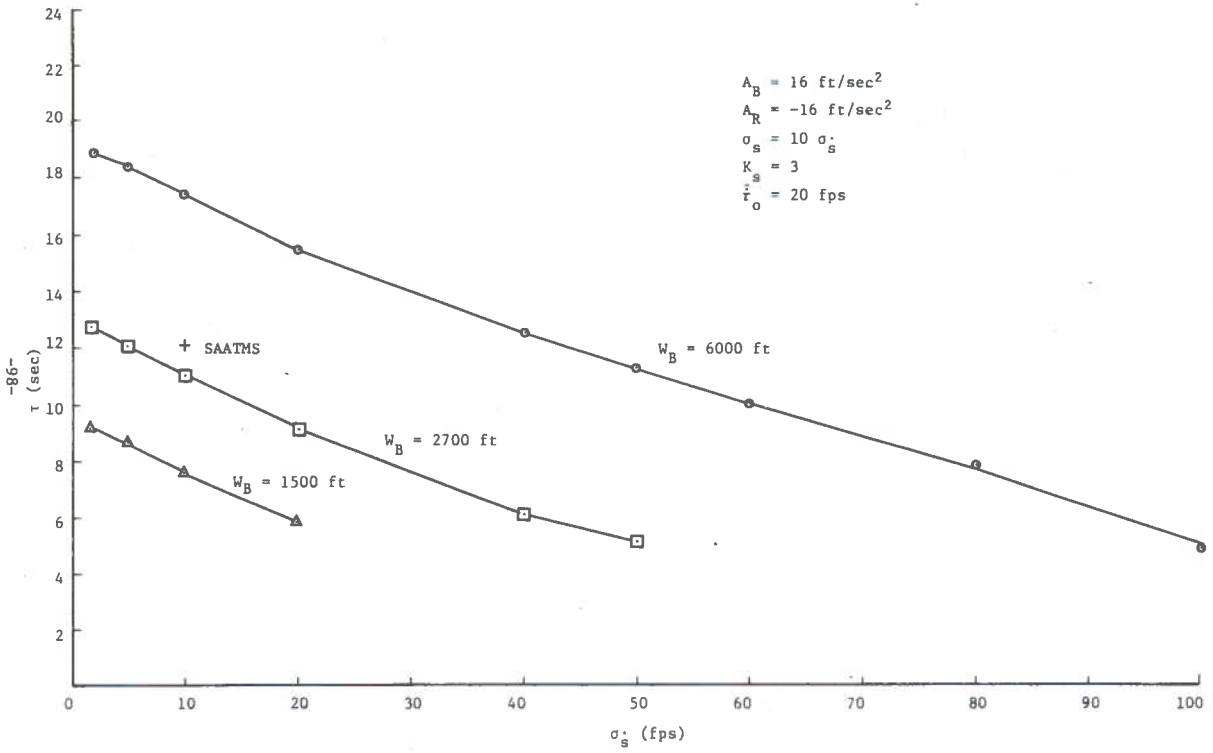

Figure 6.1-8. Surveillance Update Interval vs Surveillance Accuracy Tradeoff Curves for Buffer Distance, W_B

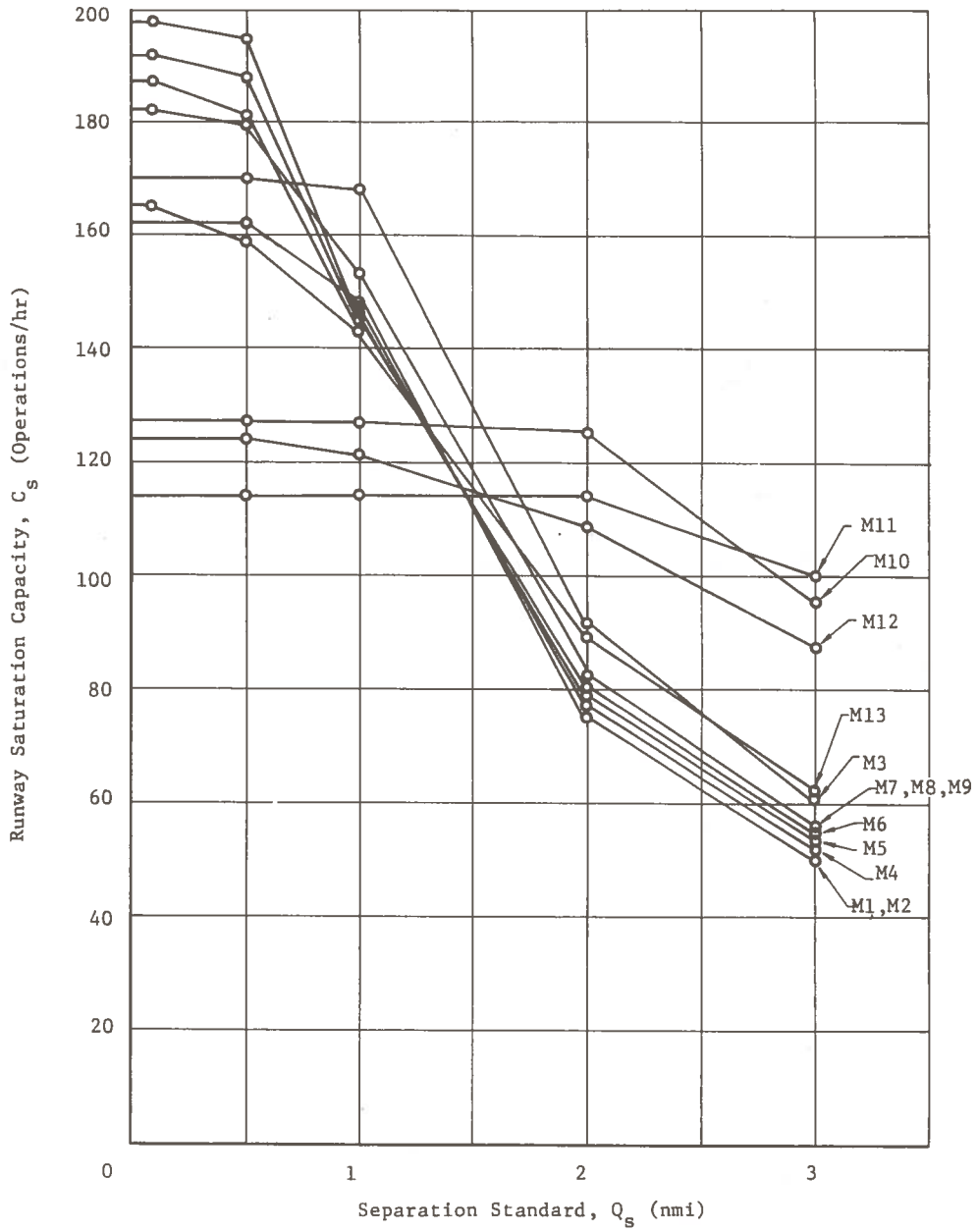

Figure 6.2-1. Runway Saturation Capacity vs Separation Standard for 13 Aircraft Mixes for VFR Conditions

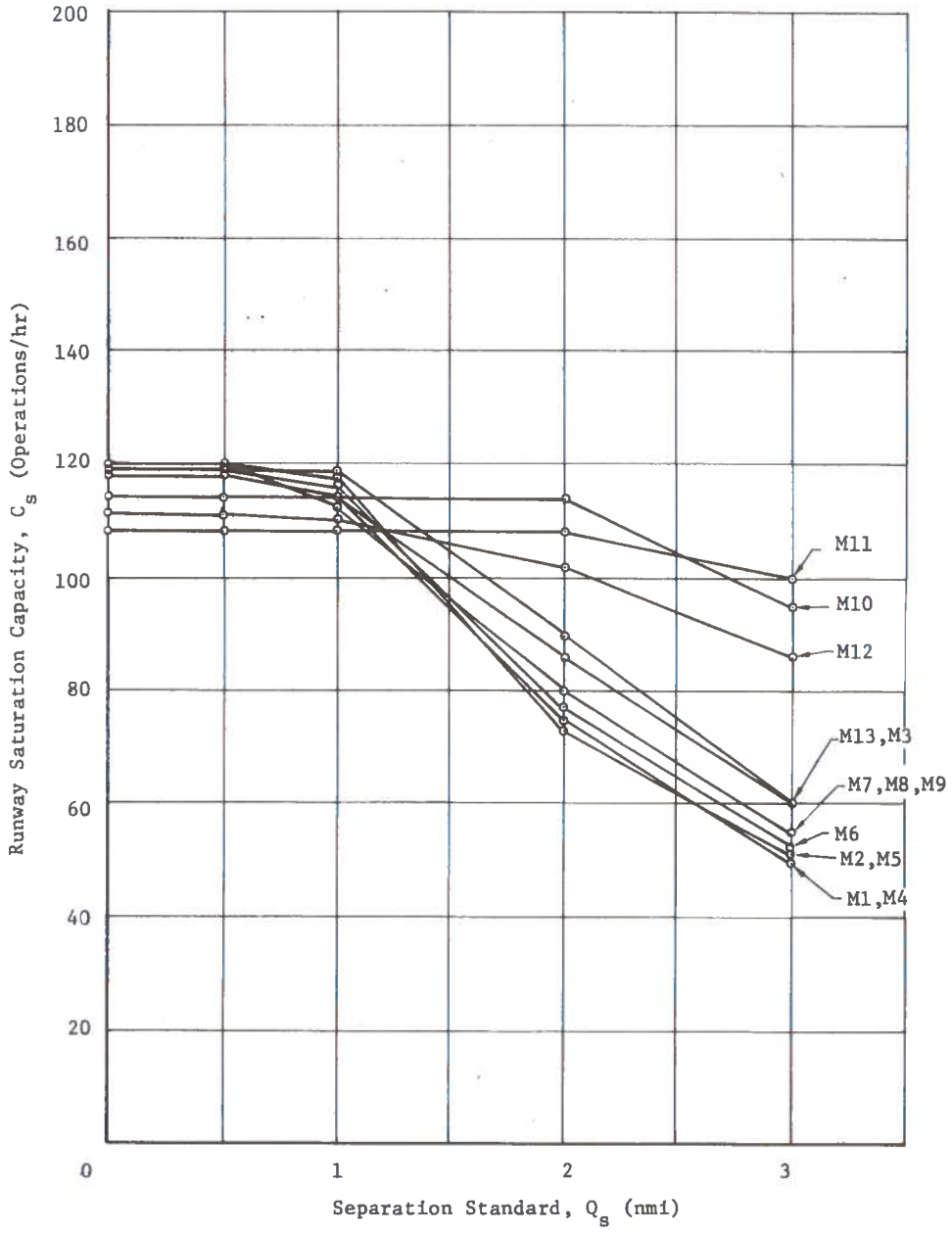

Figure 6.2-2. Runway Saturation Capacity vs Separation Standard for 13 Aircraft Mixes for IFR Conditions

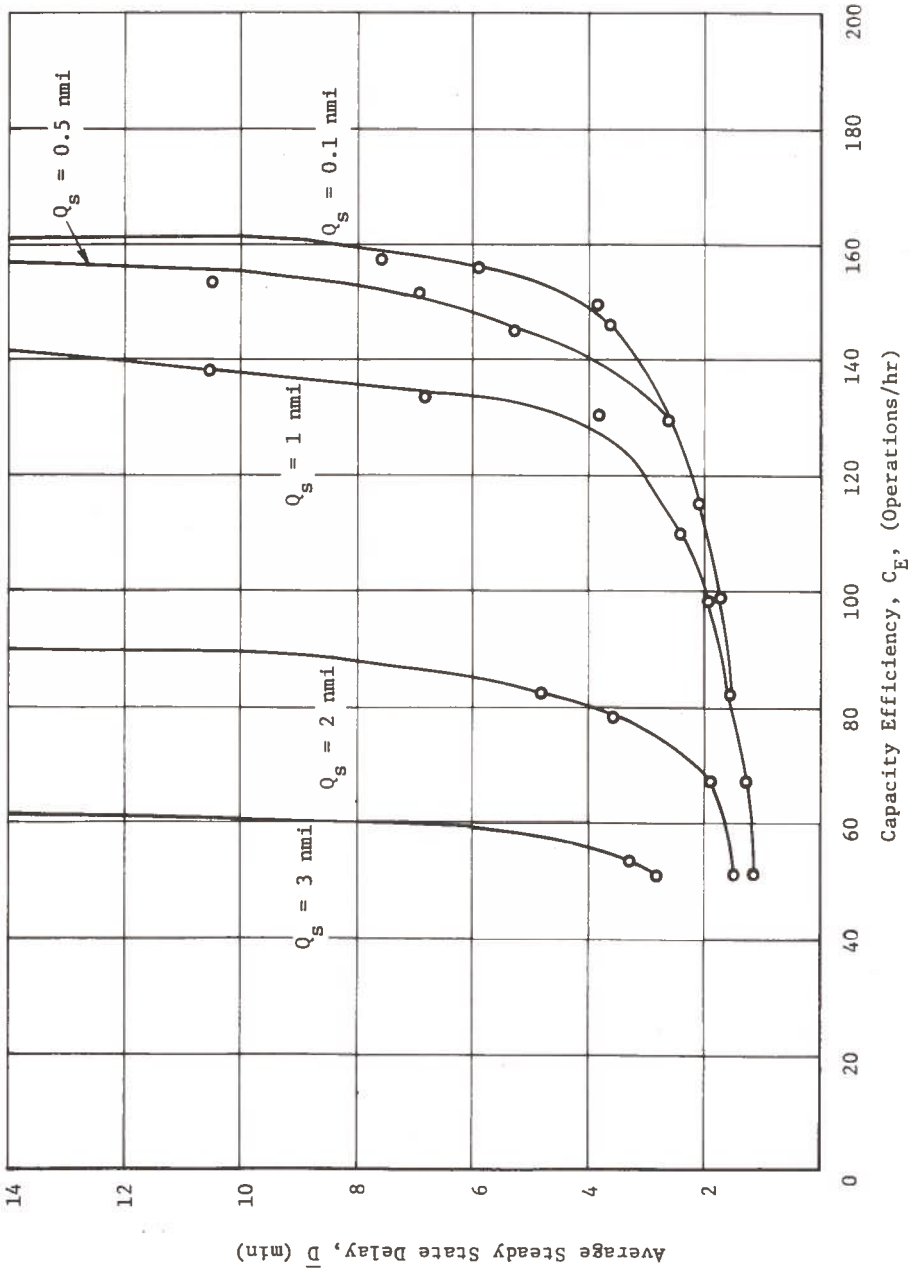

Figure 6.2-3. Runway Capacity vs Average Delay for VFR Conditions for Mix M13

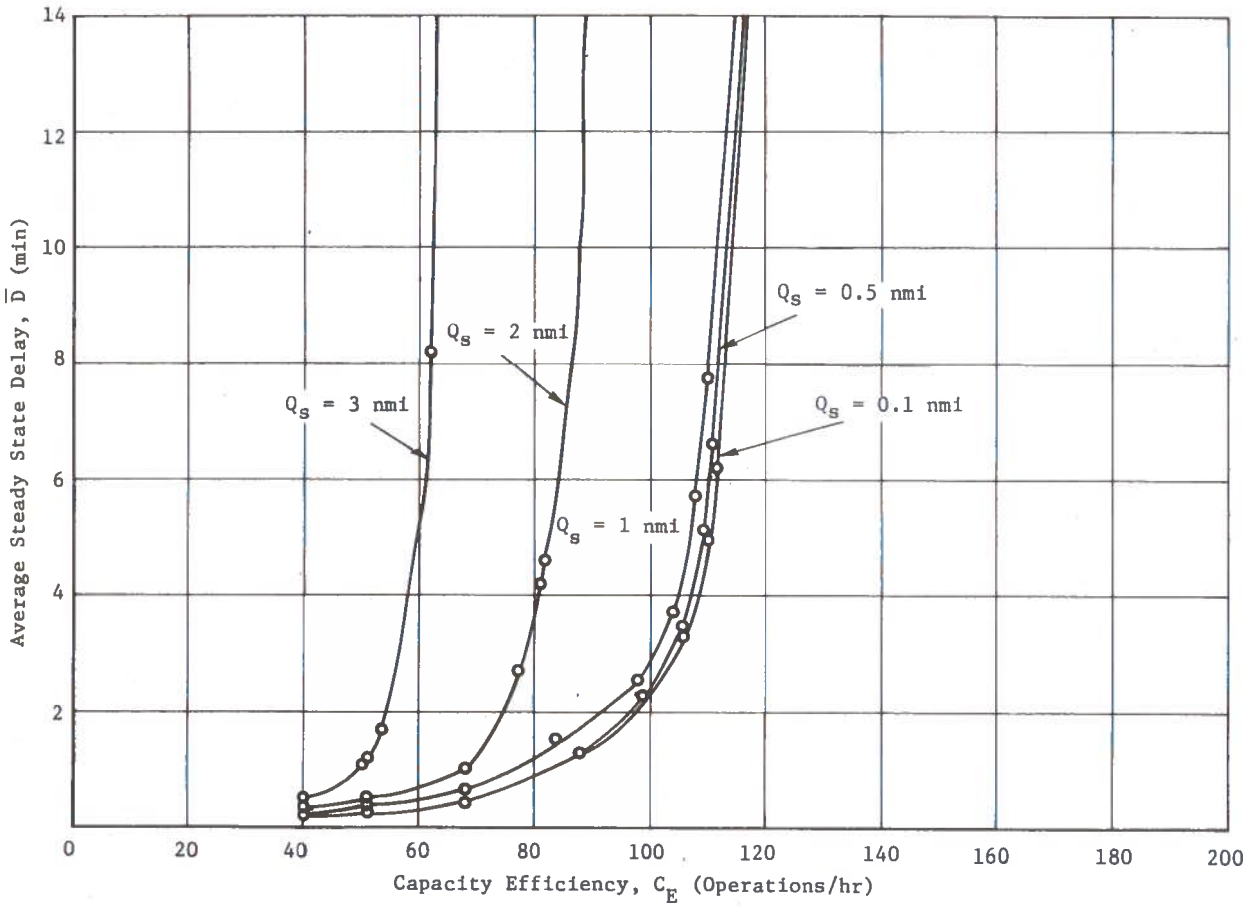

Figure 6.2-4. Runway Capacity vs Average Delay for IFR Conditions for Mix M13

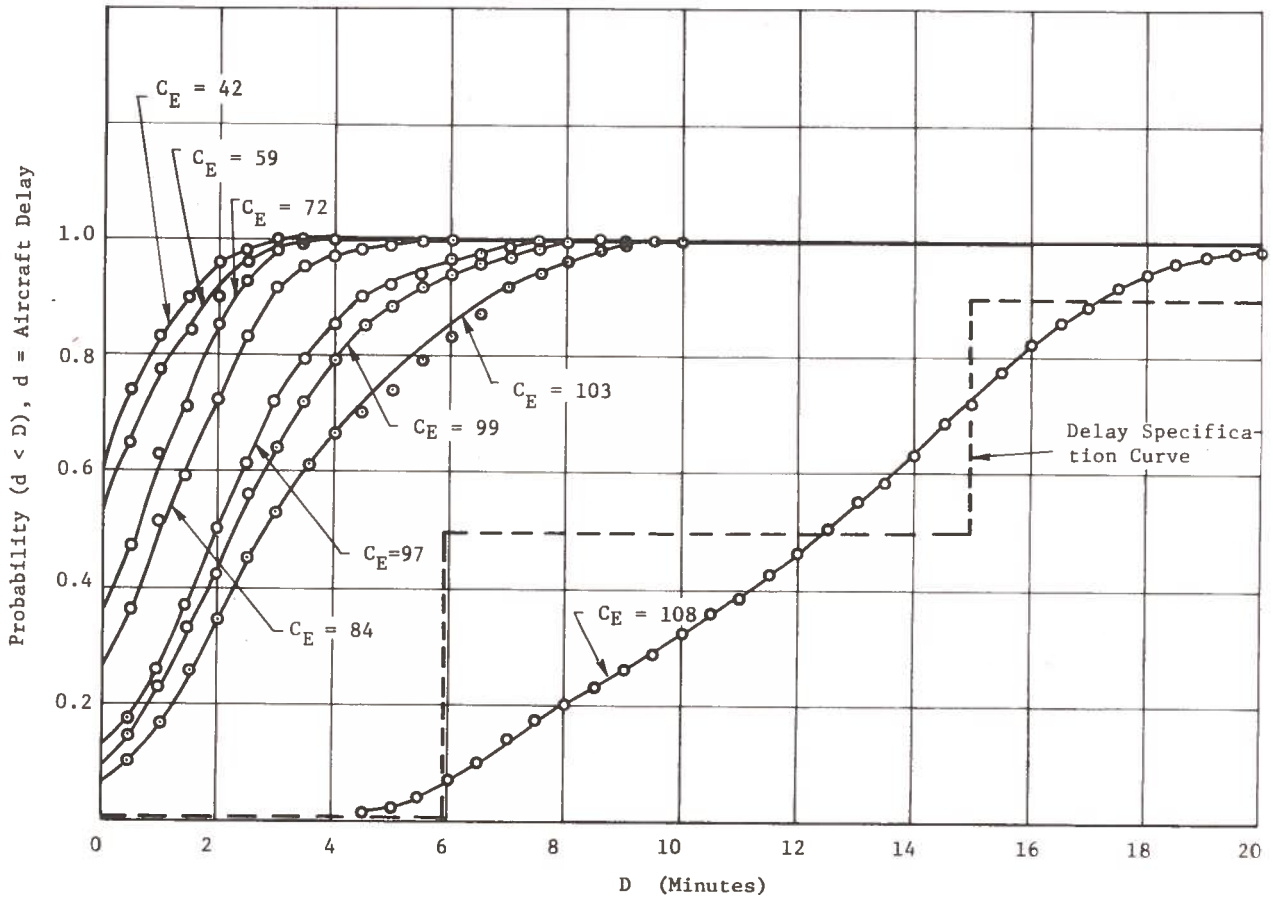

Figure 6.2-5. Runway Capacity Efficiency with Delay Given by a Probability Distribution Function for a Separation Standard of 2 NMI., and M11 Mix, and IFR Conditions

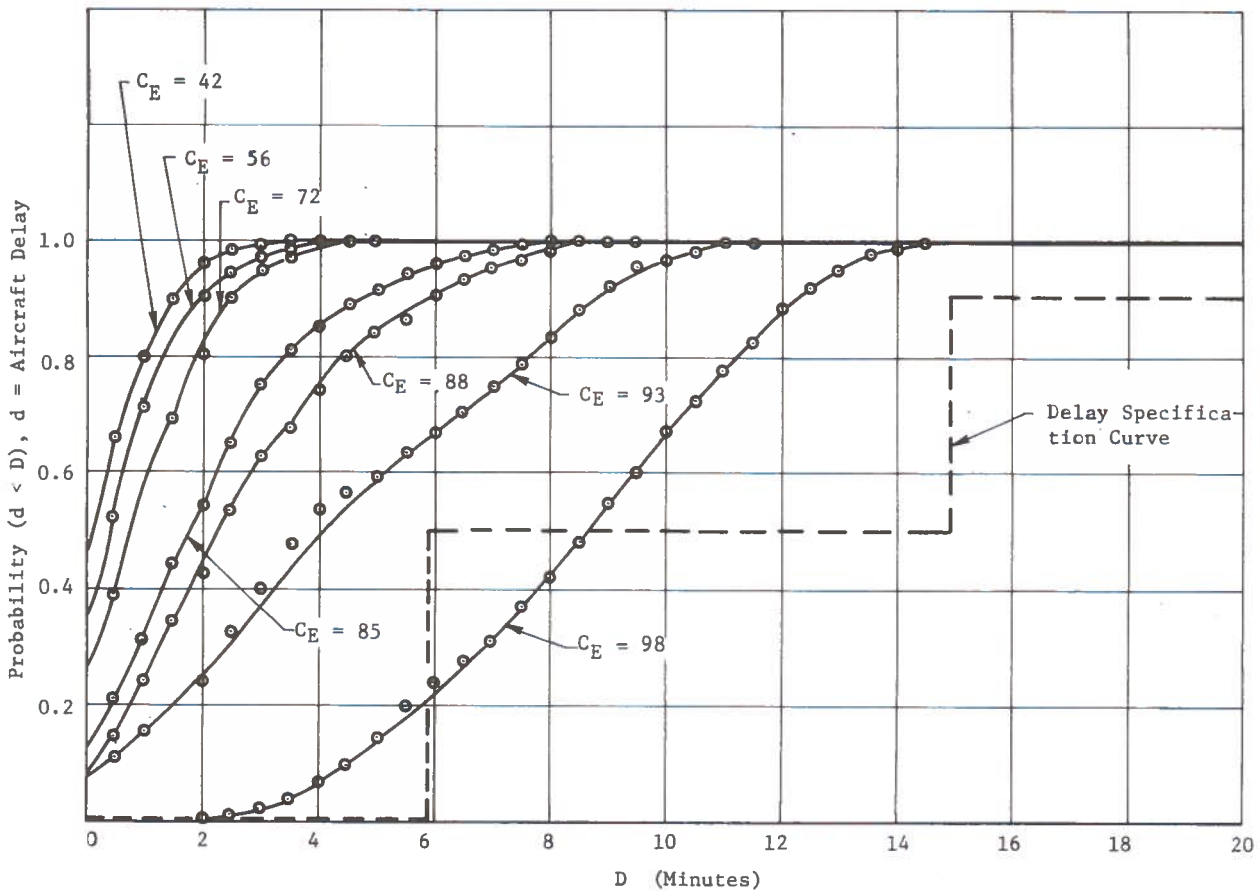

Figure 6.2-6. Runway Capacity Efficiency with Delay Given by a Probability Distribution Function for a Separation Standard 3 NMI, an M11 Mix, and IFR Conditions

aircraft, less than 15 min for 90 percent of all user aircraft, and less than 30 min for 99.9 percent of all user aircraft. A comparison of the capacity efficiency curves of these figures with the delay specification curve is necessary to determine that capacity efficiency which exactly meets the delay specification. Examination of the curves in Fig. 6.2-6 shows that the C_E (capacity efficiency) value that exactly meets the delay requirements is between 93 and 98 operations per hour. Using linear interpolation with these values as end points results in a C_E value of 95 operations per hour. This C_E curve would pass through the point where D = 6 min and the Probability (d < D) = 0.5.

6.3 Subsystem Sensitivities

This section considers the impact on the various SAATMS subsystems of variations in cost, technical risk, and schedule. The results are generally stated in relative values. The satellite and range tracking equipment and the surveillance, navigation, and communications subsystems are considered.

6.3.1 Satellite Constellation

The selected satellite constellation consists of six equatorial, geostationary satellites and nine inclined, eccentric orbit geosynchronous satellites. The geostationary satellites are precision three-axis sensing and controlling units designed for antenna pointing at selected earth-fixed points. The geosynchronous satellites are simpler in that antenna pointing is controlled to subsatellite points.

The large number of satellites is predicated on surveillance invulnerability to satellite failures, aircraft bank angle visibility dropout, and low power user dropout as well as on the desire for broad oceanic coverage. Alternate, smaller satellite constellations have been proposed on other programs but these configurations are primarily designed for navigation. The general purpose of these navigation satellites is to provide data for augmenting low cost inertial navigation units. The selected satellite constellation was predicated on the surveillance function rather than the navigation function.

Although the cost of the large number of satellites is higher than other proposed constellations, the basic intent can only be achieved through the use of this number of satellites. Reductions in the constellation size will not affect the research and development costs. Benefits will be achieved only on acquisition, launch, and maintenance costs. Reduction of the constellation size could achieve a cost savings at the expense of surveillance subsystem operational capabilities.

A potential cost savings could be achieved if a satisfactory alternate constellation design were available. This stems from the basic instability of the 80 deg inclination selected for the geosynchronous satellites. Because of the inclination angle selected, an in-plane precession of the perigee results. This will cause the use of an active station keeping mechanism. The result is that a limited useful life is implicit in the geosynchronous satellite design. Alternate satellite configurations based on a 63.4 deg inclination do not suffer these

precessions and an longer useful life could be realized. Further constellation design studies are warranted to select a more optimum design in terms of useful satellite life spans.

The technical risks and schedule sensitivities of the satellite constellation are extremely small. The technology implicit in the satellite designs are presently available. No impacts on the schedule are foreseen as a result of the availability of the technology.

6.3.2 Satellite Range Tracking

The range tracking is based on reception of the satellite emitted navigation pulses. These data are filtered and an estimation and prediction of the satellite ephemeris is formed. This system is similar to many existing satellite tracking systems presently being used.

There are few available alternate range tracking mechanizations. Any mechanization which will achieve nominal accuracies in the 10 to 60 ft rms radial error range is acceptable. There is an extremely small cost benefit to alternate mechanizations. No technical risks or schedule impacts are foreseen as a result of the selected mechanization.

6.3.3 Surveillance Subsystem

The surveillance subsystem consists of dedicated satellite surveillance RF links, tracking antennas, receivers and preprocessors, and surveillance processing equipment. Independent calibration stations are also included in this subsystem. The tracking antennas, receivers, preprocessors, and processing equipment are located at two Regional Control Centers (RCC) and one Continental Control Center (CCC).

The system design is such that approximately half of the Instantaneous Airborne Count (IAC) is tracked at each RCC with complete backup provided at the CCC. This particular arrangement is the most cost effective method of achieving system redundancy consistent with maximal oceanic coverage. Alternate segmentation of the surveillance distributions exhibited linearly increasing costs as the number of sites is increased.

These particular surveillance preprocessing, acquisition, and tracking mechanizations are cost effective. Some individual functions may be improved by the application of adroit engineering innovations, but the effect on cost will be slight.

The only suspected surveillance subsystem technical risks relate to the aircraft-to-satellite RF links. The possibility of multi-access noise creating a serious problem in surveillance is present. Some initial studies would indicate that the RF link effects could be as serious as 6 db worse than the assumed link multi-access noise effects. Although the study results are felt to be compromised by the choice of coding employed, this question should be subjected to further

scrutiny. Alternate mechanizations such as range ordering (see Volume IV, Section 2.3) are feasible if the multi-access noise proves to be a serious problem. Multi-access noise is suspected to be a limiting factor relative to system growth rather than a serious technical risk for the assumed demand levels.

Reducing the accuracy of the surveillance function would have little effect on cost or risk, since the satellite requirements are set by operational rather than functional requirements. That is, the most logical method of altering surveillance accuracy would be to reduce the number of satellites, increasing GDOP and reducing accuracy. However this would severely limit the failure mode performance and make the system susceptible to drastic degradation in the event of a satellite loss. This is clearly undesirable. Thus, the number of satellites is set by operational (failure mode) requirements rather than accuracy.

6.3.4 Navigation Subsystem

The navigation subsystem has two separate mechanizations: satellite navigation and Virtual VOR (VVOR). The satellite navigation subsystem includes a satellite RF link, user receivers, and user processors. The VVOR navigation is based on transmission of navigation signals to users over a digital communications link. The VVOR data are extracted from user surveillance data.

There is no known major sensitivity of the VVOR mechanization to schedule, cost, or technical risks. This mode is predicated simply on the availability of the surveillance data.

The satellite navigation mechanization exhibits a user cost differential, subject to the desired navigation accuracy and extent of subsidiary navigation computations. A factor of 2 higher user processor costs could be expected if the user wants a more sophisticated mechanization. This is a user option and is not a system cost penalty.

The selected basic navigation system is expected to show little sensitivity to cost, schedule, or technical risks.

An alternative to eliminate the satellite navigation and rely only on VVOR is practical but at a severe reduction in navigation accuracy. This would have a small system cost benefit but would reduce user costs. The potential for independent surveillance and navigation is obviated by this action and it is not recommended.

6.3.5 Communications Subsystem

The communications subsystem involves ground, satellite, and user RF links and associated coding/decoding processors. The RF links consist of both voice and digital channels. The user-associated digital channels are predicated on the use of spread spectrum, pseudo-noise (PN) coded signals. These signals are decoded using Analog Matched Filters (AMF).

The digital communications coding scheme for the users (via the PN/AMF combination) is based on presently existing technology. There is some cost sensitivity to the implementation of the exact coding scheme. Optimization of several links could result in some coding simplification and a potentially lower user cost. This would have minor ground system impacts.

Voice communications are equivalent to today's VHF channel complexity and show little cost or technical risk sensitivity.

The only known area of technical risk involves the asynchronous user-to-ground digital data link. This link is subject to multi-access noise similar to the surveillance link. The technical risks are less severe and alternate mechanizations are feasible.

7. REFERENCES

1. "Advanced Air Traffic Management System (AATMS) Program Preliminary Requirements Specification, Appendix K, DOT TSC, September 20, 1972
2. "Near Midair Collision Report of 1968," DOT FAA Air Traffic and Flight Standards Technical Report, July 1969
3. C71-61/301, DOT-TSC-304-1, "Fourth Generation Air Traffic Control Study," Volume II, Autonetics, Anaheim, California
4. "Working Paper, Reference Material for Air Traffic Control Separation," Compiled for Air Traffic Control Advisory Committee Group III, DOT FAA, January 1969
5. "Probability, Random Variables, and Stochastic Processes," Papoulis, McGraw-Hill, 1965
6. Proceedings IEEE, Vol 58, No. 3, March 1970, "Separation of Air Traffic by Visual Means: An Estimate of the Effectiveness of the See-and-Avoid Doctrine," W. Graham and R. H. Orr
7. "Working Paper (Project 150-2S), Altitude Distribution of Airborne Aircraft - Peak Hour, Friday, August 1963, CONUS," FAA, Systems Managment Division - Traffic and Economic Analysis, March 1963
8. Report of Department of Transportation for the Air Traffic Control Advisory Committee, December 1969
9. "Enroute IFR Air Traffic Survey Peak Day Fiscal Year 1971," DOT FAA, Information and Statistics Division Office Management Services
10. "Civil Aviation Collisions Analysis, January 1964 - December 1971," The Mitre Corporation, January 1973 Presentation at TSC, to be published
11. "Advanced Air Traffic Management System (AATMS) Program Requirements Specification," The Mitre Corporation Version, November 17, 1972
12. "Air Traffic Patterns for IFR and VFR Aviation Calendar Year 1968," DOT FAA, Office of Management Systems
13. DOT-TSC-FAA-71-27, "The Calculation of Aircraft Collision Probabilities," J. Bellantoni
14. DOT-TSC-OST-71-4, "A Theory of Aircraft Collision Avoidance System Design and Evaluation." E. Koenke
15. AOPA Presentation to Subcommittee on Advance Research and Technology on General Aviation Demand in Future Years, January 20, 1972
16. "Analaysis of Long Range Air Traffic Systems - Separation Standards II," R.A.E. Technical Report, P. G. Reich

17. Report No. TA-1358-G-1, "An Analytical Investigation of Airport Capacity," A. Blumstein, Cornell Aeronautical Laboratory, Inc., June 1960

18. "Nonstationary Queuing Probabilities for Landing Congestion of Aircraft," H. P. Galliher and R. C. Wheeler, Operations Research, Vol 6, pp 264-275, 1958

19. Technical Report No. 4102, "Models for Runway Capacity Analysis," R. M. Harris, The Mitre Corporation, October 1969

20. AIL Report No. AIL-1167-1 AD 690477, "Operational Development of Techniques for Computing Airport Capacity," E. N. Hooten, H. Burns, and M. A. Warskow, June 1969

21. Technical Report No. 46, AD-700814, "An Analytical Investigation of Air Traffic in Vicinity of Terminal Areas," A. R. Odoni, MIT Operations Reserach Center, December 1969

22. Working Paper (44WP-5000), Airspace Coverage by a Ground-based Network, February 1973, MIT for DOT/TSC-241

23. FAA-ER-240-013a DOT-FAA Specification ATCRBS Electronic Scan Antenna

APPENDIX A. SYSTEM PERFORMANCE DATA

1. INTRODUCTION

This appendix presents the complete set of data used as the basis for the airport capacity data presented in the system performance analysis. Some of the text of that section is repeated for clarity.

2. CAPACITY

2.1 Single Runway Capacity

The capacity of a single runway is a function of the mix of aircraft using the runway. The mix for each runway in the Los Angeles region was derived from the terminal area demand data supplied by The Mitre Corporation. The snapshot demand data consisted of the position, altitude, velocity, origin and destination of 1840 instantaneous airborne aircraft. The number and type of the aircraft using each runway at each of the 43 airports of concern was derived from the snapshot data. The data cover 48 airports in the region; however, the 5 military airports were not considered due to the limited demand projected for these airports in 1995.

Using the aircraft classes described in Section 3, the mix at the 43 airports of interest was determined in terms of the percentage of aircraft in each of these six classes. The resultant 43 mixes were examined for similarities; these similarities were used to combine mixes, resulting in a specification of 13 mixes which accurately represent the aircraft mix at the 43 airports. Table A-1 lists the 13 mixes; the entries in the table are the percent of each aircraft class in the specified mix. Table A-2 lists the 43 airports and the aircraft mix for each runway of those airports. The runway configuration for each airport class class as provided by The Mitre Corporation is shown in Fig. 3.3.1.

Another important factor affecting the capacity of a runway is the set of rules regarding runway use. The following five rules are assumed to apply to runway operations in the SAATMS.

(1) The minimum safety separation between two airborne aircraft on on approach will not be violated.

(2) Two aircraft may not be on the same runway at the same time.

(3) An IFR departure cannot be initiated unless the following arrival is more than 40 sec from the threshold.

(4) A departure followed by another departure must be appropriately spaced (60 sec between IFR departures).

(5) Aircraft on final approach are given priority.

TABLE A-1. BASIC AIRCRAFT MIXES

MIX DESIGNATION	AIRCRAFT CLASS					
	A SINGLE ENGINE GA	B MULTI-ENGINE & TURBO-PROP GA	C JET-GA	D ULTRA SHORT HAUL AC	E LIGHTWEIGHT AC	F HEAVY WEIGHT AC
M1	95	5	-	-	-	-
M2	90	10	-	-	-	-
M3	-	90	10	-	-	-
M4	80	20	-	-	-	-
M5	65	35	-	-	-	-
M6	55	35	10	-	-	-
M7	35	65	-	-	-	-
M8	35	60	5	-	-	-
M9	30	64	-	6	-	-
M10	-	-	-	60	24	16
M11	-	-	-	30	20	50
M12	-	15	15	10	35	25
M13	20	50	12	16	2	-

Note: Entries are percent of class in a particular mix.

TABLE A-2. MIX FOR EACH RUNWAY AT EACH AIRPORT

AIRPORT				RUNWAY TYPE, NUMBER, MIX					
				AC		MIXED (AC/GA)		GA	
NAME	DESCRIPTOR	NO.	CLASS	NO.	MIX	NO.	MIX	NO.	MIX
Burbank	BUR	8	8	2	M8, M9	2	M8, M9	2	M1, M1
Los Angeles Int'l.	LAX	4	8	2	M11, M11	2	M11, M11	2	M8, M8
Ontario Int'l	ONT	17	8	2	M10, M10	2	M3, M3	2	M1, M1
Santa Ana (Orange Co)	SNA	3	8	2	M10, M10	2	M3, M3	2	M1, M1
Palmdale	PMD	21	7	2	M12, M12	1	M3	2	M1, M1
Long Beach	LGB	1	6	-	-	2	M13, M13	2	M1, M1
Oxnard (Ventura)	CXR	16	6	-	-	2	M8, M9	2	M1, M1
Riverside	RAL	18	6	-	-	2	M9, M9	2	M1, M1
Torrance	TOA	5	6	-	-	2	M5, M5	2	M1, M1
Apply Valley	APV	26	4	-	-	1	M2	2	M1, M1
Cable (Upland)	CCB	23	4	-	-	1	M4	2	M1, M1
Chino	CNO	10	4	-	-	1	M7	2	M1, M1
Compton	CPM	13	4	-	-	1	M8	2	M1, M1
Corona	L66	18	4	-	-	1	M8	2	M1, M1
El Monte	EMT	11	4	-	-	1	M6	2	M1, M1
Fox (Lancaster)	WJF	20	4	-	-	1	M5	2	M1, M1
Fullerton	FUL	12	4	-	-	1	M3	2	M1, M1
Hawthorne	HHR	7	4	-	-	1	M3	2	M1, M1
LaVerne Bracket	POC	9	4	-	-	1	M3	2	M1, M1
Meadowlark (Huntington Beach)	L16	19	4	-	-	1	M5	2	M1, M1
San Fernando	SFR	32	4	-	--	1	M5	2	M1, M1

TABLE A-2. (CONTINUED)

AIRPORT				RUNWAY TYPE, NUMBER, MIX					
				AC		MIXED (AC/GA)		GA	
NAME	DESCRIPTOR	NO.	CLASS	NO.	MIX	NO.	MIX	NO.	MIX
Santa Monica	SMO	6	4	-	-	1	M3	2	M1, M1
Santa Paula	SZP	37	4	-	-	1	M4	2	M1, M1
Santa Susana	LO2	22	4	-	-	1	M3	2	M1, M1
Van Nuys	VNY	2	4	-	-	1	M3	2	M1, M1
Whiteman	WHP	34	4	-	-	1	M4	2	M1, M1
Agua Dulce	YO1	35	3	-	-	-	-	1	M2
Capistrano	L38	40	3	-	-	-	-	1	M1
FLA BOB (Riverside)	RIR	33	3	-	-	-	-	1	M1
Redlands	X34	29	3	-	-	-	-	1	M2
Skylark	X42	36	3	-	-	-	-	1	M1
Hemet Ryan	X17	31	2	-	-	-	-	1	M1
Hesperia Air Lodge	X18	46	2	-	-	-	-	1	M2
Rialto	L36	25	2	-	-	-	-	1	M1
Rosamond	X37	39	2	-	-	-	-	1	M1
Tri City	SBT	41	2	-	-	-	-	1	M1
Hawkins	X15	43	1	-	-	-	-	1	M2
Morrow	X25	42	1	-	-	-	-	1	M1
Perris Valley	X31	44	1	-	-	-	-	1	M2
Quartz Hill	X32	38	1	-	-	-	-	1	M1
Rancho Calif.	X33	45	1	-	-	-	-	1	M2
Sterks Ranch	X43	48	1	-	-	-	-	1	M1
Sunhill Ranch	X44	47	1	-	-	-	-	1	M2

Rules 3 and 4 contain timing restrictions on IFR operations. These same constraints are assumed not to exist for VFR conditions. Thus, runway capacity will be a function of meteorological conditions, and runway capacity was thus determined for both VFR and IFR conditions.

Table A-3 shows capacity values for each of the 13 mixes of aircraft and for various separation standard values, Q_s, under IFR conditions. Three different capacity values are shown for each of five separation standard values and each aircraft mix. The first capacity value shown in Table A-4 is the runway saturation capacity. The second is a capacity efficiency value, corresponding to a landing or departure delay for each aircraft that satisfies the most constraining the following specified delay conditions:

1. The probability that the delay is 6 minutes or less is 0.5 (This can be written as $P(D \leq 6) = 0.5$)
2. The probability that the delay is 15 minutes or less is 0.9 ($P(D \leq 15) = 0.9$)
3. The probability that the delay is 30 minutes or less is 0.999 ($P(D \leq 30) = 0.999$)

The third capacity measure in Table A-3 is the capacity efficiency value for an average aircraft delay of three minutes.

Aircraft delay depends on the time spacing between successive aircraft. This spacing was determined from the snapshot data mentioned earlier. The statistics of this time spacing was found to be Poisson. Thus, the values shown in Table A-3 were obtained by use of the network simulation model using Poisson statistics for aircraft arrivals. The saturation capacity figures were also determined analytically as a check on the simulation results. These results are shown for mixed operations of arrivals and departures on each runway with a departure/arrival ratio of one. This case is denoted by the description, A/D_R.

Table A-4 lists the corresponding capacity values under VFR conditions. The notation, A/D_V, is used for this case. Capacity figures for arrivals only (notation A_O) are shown in Table A-5 and for departures only (notation D_O) are shown in Table A-6. Table A-6 shows the departure case for both IFR (at least 60 sec required between departures) and VFR (departure interval limited only by takeoff runway occupancy time) conditions. Capacity figures for arrivals or departures only a runway are of interest for the case of dependent dual runways.

TABLE A-3. RUNWAY CAPACITIES FOR EACH MIX A/D_R CASE

RUNWAY MIX	Saturation Capacity (OPS/HR)					CAPACITY EFFICIENCY (OPS/HR)									
						P(D≤6) = .5, P(D≤15) = .9, P(D≤30) = .999					Average Delay = $\bar{D}$ = 3 (Min)				
	Q_s = nmi					Q_s = nmi					Q_s = nmi				
	3	2	1	.5	.1	3	2	1	.5	.1	3	2	1	.5	.1
M1	50	75	114	114	114	47	71	110	110	110	42	62	94	94	94
M2	51	76	113	113	113	46	72	111	111	111	38	60	101	101	101
M3	60	90	119	119	119	59	89	116	116	116	54	81	103	104	104
M4	50	73	118	120	120	48	70	113	113	113	42	64	106	106	106
M5	51	75	118	120	120	49	71	116	116	116	46	67	102	102	102
M6	53	77	116	119	119	49	76	117	117	117	42	64	102	102	102
M7	55	80	118	120	120	52	77	115	115	115	45	65	104	104	104
M8	55	80	117	120	120	53	79	117	118	118	46	65	104	104	104
M9	56	81	117	120	120	55	81	113	113	113	51	74	101	102	103
M10	95	114	114	114	114	91	112	112	112	112	84	106	106	106	106
M11	100	108	108	108	108	96	104	104	104	104	89	102	102	102	102
M12	86	102	110	111	111	84	99	106	109	109	77	92	101	103	103
M13	61	86	114	118	118	59	85	109	111	112	56	77	101	103	103

TABLE A-4. RUNWAY CAPACITIES FOR EACH MIX FOR A/D_V CASE

RUNWAY MIX	Saturation Capacity (OPS/HR)					Capacity Efficiency (OPS/HR) P(D≤6) = .5; P(D≤15) = .9; P(D≤30) = .999					Capacity Efficiency (OPS/HR) Average Delay = $\bar{D}$ = 3 (Min)				
	Q_s = nmi					Q_s = nmi					Q_s = nmi				
	3	2	1	.5	.1	3	2	1	.5	.1	3	2	1	.5	.1
M1	50	75	148	162	162	47	71	143	157	157	42	62	123	133	133
M2	51	76	147	161	161	46	72	146	159	159	38	60	130	143	143
M3	61	91	168	170	170	59	89	163	163	163	54	81	148	150	150
M4	52	77	147	195	198	48	70	139	189	192	42	64	128	171	174
M5	53	78	147	188	192	48	74	145	184	188	46	67	131	169	171
M6	55	80	146	181	187	49	76	144	180	186	44	64	118	159	165
M7	56	82	153	179	182	52	77	143	171	176	45	65	132	154	154
M8	56	83	152	178	181	53	79	142	176	180	47	73	135	160	162
M9	57	83	153	177	180	56	82	148	168	171	51	74	127	146	149
M10	95	125	127	127	127	93	123	125	125	125	84	110	114	114	114
M11	100	114	114	114	114	96	111	112	112	112	89	106	108	108	108
M12	89	109	121	124	124	84	105	116	118	121	77	94	111	111	112
M13	62	89	143	159	165	59	88	133	150	157	56	77	121	135	140

TABLE A-5. RUNWAY CAPACITIES FOR EACH MIX FOR A_0 CASE (ARRIVALS ONLY)

Runway Mix	Saturation Capacity (Ops/Hr) Q_s = nmi					Capacity Efficiency (Ops/Hr) P(D 6)=.5; P(D≤15)=.9; P(D≤30)=.999 Q_s = nmi					Average Delay = 5 = 3 (min) Q_s = nmi				
	3	2	1	.5	.1	3	2	1	.5	.1	3	2	1	.5	.1
M1	25	38	74	145	155	23	36	73	143	153	20	33	68	142	153
M2	25	38	74	140	153	24	35	72	135	152	20	31	66	132	146
M3	30	45	89	170	186	28	42	87	168	184	23	34	76	165	181
M4	26	38	74	136	219	23	34	71	134	218	20	30	68	129	217
M5	27	39	74	133	202	25	37	73	133	201	19	31	69	130	199
M6	27	40	74	127	184	25	38	72	125	182	21	32	69	121	199
M7	28	41	78	139	187	26	39	73	133	182	19	35	68	130	175
M8	28	41	77	136	183	26	37	75	133	180	22	31	61	129	174
M9	28	42	78	137	181	26	40	75	127	166	22	33	70	119	155
M10	48	70	132	160	160	46	67	128	154	158	43	60	122	118	151
M11	51	74	132	149	149	47	69	128	145	149	45	62	123	139	145
M12	43	61	103	122	132	41	53	99	117	127	39	49	92	110	123
M13	31	45	79	122	149	29	43	75	122	142	26	37	72	108	130

TABLE A-6. RUNWAY CAPACITIES FOR EACH MIX FOR D_Q CASE (DEPARTURES ONLY)

Runway Mix	Saturation Capacity (Ops/Hr)		Capacity Efficiency (Ops/Hr)			
			P (D ≤ 6)=. 5, P(D≤15)=. 9 P(D≤30)=. 999		Average Delay = 3 min.	
	IFR	VFR	IFR	VFR	IFR	VFR
M1	60	171	58	170	54	169
M2	60	170	58	169	54	169
M3	60	157	58	156	53	151
M4	60	168	59	167	55	163
M5	60	166	59	164	55	163
M6	60	164	58	162	53	159
M7	60	161	57	161	53	157
M8	60	161	58	161	53	155
M9	60	161	59	157	57	152
M10	60	105	58	104	55	102
M11	60	92	59	92	55	88
M12	60	104	59	102	56	94
M13	60	150	58	144	54	141

Capacity values for very small separation standard values (0.1 and 0.5 nm) were obtained from the network simulation model in order to determine the effect of runway occupancy rules on capacity. The limits on capacity for small values of Q_s are due to runway constraints (rules 2-4 above). Examination of Table A-3 shows that for IFR condition there is little increase in capacity as Q_s decreases below 1 nm. For all of the cases in Tables A-3 and A-4, there is a departure between each arrival pair under saturation conditions. Under VFR conditions, where rules 3 and 4 do not apply, examination of Table A-4 shows that there is a significant increase in capacity with decreasing Q_s (for Q_s greater than or equal to 0.5 nm) for all mixes composed primarily of GA aircraft (all mixes except M10, M11, M12). For arrivals only, Table A-5 shows an increase in capacity for decreases in Q_s down to 0.1 nm for all mixes except the air carrier mixes (M10, M11).

2.2 Airport Capacity

The capacity for each airport as a function of separation standard for each case (VFR, IFR with either dual or independent parallel runway operation) can be determined by summing the appropriate capacity values based upon the capacities for each runway from Table A-3 through A-6 and the runway and mix assignment of Table A-2. Tables A-7 through A-9 show the capacity for each of 43 airports in the designated scenario for each of these three cases. As in Tables A-3 through A-6, values are given for each airport for three different measures of capacity and five different separation standards.

The busy hour operations shown in these tables are for demand level two and were furnished by the Mitre Corporation. A comparison between demand and capacity is given by the curves and discussion of Section 5.4 and Figures 5.3-1 and 5.3-2.

TABLE A-7. AIRPORT CAPACITY FOR IFR CONDITIONS MIX DEPARTURES/ ARRIVAL RUNWAY OPERATION CASE A/D_R

Airport	No. of Runways	Airport	Busy Hour Operations	Saturation Capacity (ops/hr)					Capacity Efficiency (ops/hr)									
									$P(D\leq 6)$ 0.5; $P(D\leq 15)$ 0.9; $P(D\leq 30) = 0.999$					Average Delay = $\bar{D}$ = 3 min				
				Q_s (nmi)					Q_s (nmi)					Q_s (nmi)				
				3	2	1	0.5	0.1	3	2	1	0.5	0.1	3	2	1	0.5	0.1
Primary	6	BUR	197	322	472	696	708	708	310	462	680	682	682	278	402	598	600	602
	6	LAX	200	510	592	666	672	672	490	574	650	652	652	448	538	616	616	616
	6	ONT	226	410	558	694	694	694	394	544	676	676	676	360	498	606	608	608
	6	SNA	217	410	558	694	694	694	394	544	676	676	676	360	498	606	608	608
	5	PMD	122	332	444	567	569	569	321	429	548	554	554	292	389	493	498	498
Secondary	4	LGB	240	222	322	456	464	464	212	312	438	442	444	196	278	390	394	394
	4	OXR	210	211	311	462	468	468	202	302	450	451	451	181	263	393	394	395
	4	RAL	211	212	312	462	468	468	204	304	446	446	446	186	272	390	392	394
	4	TOA	246	202	300	464	468	468	192	284	452	452	452	176	256	392	392	392
Feeder	3	APV	134	151	226	341	341	341	140	214	331	331	331	122	184	289	289	289
	3	CCB	198	150	223	346	348	348	142	212	333	333	333	126	188	294	294	294
	3	CNO	206	155	230	346	348	348	146	219	335	335	335	129	189	292	292	292
	3	CPM	218	155	230	345	348	348	147	221	337	338	338	130	189	292	292	292
	3	L66	162	155	230	345	348	348	147	221	337	338	338	130	189	292	292	292
	3	EMP	195	153	227	344	347	347	143	218	337	337	337	126	188	290	290	290
	3	WJF	183	151	225	346	348	348	143	213	336	336	336	130	191	290	290	290
	3	FUL	181	160	240	347	347	347	153	231	336	336	336	138	205	291	292	292
	3	AHR	187	160	240	347	347	347	153	231	336	336	336	138	205	291	292	292
	3	POC	190	160	240	347	347	347	153	231	336	336	336	138	205	291	292	292
	3	L16	218	151	225	346	348	348	143	213	336	336	336	130	191	290	290	290
	3	SFR	180	151	225	346	348	348	143	213	336	336	336	130	191	290	290	290
	3	SMO	190	160	240	347	347	347	153	231	336	336	336	138	205	291	292	292

TABLE A-7. (CONTINUED)

Airport Class	No. of Runways	Airport	Busy Hour Operations	Saturation Capacity (ops/hr)					Capacity Efficiency (ops/hr) P(D≤6) = 0.5; P(D<15) = 0.9; P(D≤30) = 0.999					Capacity Efficiency (ops/hr) Average Delay = $\bar{D}$ = 3 min				
				Q_S (nmi)					Q_S (nmi)					Q_S (nmi)				
				3	2	1	0.5	0.1	3	2	1	0.5	0.1	3	2	1	0.5	0.1
Feeder	3	SZP	148	150	223	346	348	348	142	212	333	333	333	126	188	294	294	294
	3	L02	164	160	240	347	347	347	153	231	336	336	336	138	205	291	292	292
	3	VNY	246	160	240	347	347	347	153	231	336	336	336	138	205	291	292	292
	3	WHP	176	150	223	346	348	348	142	212	333	333	333	126	188	294	294	294
	1	X01	129	51	76	113	113	113	46	72	111	111	111	38	60	101	101	101
	1	L38	128	50	75	114	114	114	47	71	110	110	110	42	62	94	94	94
	1	RIR	166	50	75	114	114	114	47	71	110	110	110	42	62	94	94	94
	1	X34	101	51	76	113	113	113	46	72	111	111	111	38	60	101	101	101
	1	X42	95	50	75	114	114	114	47	71	110	110	110	42	62	94	94	94
	1	X17	95	50	75	114	114	114	47	71	110	110	110	42	62	94	94	94
	1	X18	27	51	76	113	113	113	46	72	111	111	111	38	60	101	101	101
	1	L36	168	50	75	114	114	114	47	71	110	110	110	42	62	94	94	94
	1	X37	98	50	75	114	114	114	47	71	110	110	110	42	62	94	94	94
	1	SBT	126	50	75	114	114	114	47	71	110	110	110	42	62	94	94	94
	1	X15	61	51	76	113	113	113	46	72	111	111	111	38	60	101	101	101
	1	X25	132	50	75	114	114	114	47	71	110	110	110	42	62	94	94	94
	1	X31	49	51	76	113	113	113	46	72	111	111	111	38	60	101	101	101
	1	X32	68	50	75	114	114	114	47	71	110	110	110	42	62	94	94	94
	1	X33	49	51	76	113	113	113	46	72	111	111	111	38	60	101	101	101
	1	X43	91	50	75	114	114	114	47	71	110	110	110	42	62	94	94	94
	1	X44	23	51	76	113	113	113	46	72	111	111	111	38	60	101	101	101

TABLE A-8. AIRPORT CAPACITY FOR VFR CONDITIONS, MIXED DEPARTURE/ARRIVAL RUNWAY OPERATION CASE A/D_V

Airport Class	No. of Runways	Airport	Busy Hour Operations	Saturation Capacity (ops/hr)					Capacity Efficiency (ops/hr)									
									$P(D\leq 6) = 0.5$; $P(D<15) = 0.9$; $P(D\leq 30) = 0.999$					Average Delay = $\bar{D}$ = 3 min				
				Q_s (nmi)					Q_s (nmi)					Q_s (nmi)				
				3	2	1	0.5	0.1	3	2	1	0.5	0.1	3	2	1	0.5	0.1
	6	BUR	197	326	482	906	1034	1046	312	464	866	1002	1016	280	418	770	878	888
Primary	6	LAX	200	512	622	760	812	818	490	602	732	800	808	450	570	702	752	756
Primary	6	ONT	226	412	582	886	918	918	398	566	862	890	890	360	506	770	794	794
Primary	6	SNA	217	412	582	886	918	918	398	566	862	890	890	360	506	770	794	794
Primary	5	PMD	122	335	459	706	742	742	321	441	681	713	719	292	393	616	638	640
Secondary	4	LGB	240	224	328	582	642	654	212	318	552	614	628	196	278	488	536	546
Secondary	4	OXR	210	213	316	601	679	685	203	303	576	658	665	182	271	508	572	577
Secondary	4	RAL	211	214	316	602	678	684	206	306	582	650	656	186	272	500	558	564
Secondary	4	TOA	246	206	306	590	700	708	190	290	576	682	690	176	258	508	604	608
Feeder	3	APV	134	151	226	443	485	485	140	214	432	473	473	122	184	376	409	409
Feeder	3	CCB	198	152	227	443	519	522	142	212	425	503	506	126	188	374	437	440
Feeder	3	CNO	206	156	232	449	503	506	146	219	429	485	490	129	189	378	420	420
Feeder	3	CPM	218	156	233	448	502	505	147	221	428	490	494	131	197	381	426	428
Feeder	3	L66	162	156	233	448	502	505	147	221	428	490	494	131	197	381	426	428
Feeder	3	EMT	195	155	230	442	505	511	143	218	430	494	500	128	188	364	425	431
Feeder	3	WJF	183	153	228	443	512	516	142	216	431	498	502	130	191	377	435	437
Feeder	3	FUL	181	161	241	464	494	494	153	231	449	477	477	138	205	394	416	416
Feeder	3	AHR	187	161	241	464	494	494	153	231	449	477	477	138	205	394	416	416
Feeder	3	POC	190	161	241	464	494	494	153	231	449	477	477	138	205	394	416	416
Feeder	3	L16	218	153	228	443	512	516	142	216	431	498	502	130	191	377	435	437
Feeder	3	SFR	180	153	228	443	512	516	142	216	431	498	502	130	191	377	435	437
Feeder	3	SMO	190	161	241	464	494	494	153	231	449	477	477	138	205	394	416	416

TABLE A-8. (CONTINUED)

Airport Class No. of Runways	Airport	Busy Hour Operations	Saturation Capacity (ops/hr)					Capacity Efficiency (ops/hr)									
								P(D<6) = 0.5; P(D<15) = 0.9; P(D<30) = 0.999					Average Delay = $\bar{D}$ = 3 min				
			Q_s (nmi)					Q_s (nmi)					Q_s (nmi)				
			3	2	1	0.5	0.1	3	2	1	0.5	0.1	3	2	1	0.5	0.1
Feeder 3	SZP	148	152	227	343	519	522	142	212	425	503	506	126	188	374	437	440
3	L02	164	161	241	464	494	494	153	231	449	477	477	138	205	394	416	416
3	VNY	246	161	241	464	494	494	153	231	449	477	477	138	205	394	416	416
3	WHP	176	152	227	343	519	522	142	212	425	503	506	126	188	374	437	440
1	X01	129	51	76	147	161	161	46	72	146	159	159	38	60	130	143	143
1	L38	128	50	75	148	162	162	47	71	143	157	157	42	62	123	133	133
1	RIR	166	50	75	148	162	162	47	71	143	157	157	42	62	123	133	133
1	X34	101	51	76	147	161	161	46	72	146	159	159	38	60	130	143	143
1	X42	95	50	75	148	162	162	47	71	143	157	157	42	62	123	133	133
1	X17	95	50	75	148	162	162	47	71	143	157	157	42	62	123	133	133
1	X18	27	51	76	147	161	161	46	72	146	159	159	38	60	130	143	143
1	L36	168	50	75	148	162	162	47	71	143	157	157	42	62	123	133	133
1	X37	98	50	75	148	162	162	47	71	143	157	157	42	62	123	133	133
1	SBT	126	50	75	148	162	162	47	71	143	157	157	42	62	123	133	133
1	X15	61	51	76	147	161	161	46	72	146	159	159	38	60	130	143	143
1	X25	132	50	75	148	162	162	47	71	143	157	157	42	62	123	133	133
1	X31	49	51	76	147	161	161	46	72	146	159	159	38	60	130	143	143
1	X32	68	50	75	148	162	162	47	71	143	157	157	42	62	123	133	133
1	X33	49	51	76	147	161	161	46	72	146	159	159	38	60	130	143	143
1	X43	91	50	75	148	162	162	47	71	143	157	157	42	62	123	133	133
1	X44	23	51	76	147	161	161	46	72	146	159	159	38	60	130	143	143

TABLE A-9. AIRPORT CAPACITY FOR IFR CONDITIONS DUAL RUNWAY OPERATION ON CLOSE SPACED PARALLEL RUNWAYS, MIXED A/D ON OTHERS

Airport Class	No. of Dual Runways	No. of Mixed Runways	Airport	Busy Hour Operations	Saturation Capacity (ops/hr)					Capacity Efficiency (ops/hr)									
										$P(D\leq 6) = 0.5$; $P(D<15) = 0.9$; $P(D\leq 30) = 0.999$					Average Delay = $\bar{D}$ = 3 min				
					Q_s (nmi)					Q_s (nmi)					Q_s (nmi)				
					3	2	1	0.5	0.1	3	2	1	0.5	0.1	3	2	1	0.5	0.1
Primary	2	2	BUR	197	212	316	468	468	468	198	296	454	454	454	172	252	408	408	408
Primary	2	2	LAX	200	314	400	474	480	480	294	394	470	472	472	272	350	428	428	428
Primary	2	2	ONT	226	256	380	468	468	468	242	342	452	452	452	216	302	404	404	404
Primary	2	2	SNA	217	256	380	468	468	468	242	342	452	452	452	216	302	404	404	404
Primary	2	1	PMD	122	196	286	359	359	359	187	267	350	350	350	172	245	323	324	324
Secondary	1	2	LGB	240	172	248	348	356	356	164	242	334	338	340	152	220	310	314	314
Secondary	1	2	OXR	210	161	237	354	360	360	154	232	346	347	347	137	205	313	314	315
Secondary	1	2	RAL	211	162	238	354	360	360	156	234	342	342	342	142	214	310	312	314
Secondary	1	2	TOA	246	152	226	356	360	360	144	214	348	348	348	132	200	312	312	312
Feeder	1	1	APV	134	101	152	233	233	233	92	144	227	227	227	78	126	209	209	209
Feeder	1	1	CCB	198	100	149	238	240	240	94	142	229	229	229	82	130	214	214	214
Feeder	1	1	CNO	206	105	156	238	240	240	98	149	231	231	231	85	131	212	212	212
Feeder	1	1	CPM	218	105	156	237	240	240	99	151	233	234	234	86	131	212	212	212
Feeder	1	1	L66	162	105	156	237	240	240	99	151	233	234	234	86	131	212	212	212
Feeder	1	1	EMP	195	103	153	236	239	239	95	148	233	233	233	82	130	210	210	210
Feeder	1	1	WJF	183	101	151	238	240	240	95	143	232	232	232	85	133	210	210	210
Feeder	1	1	FUL	181	110	166	239	239	239	105	161	232	232	232	94	147	211	212	212
Feeder	1	1	AHR	187	110	166	239	239	239	105	161	232	232	232	94	147	211	212	212
Feeder	1	1	POC	190	110	166	239	239	239	105	161	232	232	232	94	147	211	212	212
Feeder	1	1	L16	218	101	151	238	240	240	95	143	232	232	232	86	133	210	210	210
Feeder	1	1	SFR	180	101	151	238	240	240	95	143	232	232	232	86	133	210	210	210
Feeder	1	1	SMO	190	110	166	239	239	239	105	161	232	232	232	94	147	211	212	212

TABLE A-9. (CONTINUED)

Airport Class	Dual	No. of Mixed Runways	Airport	Busy Hour Operations	Saturation Capacity (ops/hr)					Capacity Efficiency (ops/hr)									
										P(D≤6) = 0.5; P(D<15) = 0.9; P(D≤30) = 0.999					Average Delay = $\bar{D}$ = 3 min				
					Q_s (nmi)					Q_s (nmi)					Q_s (nmi)				
					3	2	1	0.5	0.1	3	2	1	0.5	0.1	3	2	1	0.5	0.1
	1	1	SZP	148	100	149	238	238	238	94	142	229	229	229	82	130	214	214	214
	1	1	L02	164	110	166	239	239	239	105	161	232	232	232	94	147	211	212	212
	1	1	VNY	246	110	166	239	239	239	105	161	232	232	232	94	147	211	212	212
	1	1	WHP	176	100	149	238	238	238	94	142	229	229	229	82	130	214	214	214
	0	1	X01																
	0	1	L38																
	0	1	RIR																
	0	1	X34																
	0	1	X42						Same as in Table A-7										
Feeder	0	1	X17																
	0	1	X18																
	0	1	L36																
	0	1	X37																
	0	1	SBT																
	0	1	X15																
	0	1	X25																
	0	1	X31																
	0	1	X32																
	0	1	X33																
	0	1	X43																
	0	1	X44																

APPENDIX B. ENROUTE SAFETY

1. INTRODUCTION

The system performance discussion of Sections 4.2.3 and 5.5 presented the models used to analyze enroute safety and described the results of that analysis. The results covered three aspects of system safety:

(1) The number of enroute conflicts for the year 1995 for CONUS

(2) The effect of limited surveillance coverage

(3) The effect of not providing surveillance at nontower airports

This appendix presents the data used in running the models and some additional discussion of the results. Additional results are also presented including the relationship between the number of CONUS radar sites and mid-air collisions.

2. ENROUTE CONFLICTS

2.1 Enroute IFR/IFR Conflicts

The number of enroute IFR/IFR conflicts was calculated using Eq. (4) of Section 4.2. Use of this conflict equation requires specification of aircraft passages and crossings (number and separation distance at point of closest approach), aircraft position keeping accuracies, and collision cross-sectional areas.

The number of aircraft crossings and passages per year for 1968 and those projected for 1995 were obtained by appropriate processing of the Autonetics enroute demand data (see Section 4.2.3.3). (Two aircraft on crossing paths which come within some prescribed distance of each other constitute a crossing. The same condition for two aircraft on the same path constitutes a passage.) The number of crossings and passages in each altitude band was obtained and is presented in Table B-1. This is for the 1995 scenario, with 10-min crossings, using a demand consisting of 6700 aircarriers, 500,000 General Aviation, and 20,000 military aircraft (Ref. 3).

Table B-1. Number of Enroute Crossings and Passages per Year for 1968 and 1995

Altitude Band (ft.)	Crossings Per Year		Passages Per Year	
	1968	1995	1968	1995
0 - 10,000	1,251,200	11,257,500	48,200	624,200
10,000 - 20,000	2,297,200	20,282,700	42,400	557,500
20,000 - 28,000	1,243,800	11,187,700	800	9,800
28,000 - 40,000	924,200	8,315,700	800	9,800

The average value of the separation distance at the point of closest approach for aircraft crossings was assumed to correspond to the existing 10-min separation requirement and the present airway structure. For aircraft passages, this distance was assumed to be 7 nmi. Due to different aircraft speeds, the 10-min separation requirement results in different separation distances. The mix of aircraft in each altitude band (Ref. 3, 12) was used to determine the average separation distance as presented in Table B-2. These values are predicated on average aircraft velocities of 140, 220, 444, and 474 knots for single engine, multiple engine, turboprop, and turbojet, respectively. The aircraft position keeping errors were assumed to be the same as the ATM surveillance errors since the surveillance errors indicate the uncertainty in aircraft relative position as seen by the system. These surveillance data are used to keep aircraft separated, whereas navigation and pilotage errors determine the nominal route separation distances which result in acceptable intervention rates. The relative position errors were treated as independent errors in the horizontal and vertical dimensions. The horizontal accuracy values estimated for the present and GAATMS assume the aircraft are uniformly distributed within the radar range and that the angle of the relative position vector to the radar line of sight is uniformly distributed. The relative surveillance position errors for the present and the GAATMS systems were calculated from published data (Ref. 1) and the errors are shown in Table B-3.

Table B-2. Crossing Distance for a 10-min Separation as a Function of Altitude Band

h	Altitude Band (ft.)	$r_c(h)$ - Average Separation Distance at Crossing (ft.)
1	0 - 10,000	284,100
2	10,000 - 20,000	356,400
3	>20,000	465,000

Table B-3. System Relative Position Surveillance Errors

System	Standard Deviation of Surveillance Position Error (ft)		Comment
	Horizontal, σ_H	Vertical, σ_z	
Present	11,400	350	200 nmi Radar Coverage
GAATMS	900	350	100 nmi Radar Coverage
SAATMS	100	100	Satellite Coverage

The collision cross-section area is a function of the conflict distance (150 ft) and the physical dimensions of the aircraft involved in the conflict. The mix of aircraft by altitude bands was used to determine the average aircraft dimensions. Combining the conflict distance with the average aircraft dimensions yields the average collision cross-section area as indicated in Table B-4. Since the statistics of wake turbulence are presently unknown, it is not feasible to increase the collision cross-section area by an average wake turbulence value determined from the average aircraft mix in each altitude band. The horizontal and vertical values chosen for the probability distribution ellipsoid, Equation (8), Section 4.2, were 22,800 and 0 ft, respectively (no altitude separation).

Table B-4. Collision Cross-Section Area at Altitude Band h

h	Altitude Band (ft)	Horizontal Dimension (ft)	Vertical Dimension (ft)
1	0 - 10,000	480	360
2	10,000 - 20,000	540	380
3	>20,000	600	400

The normalization factor was determined using 1968 demand and conflict data (Ref. 2). The 1968 conflict data were assumed to be 106 crossing conflicts and 11 passage conflicts. This value has been adjusted to include the average number of IFR/IFR mid-air collisions per year and the conflicts are multiplied by a factor of 4 which is based on the frequency of unreported incidents (Ref. 2). The conflicts were classed as Critical Near Mid-Air Collisions (CNMAC) where aircraft were separated by 150 ft or less at their point of closest approach.

The results are shown in Fig. 5.5-1. The curves would look more like straight lines (dotted line extensions) if the vertical system accuracies were all the same.

The results are plotted for crossing separations of 10 and 2 min. The relationship between crossing separation time and conflicts can be determined from Equation (4), Section 4.2, to be as follows:

$$\text{Number of conflicts for 1995 for X-min separation} = \frac{10}{X} \text{ (Number of conflicts for 1995 for 10-min separation)}$$

when the cube of the length of the horizontal axes of the probability distribution ellipsoid, Equation (8), Section 4.2, is small as compared to the crossing separation distance X. For a 2-min separation, this is a reasonable assumption and is used to obtain the "2-min crossing separation" curve in Fig. 5.5-1. Better IFR/IFR enroute safety than that existing in the 1968 (117 conflicts) is obtained with the GAATMS and SAATMS for 2-min separation.

The values in Fig. 5.5-1 have not been adjusted by an automation factor. This factor would be based on the ability of the system to reduce or eliminate gross errors on the part of the pilot, controller, or equipment. Reference 12 indicates that possibly greater than 57 percent of the IFR/IFR NMAC's are due to these causes.

2.2 Enroute IFR/VFR and VFR/VFR Conflicts

For the case of IFR/VFR and VFR/VFR conflicts in airspace under surveillance, the normalization of the conflict equation using 1968 data is not possible since VFR aircraft were not controlled by the ATC system in 1968. The IFR/IFR normalization factor should provide a reasonable estimate for this case, however, and this was used to estimate SAATMS performance. The IFR/VFR and VFR/VFR crossings and passages were determined from the Autonetics enroute demand data. The minimum separation distance at the point of closest approach in this case was assumed to be 1 nmi. This corresponds roughly to the separation standard for the SAATMS given in Section 5.2.

The crossing model was used to calculate the number of 1 nmi crossings per year. The number of crossings and passages used in the conflict equation is indicated in Table B-5 for the four demand levels. The collision cross-section area, relative position keeping accuracy, and q factor are obtained as before. The IFR/VFR and VFR/VFR conflicts for SAATMS are indicated in Table B-5. The relative safety performance for the system was determined and is indicated in Table B-6. The SAATMS system is safer than the GAATMS by a factor of 52.7.

Table B-5. SAATMS VFR/VFR and IFR/VFR Enroute Conflict Estimates (0 to 12,000 ft)

Demand Level	Crossings at 1 Mile	Passages	Crossing Conflicts	Passage Conflicts	Total Conflicts
1	632,600	355,500	0.7990	0.0197	0.8180
2	1,596,200	1,331,100	2.020	0.0736	2.090
3	4,864,100	2,803,800	6.140	0.1550	6.300
4	19,849,300	12,195,300	25.10	0.6740	31.80

Table B-6. IFR/VFR and VFR/VFR Normalized System Safety for Crossing and Passage Conflicts

System Designation	Surveillance Errors		Normalized Conflicts
	σ_H (ft)	σ_z (f)	
A	50	50	0.20
B SAATMS	100	100	1.00
C	500	350	32.9
D GAATMS	900	350	52.7

Estimates of the number of conflicts for the GAATMS can be obtained from Table B-5 and B-6. For example, the GAATMS with surveillance coverage down to ground would have 110 conflicts for demand level 2 (2.09 for the SAATMS times a relative factor between the SAATMS and GAATMS of 52.7, Tables B-5 and B-6). This estimate has not included a see-and-avoid factor which would reduce the number of conflicts.

3. THE EFFECTS OF SURVEILLANCE COVERAGE

3.1 Enroute Safety as a Function of Altitude Coverage

For an ATC system to prevent aircraft conflicts, it must have surveillance data giving relative aircraft states (e.g., position and velocity). If surveillance data are not available below a certain altitude, the ATC system cannot prevent conflicts below that altitude. To determine the effect of limited altitude surveillance coverage, the curves of Fig. B-1 and B-2 were generated. The lower curve of Fig. B-1 shows the number of IFR/VFR and VFR/VFR collisions that occurred in the year 1968 below a certain altitude (as given by values along the X-axis). The upper four curves represent the same relationship for the four projected demand levels. For demand level 2, if coverage were limited to altitudes 6,000 ft and above, over 60 mid-air collisions would occur below this altitude (where there is no surveillance).

The curves of Fig. B-1 indicate the importance of providing surveillance coverage to ground level to keep safety comparable to that achieved in 1968. For example, for demand level 2 if coverage is not provided down to 1500 ft, the number of collisions in the uncovered airspace will exceed the total number of collisions that occurred in 1968.

The VFR/VFR and VFR/IFR results indicate that fewer than 110 conflicts would result for the GAATMS with coverage down to the ground and demand level 2. Also, 5391 and 3641 conflicts would result when no surveillance is available below 12,000 and 6,000 ft, respectively. Correspondingly, the number of CNMAC for 1968 below positive control airspace was estimated to be 1370. In order to get GAATMS performance comparable to the 1968 safety level, coverage must be down to 1500 ft. In comparison, the SAATMS with coverage to ground would have fewer than 2.09 conflicts.

The high density of VFR itinerant aircraft between 1000 and 4000 ft (Ref. 7) results in the steep slope of the curves in this altitude band. The change of slope of the curves at 8000 ft is due to the assumption that VFR traffic formerly flying from 10,000 ft to positive controlled airspace will now be assumed to be uniformly distributed between 8000 and 12,000 ft (1995 positive control).

The number of conflicts is calculated using Equations (9) and (10), Section 4.2, along with the number of random crossings and passage of Table B-7. The average number of crossings and passages are indicated assuming randomly spaced flight of aircraft on city pair routes and that the pilots could not see and avoid other aircraft.

Figure B-1 was obtained from Fig. B-2 by using a factor of 0.0174 mid-air collisions per CNMAC. The number of mid-air collisions per 150 ft CNMAC was calculated by two different methods. The first approach is from Reference 6. If the pilots fail to see each other, then it can be assumed that the relative velocity vector is equally likely to penetrate any point in the plane normal to this vector containing the point of closest approach (Ref. 6). We can then estimate from the number of incidents in a radius of 150 ft the expected number of actual collisions as the ration of the collision cross-section of two aircraft to the area of the

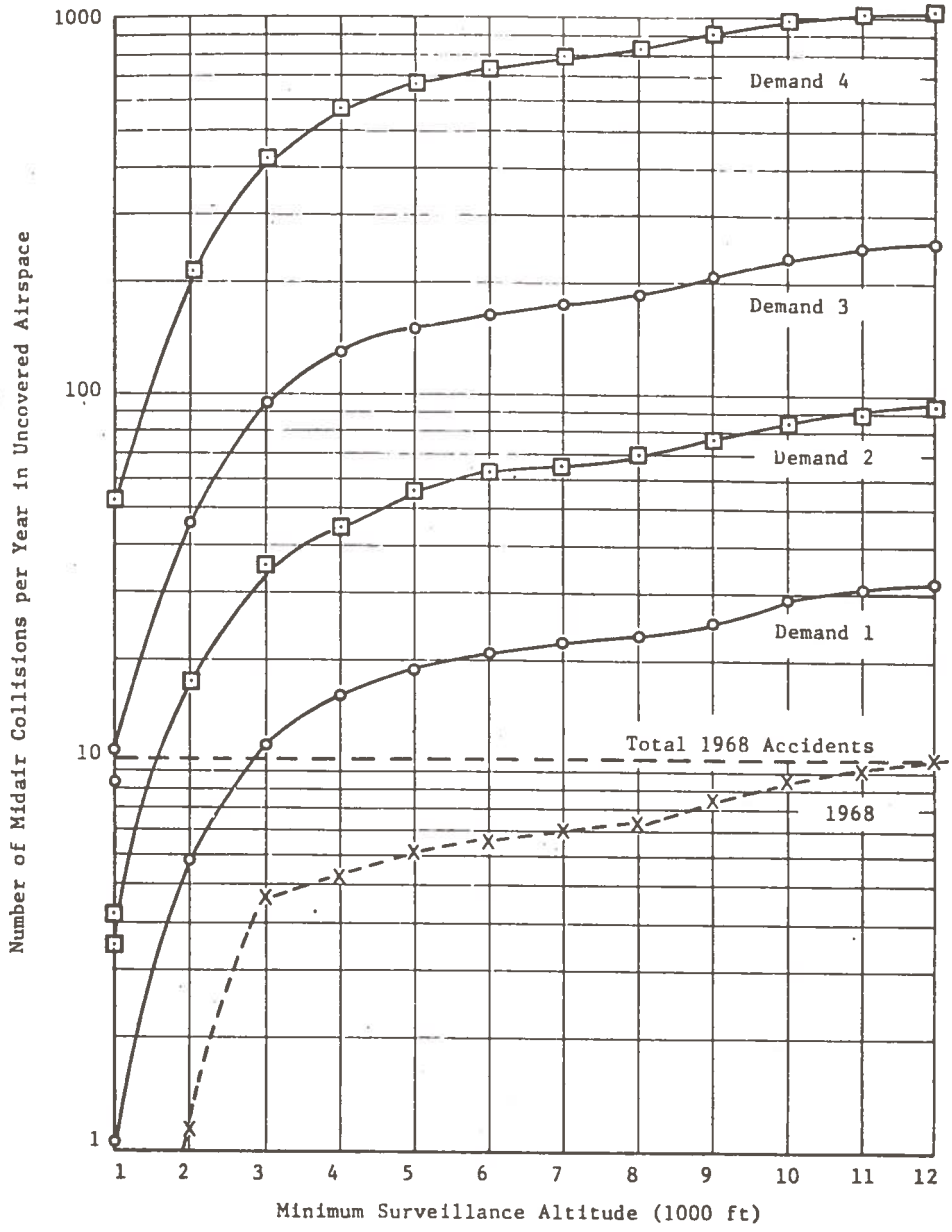

Figure B-1. Mid-Air IFR/VFR, VFR/VFR Enroute Collisions as a Function of Minimum Surveillance Attitude

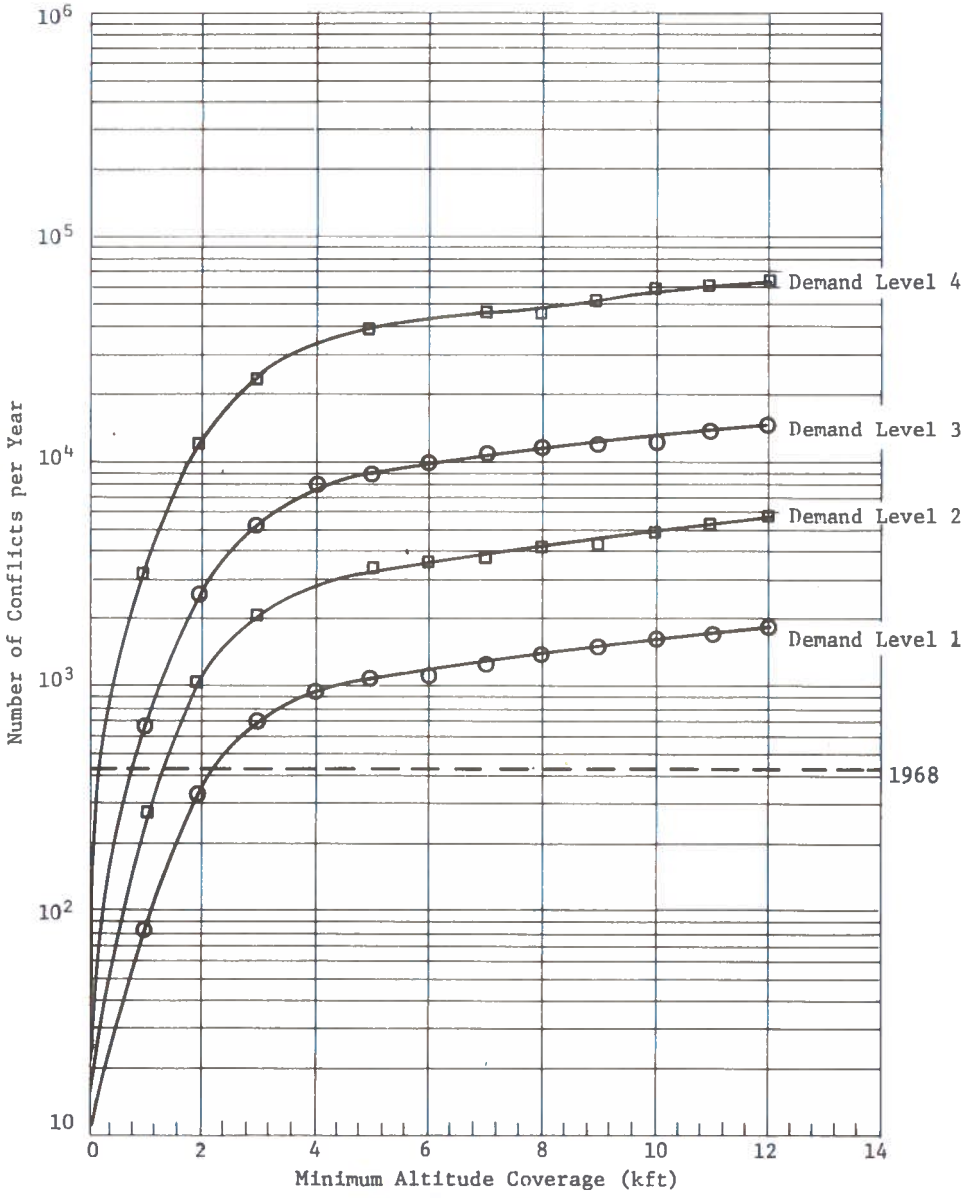

Figure B-2. Safety as a Function of Coverage

TABLE B-7. VFR/VFR AND VFR/IFR RANDOM CROSSINGS AND PASSSAGES

	150 ft Crossings		500 ft Crossings		Passages	
Demand Level	Altitude 0-10,000 ft	Altitude 10,000'- Positive Control	Altitude 0-10,000 ft	Altitude 10,000'-Positive Control	Altitude 0-10,000 ft	Altitude 10,000'-Positive Control
1	10,500	5,100	-	-	3,200	200
2	27,600	11,700	-	-	12,500	600
3	85,300	34,500	-	-	25,500	2,000
4	379,500	109,200	-	-	110,900	8,600
1968	-	-	8,700	4,300	1,700	100

circle of 150 ft radius. We take as the collision cross-section the sum of the product of the tail height of the first aircraft and the wing span of the second aircraft and the product of the tail height of the second aircraft and the wing span of the first aircraft. If we use for a light aircraft a tail height of 10 ft and a wing span of 38 ft and if we use for a heavy aircraft a tail height of 35 ft and a wing span of 125 ft, we get as the collision cross-section in an encounter between two light aircraft 760 sq ft and between a light and a heavy aircraft, 2580 sq ft. The average collision cross-section was calculated by weighing the light-light and light-heavy involvement collision cross-section by the relative densities of GA and AC aircraft (Ref. 12). The resulting average collision cross-section is 978 sq ft. The area of the circle of radius 150 ft is 70,686 sq ft, so we predict that the expected number of collisions per 150 ft near miss will be 978/70,686 - 0.0138.

Another factor was calculated using the 150 ft CNMAC data and the actual number of random flight mid-air collisions. For this calculation, it was estimated that 404 VFR/VFR and VFR/IFR CNMAC occurred below positive controlled airspace in 1968. This estimate is obtained using Reference 2 data and the assumption that only 25 percent of the near misses are reported. There were 11 mid-air collisions of this type in 1968 and only 64 percent of them were of a random flight nature. Therefore,

$$\frac{11 \times 0.64}{404} = 0.0174$$

mid-air collisions occurred per CNMAC for random flight in 1968. The two estimates of this parameter exhibit reasonable agreement.

3.2 Relationship Between the Number of Radar CONUS Sites and Mid-Air Collisions

An analysis of the airspace coverage by ground-based networks (Ref. 22) was used to determine the number of mid-air collisions resulting from lack of coverage as a function of the number of radar sites in the network. The radar coverage is parameterized on the following variables: antenna height (h), minimum antenna elevation angle (θ_{min}) and network geometry as indicated by the spacing between stations ($2d_o$). Figure B-3 indicates the results with the number of CONUS sites as the abscissa and with the number of mid-air collisions as the ordinate and parameterized on θmin and demand level. The antenna height was kept constant at 100 ft, and optimistic choice except in the case of radar sites on hills; however, the results are not too sensitive to this parameter. An estimate of 0.85 deg for θ_{min} is obtained for ATCRBS from Ref. 23. The results indicate for 300 radar sites for demand level 2 and a ground-based radar system, approximately 40 mid-air collisions would result as compared to 11 mid-air collisions in 1968 for enroute VFR/VFR and VFR/IFR.

FIGURE B-3. VFR/VFR AND VFR/IFR SAFETY VS COVERAGE